UNIVERSITE CATHOLIQUE DE LOUVAIN
Faculty of Pharmacy and Biomedical Sciences
Institute of Neurosciences (IoNS)
Aging and Dementia Research team (AGAD)

Advancing Alzheimer's Disease Diagnosis: From Bood Soluble Biomarkers to EVs

Emilien Boyer

Thesis submitted for the degree of
Doctor in Biomedical and Pharmaceutical sciences
Thèses du secteur des sciences de la santé

Submission date: 02-09-2024

Promotor: Pascal Kienlen-Campard
Co-promotor: Bernard Hanseeuw

Composition of the Jury

Promotors:

Prof. Pascal Kienlen-Campard
(UCL, Institute of Neurosciences, CEMO, AGAD)

Prof. Bernard Hanseeauw
(UCL, Institute of Neurosciences, NEUR, LAB)

President:

Prof. Emmanuel Hermans
(UCL, Institute of neurosciences, CEMO, NFAR)

Internal members:

Prof. Phillipe Gailly
(UCL, Institute of neurosciences, CEMO, Physiologie cellulaire)

Prof. Vincent Van Pesch
(UCL, Institute of neurosciences, CEMO, Neurochimie)

External members:

Prof. Sylvain Lehmann
(CHU de Montpellier, Director of Inserm UMR 1298 at the Institute for Neurosciences of Montpellier, Montpellier, France)

Prof. Charles Ramassamy
(Full professor at the Institut national de la recherche scientifique, Quebec, Canada)

Remerciements

Je tiens tout d'abord à remercier mon promoteur, Pascal Kienlen-Campard, pour son aide et son soutien durant ces quatre années, pour la confiance qu'il a accordée à mes décisions, pour avoir été toujours à l'écoute lorsque j'avais des doutes quant aux résultats de mes expériences, et surtout, pour m'avoir permis de rejoindre son laboratoire et son équipe de chercheurs extraordinaires. Un grand merci également à mon co-promoteur, Bernard Hanseeuw, sans qui toute cette aventure n'aurait pu être possible. Tu as été le premier à me faire confiance pour porter ce projet, dès notre rencontre lors d'un cours de master 3, et tu as été le fil conducteur pour l'interprétation de mes résultats et la rédaction des articles. Merci à l'ensemble des membres de mon jury de thèse pour leurs commentaires constructifs et leur suivi pendant ces 4 années de doctorat.

Je remercie chaleureusement Lise, avec qui j'ai commencé ma thèse. Sans ton travail et ta détermination, nous n'aurions jamais pu recruter nos participants, et l'ensemble de ce travail n'aurait pas été possible. Nuria, tu as été la première personne, avec Céline à l'époque, à m'accueillir au laboratoire, et je vous dois beaucoup pour cette formation express en techniques de laboratoire durant mes trois premiers mois de thèse. Tu as su prendre le temps de m'expliquer les techniques, de m'apprendre à penser scientifiquement, à interpréter les résultats et à mener un projet de thèse. Un immense merci pour tout ce que tu as fait, et j'espère que ta carrière académique se poursuivra aussi loin que tu le souhaites ; tu le mérites amplement.

J'ai une pensée particulière pour Marion et Louise, que j'ai eu la chance de superviser pendant mon doctorat. Merci à vous deux de m'avoir fait confiance pour vous encadrer, alors que je n'avais pas vraiment eu l'occasion de le faire auparavant, de ne pas m'en avoir voulu pour mes multiples gaffes lors de nos

manipulations (le fameux FBS renversé sous la hotte lors de vos premiers jours de stage, on s'en souvient tous !), mais surtout merci pour le soutien que vous m'avez apporté une fois devenues doctorantes au laboratoire. Dans les bons moments comme dans les plus difficiles, nous avons su nous épauler et persévérer. Merci aussi à Shirine et Debora pour les moments partagés au labo et en dehors (hâte d'une revanche sur Mario Kart, Shi !). En quatre ans, vous êtes devenus bien plus que des collègues, vous êtes devenus des amis.

Je tiens aussi à remercier Esther pour le temps qu'elle a consacré à m'aider dans mes expériences, ses conseils avisés sur les techniques de laboratoire, nos après-midis passés à extraire des vésicules sur colonnes (cette journée aux cent extractions restera gravée dans nos mémoires !), ainsi que Romélia, qui s'est occupée de ma colonie de souris et de l'entretien du labo.

Merci à toute l'équipe clinique : Daniela et Fiona pour le suivi des patients, Thomas et Renaud pour la partie médecine nucléaire, Yasmine et Vincent pour les acquisitions d'IRM, Lisa et Lara pour le suivi neuropsychologique des patients, et bien sûr Adrian et Bernard pour la gestion du projet et leurs précieux conseils. Sans vous tous, ce travail n'aurait pu voir le jour.

Je souhaite également remercier mes parents et ma sœur, qui m'ont toujours soutenu malgré la distance, qui m'ont permis de venir en Belgique pour faire mes études de médecine et qui m'ont épaulé dans les moments difficiles de ces dix dernières années. Un grand merci enfin à Florian, pour son soutien inconditionnel, pour être la personne sur qui je peux toujours compter, sans qui rien de tout cela n'aurait pu se réaliser. Merci de m'avoir donné l'envie et le courage de me lancer dans cette grande aventure qu'a été le doctorat ; je t'en serai éternellement reconnaissant.

Enfin, merci à tous mes amis pour leur soutien et leur amitié indéfectible. Malgré nos emplois du temps chargés, nous avons su rester proches et nous voir aussi souvent que possible.

Table of contents

Résumé

Le diagnostic précoce de la maladie d'Alzheimer (MA) est devenu un impératif majeur ces dernières années, en particulier depuis l'approbation par la FDA (Food and Drug Administration) de traitements tels que l'Aducanumab et plus récemment le Lecanemab, deux thérapies anti-amyloïde. Un des principaux axes de recherche actuels vise à faciliter l'identification des patients atteints de la MA à des stades précliniques, avant l'apparition des premiers symptômes de dysfonctionnement cognitif et de neurodégénérescence, afin de leur offrir ces nouvelles thérapies à l'avenir.

Trois axes de recherche principaux sont explorés : le développement de nouveaux tests neuropsychologiques, le perfectionnement des traceurs et techniques d'imagerie permettant de détecter les dépôts de protéine tau / amyloïde, et l'utilisation de biofluides pour détecter les biomarqueurs spécifiques de la maladie. La MA étant la première cause de démence dans le monde, affectant plus de 50 millions de personnes, l'utilisation de biofluides comme le plasma sanguin semble être le candidat de choix pour une application au plus grand nombre.

Le peptide β amyloïde (Aβ) et la protéine tau, peuvent désormais être quantifiées dans des échantillons de plasma à l'aide de techniques ultrasensibles telles que la Single molecule array (Simoa). Cependant, ces protéines circulent non seulement dans le plasma sous forme soluble mais sont également présentes dans les vésicules extracellulaires dérivées du neurone (NDEVs) sécrétées par les neurones et traversant la barrière hématoencéphalique vers le plasma. L'objectif de ce travail de thèse est (i) d'identifier le candidat le plus prometteur pour le diagnostic de la MA dans le plasma, (ii) d'évaluer le rôle des NDEVs en tant que biomarqueur de la MA,

notamment par une approche in vitro d'étude des vésicules, et (iii) d'explorer leur possible impact sur les quantifications de biomarqueurs solubles plasmatiques.

Une cohorte de patients atteints de la MA et de participants contrôles sans troubles cognitifs a été recrutée, dont une partie ont eu accès aux techniques d'imagerie PET-Amyloïde et PET-Tau. La quantification des peptides amyloïdes 42–40, protéine Tau totale et pTau 181 dans le plasma et NDEVs a été réalisée via SIMOA, et le dosage immuno-enzymatique DELFIA ELISA a été utilisé pour la quantification relative des NDEVs circulant dans le plasma.

Les principales conclusions de ce travail de thèse indiquent que le rapport Aβ42/40 s'avère être un indicateur efficace pour le dépistage de la MA, réduisant la probabilité de MA à 5,2% à l'âge de 60 ans (vs 15,8% sans test) et à 12,5% à l'âge de 80 ans (vs 32,6% sans test) en cas de résultat négatif du test, des résultats similaires furent trouvés concernant le pTau181 plasmatique, et l'association des deux mesures réduisit la probabilité de MA à 2% à l'âge de 60 ans et 4% à l'âge de 80 ans. Une étude in vitro menée sur des neurones a démontré que le contenu des vésicules extracellulaires sécrétés reflète les altérations survenant au niveau cellulaire. La présence de NDEVs dans le plasma a été identifiée comme un facteur de confusion significatif dans les mesures de biomarqueurs plasmatiques, bien que leur contenu ne semble pas constituer un biomarqueur pertinent pour le dépistage des individus à risque de développer la maladie, du moins selon les quantifications menées par SIMOA.

Abstract

Early diagnosis of Alzheimer's disease (AD) has become a major imperative in recent years, especially since the FDA's approval of treatments such as Aducanumab and more recently Lecanemab, two anti-amyloid therapies. One of the main current research directions aims to facilitate the identification of AD patients at preclinical stages, before the appearance of initial symptoms of cognitive dysfunction and neurodegeneration, in order to offer these new therapies in the future.

Three main research areas are being explored: the development of new neuropsychological tests, the refinement of tracers and imaging techniques to detect tau/amyloid protein deposits, and the use of biofluids to detect specific disease biomarkers. Since AD is the leading cause of dementia worldwide, affecting more than 50 million people, the use of biofluids like blood plasma appears to be the preferred candidate for widespread application.

The β-amyloid (Aβ) peptide and tau protein can now be quantified in plasma samples using ultra-sensitive techniques such as Single Molecule Array (Simoa). However, these proteins circulate not only in plasma in soluble form but are also present in extracellular vesicles derived from neurons (NDEVs) secreted by neurons and crossing the blood-brain barrier into plasma. The aim of this thesis work is (i) to identify the most promising candidate for AD diagnosis in plasma, (ii) to assess the role of NDEVs as an AD biomarker, notably through an in vitro approach studying vesicles, and (iii) to explore their possible impact on the quantification of soluble plasma biomarkers.

A cohort of AD patients and control participants without cognitive disorders was recruited, some of whom had access to PET-Amyloid and PET-Tau imaging

techniques. Quantification of amyloid peptides 42–40, total Tau protein, and pTau 181 in plasma and NDEVs was performed via SIMOA, and the DELFIA ELISA immunoenzymatic assay was used for the relative quantification of circulating NDEVs in plasma.

The main conclusions of this thesis work indicate that the Aβ42/40 ratio proves to be an effective indicator for AD screening, reducing the probability of AD to 5.2% at age 60 (vs 15.8% without the test) and to 12.5% at age 80 (vs 32.6% without the test) in case of a negative test result, and plasma pTau 181 performed as well, and their association reduced probability of AD to 2% at age 60 and 4% at age 80. An in vitro study conducted on neurons demonstrated that the content of extracellular vesicles secreted reflects the cellular AD alterations occurring. The presence of NDEVs in plasma was identified as a significant confounding factor in plasma biomarker measurements, although their content does not seem to be a relevant biomarker for screening individuals at risk of developing the disease, at least according to quantifications performed by SIMOA.

INTRODUCTION

1. Background

Alzheimer's disease (AD) stands as the most prevalent form of dementia, a condition characterized by acquired or inherited progressive, and irreversible cognitive impairment significant enough to interfere with daily activities [1]. Currently, there are approximately 50 million individuals worldwide affected by dementia, with over 10 million new cases appearing annually. Such statistics anticipate that one in every four individuals will eventually experience dementia, marking it as one of the most pressing global health crises of the 21st century [2].

AD is a progressive, irreversible neurodegenerative disease impacting cognition, function, and behavior. AD progresses along a continuum from preclinical disease to mild cognitive and/or behavioral impairment and finally dementia.

First described by Alois Alzheimer in 1906, AD was identified through the brain autopsy of a patient with dementia. Alzheimer's initial observations revealed two distinct lesions: extracellular deposits and tangles [3]. This seminal discovery laid the groundwork for understanding the pathophysiology underlying neurodegenerative diseases that lead to dementia. It deeply revolutionized the vision of dementia, which was no longer a stage in the aging process associated with a form of arteriosclerosis, but a pathology in its own right, whose signature could be observed in the brains of afflicted individuals.

In the mid-1980s, the definition of Alzheimer's disease evolved with the discovery of the tau protein and its phosphorylated forms as key components of neurofibrillary tangles (NFT) [4], alongside the identification of amyloid-beta peptide (Aβ) as the structural element of senile plaques, now termed amyloid plaques [5]. These early breakthroughs propelled the development of neuropathologic assessments, which subsequently acknowledged multiple comorbid neuropathologies contributing to clinical dementia [6-8]. Currently, the clinical diagnosis of AD relies on three primary axes: neuropsychological assessments, brain imaging, and biofluid analysis for AD-specific biomarkers. However, there are significant differences in cost, hospital availability, application in clinical routine, and even accuracy for diagnosis among the various diagnostic techniques. The emerging field of blood biomarkers shows promise, addressing issues of accessibility for large-scale screening in an era of new treatment discoveries. Blood biomarkers offer hope for early pre-clinical diagnosis of AD and the potential for treatments before the first signs of irreversible neuronal impairment. There is a need to bridge the gap between AD pathogenesis and the presence of biomarkers in the blood to identify those that are most likely to predict AD development, and that could be accurately tracked in clinical trials.

2. Alzheimer's disease etiology

Dementia cases in Europe are estimated to increase from 7.7 million in 2001 to 15.6 million in 2040 [9], with AD accounting for 60 to 80% of cases [10, 11]. The prevalence of AD across the population is dependent on the age of symptoms onset. More than 85% of AD cases appear after the age of 65 and constitute the late-onset branch of the disease (LOAD for late-onset Alzheimer's disease). The other 10-15% are AD cases appearing before the age of 65 and are considered as early-onset Alzheimer's disease (EOAD)[12, 13]. The hallmark of the disease remains the same in EOAD and LOAD, but there is evidence suggesting differences in several aspects of the disease. The progression of the disease is more rapid in EOAD [14, 15], with differences in the initial clinical presentation. For instance, studies have shown greater behavioral problems, increased language difficulties [16], and higher tendency toward depression and anxiety in EOAD when compared to

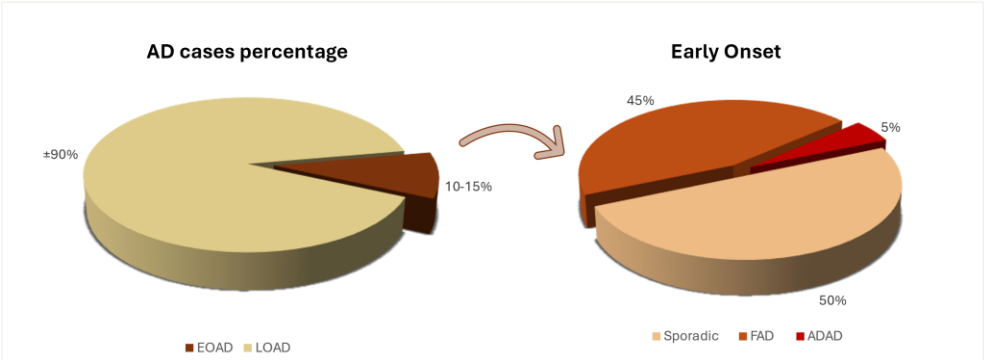

Figure 1. Distribution of early-onset (EOAD) and late-onset (LOAD) cases among total AD cases. Adapted from R. Cacace et al. Alzheimer's & Dementia- (2016). ADAD represent the familial inherited forms of AD.

LOAD [17]. One major difference between those groups is AD etiology distribution. Factors that increase AD development risk can be classified in three categories: (i) sporadic AD, linked to several risk factors (aging, genetic and environmental), increasing AD occurrence, (ii) the familial forms of the disease (FAD), with inherited mutation leading usually to AD pathogenesis, representing most of the EOAD cases, and (iii) autosomal dominant Alzheimer's disease (or ADAD), with causal AD mutations leading always to EOAD. The repartition of those different etiologies is summarized in Figure 1.

The main risk factor in LOAD is aging. It is estimated that the number of people over the age of 65 will increase from 420 million to almost 1 billion from 2000 to 2030 [18]. After the age of 65, the incidence of AD rises almost exponentially, from 10% of incidence at age 70, to 50% at age 85 [19]. This increased incidence with age can be attributed to aging-related biological processes, psychosocial factors, and environmental exposures throughout life. For instance, there is strong evidence that a cardiovascular history, such as high blood pressure with high body mass index, cerebrovascular disease, smoking history, and chronic alcohol consumption increases the risk of developing dementia, including AD. Studies have shown that overweight patients develop brain white matter atrophy, possibly linked to chronic neuroinflammatory processes and metabolic disorders as type 2 diabetes [20].

The main genetic risk determinant in LOAD is the apolipoprotein E gene (*APOE*) coding for the apolipoprotein E (apoE). There are three different *APOE* alleles in humans: ε2, (*APOE2*), ε3 (*APOE3*) and ε4 (*APOE4*); each conferring varying levels of disease risk [21]. *APOE4* carries the highest risk for AD and other dementias, particularly in homozygotes, and decreased age of disease onset (Figure 2). On the other hand, *APOE2* reduces AD risk by almost half. *APOE3* is identified as non-promoting AD development but does not offer protection against the disease either. In the general population, those different alleles are not distributed equally, varying by ethnicity group [22]. In Belgium, in the non-demented population, 6.9% are *APOE2*, 76.2% are *APOE3* and 16.9% *APOE4* carriers (for at least 1 allele) [23]. However, APOE4 is not a causing allele gene, and it should be remembered that only 12-18% of the AD cases appear to be attributed to the *APOE4* allele.

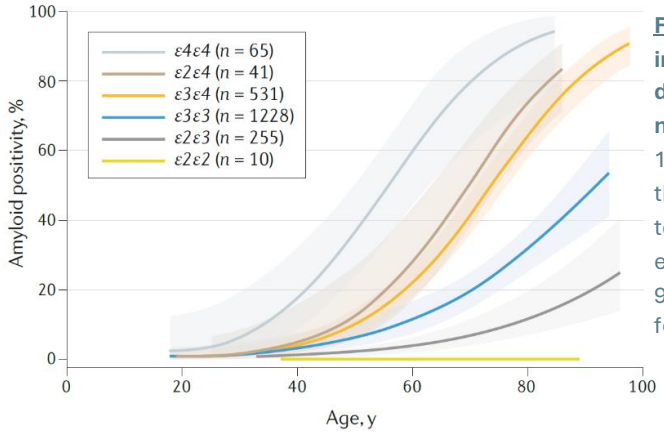

Figure 2. APOE genotype influence amyloid pathology development in cognitively normal individuals. (AlzForum 19 May 2015). People carrying the ApoE4 allele are more likely to become amyloid positive earlier in life. Shading represents 95 percent confidence interval for each curve.

The causal role of the apolipoprotein E in AD development is still not fully understood, but there is evidence linking it to Aβ clearance

mechanisms, with reduce clearance of amyloid throw the blood brain barrier (BBB) and impaired amyloid uptake by microglial cells in *APOE4* carrier [21]. Compared to apoE3 and apoE2, apoE4 enhances Aβ seeding and aggregation in both oligomers and fibrils, while also hindering its clearance from the interstitial fluid. This may potentially result in the deposition of Aβ as dense-core amyloid plaques and cerebral amyloid angiopathy, in conjunction with apoE [24]. However, there is no clear direct interaction to tau accumulation. But recent studies shown that, apoE4 could promote tau-induced neurodegeneration, mediated by apoE4 proinflammatory effect on microglia [25].

The mains etiology in EOAD are FAD mutations, but the incidence of ADAD is here more important. They are inherited causal mutations which will lead to amyloid and tau accumulation in the brain. Mutations in presenilin 1 gene (*PSEN1*); located in chromosome 14, mutations in the amyloid precursor protein gene (*APP*), on chromosome 21, and mutation in presenilin 2 gene (*PSEN2*) on chromosome 1, represent most of the cases. Mutations in APP will modulate its cleavage, with increased Aβ42 production in codons 714-717 mutation, or in the Swedish mutation (K670N/M671L) changes in the β-secretase cleavage which elevate both levels of Aβ40 and Aβ42. *PSEN* mutation will directly influence APP processing causing an increased production of Aβ42. *PSEN1* mutations are the most frequent cause of FAD, accounting for 18-50% of EOAD. More than 200 mutations in PSEN1 have been described [26], while *PSEN2* mutation are substantially less frequent with less than 40 mutations identified [27].

3. Physiopathology of AD

There are two main lesions in AD due to the deposition of two proteins: the Aβ peptide, accumulating outside the cells in the brain parenchyma into plaques (Figure 3**,** A), and the tau protein and specially its phosphorylated forms (ptau) inside the neurons forming the NFT (Figure 3, B). Both lesions lead to neurodegeneration through different cellular aspects, leading to brain atrophy and cognitive decline. But those proteins do not appear at the same time and not in the same areas of the brain parenchyma in AD development.

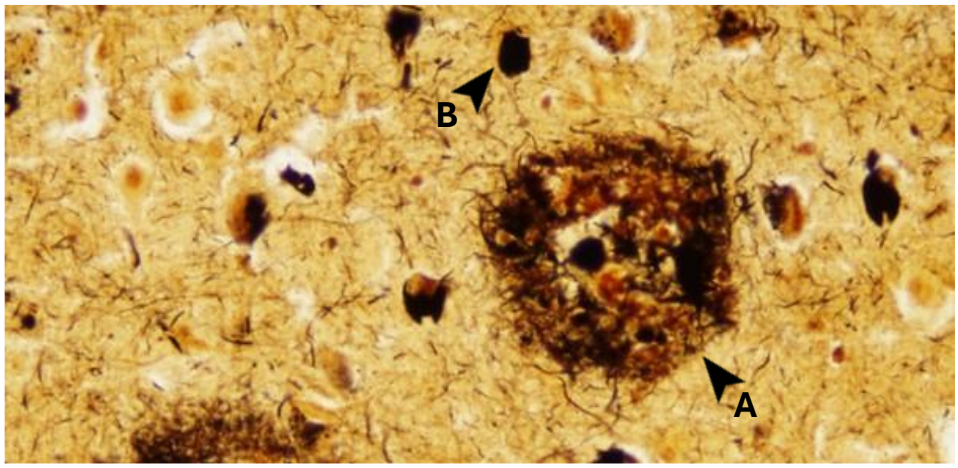

Figure 3. Histological lesions in Alzheimer's disease. A. Amyloid plaques; **B.** Neurofibrillary tangles. Silver stain. Adapted from Canet et al. 2020.

3.1. The amyloid-β peptide

3.1.1. Generalities

As the primary constituent of senile plaques, a key hallmark of AD, the Aβ peptide is crucial for understanding the disease's pathology. Consequently, extensive research has been dedicated to investigating the Aβ peptide and its role in the progression of AD.

The amyloid peptide is produced from the cleavage of the APP. APP is a transmembrane protein expressed ubiquitously by cells, encoded by a gene of the same name [28]. APP is a type I single-pass transmembrane protein with large extracellular domain and a short cytoplasmic tail, called C - terminal APP intracellular domain (AICD). The extracellular domain of APP, which constitute the major part of the protein, can be divided into domains E1 and E2. APP will be cleaved into diverse proteins with several physiological functions. This transmembrane protein is encoded by a single gene located on chromosome 21 in

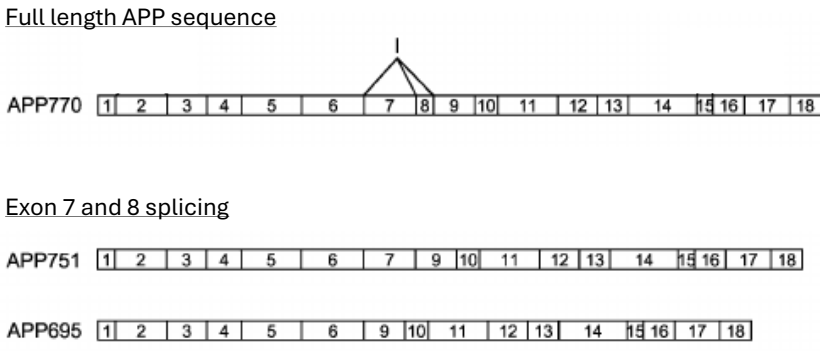

Figure 4. Alternative splicing of human APP gene. Alternative splicing of exons 7 and 8 lead to formation of isoform APP751 (exon 8 splicing) and APP695 (Exons 7 and 8 splicing).

humans, coding for three major isoforms from alternative splicing: APP_{695}, APP_{751} and APP_{770} (containing 695, 751 and 770 amino acids, respectively) [29, 30] (see Figure 2). APP_{695} is mainly expressed in neurons whereas APP_{751} and APP_{770} are found in peripheral tissues, fibroblasts, and glial cells.

APP is one of three members of transmembrane protein family in human. The two other family members, also type 1 integral membrane proteins, are the APP-related proteins APLP1 and APLP2. Both share similar structural domains with APP, and are possibly involved in cell adhesion, neuronal migration, and neurite growth [31].

3.1.2. Cellular trafficking and cleavage of APP

In neurons APP is found mainly in the somatodendritic and the axonal compartments. APP is synthetized in the endoplasmic reticulum and transported through the Golgi apparatus to the trans-Golgi network [32]. APP is abundant in intracellular membrane compartments, before being addressed to the cell membrane in secretory vesicles [29]. At the cell surface, APP is either cleaved by a α-secretase, liberating APPsα, or re-internalized via an endosomal/lysosomal pathway where β-secretase cleavage is more prone to occur. The cellular distribution of APP influences the way in which it is processed by those membrane secretases. There are two mains APP processing pathways: the non-amyloidogenic pathway which represents the major APP processing route, and the amyloidogenic pathway, leading to amyloid-β production (Figure 5.A). Non-amyloidogenic pathway is initiated by α-secretase

which cleave APP within the Aβ region, preventing Aβ production (see Figure 5.B, Aβ sequence is highlighted in red with α cleavage in blue) and liberating APPsα. ADAM10 (disintegrin and metalloproteinase domain-containing protein 10) is the major component of α-secretase in the brain [33]. On the contrary, within the amyloidogenic pathway, β-secretase cleaves APP at the amino terminus of Aβ, releasing APPsβ. β-secretase is composed of the enzyme BACE-1. In both pathways, there remain membrane-tethered C-terminal fragments (CTFα when cleaved by α-secretase and CTFβ, or C99 due to its 99-amino acid composition, when cleaved by β-secretase). These CTFs are then processed by γ-secretase.

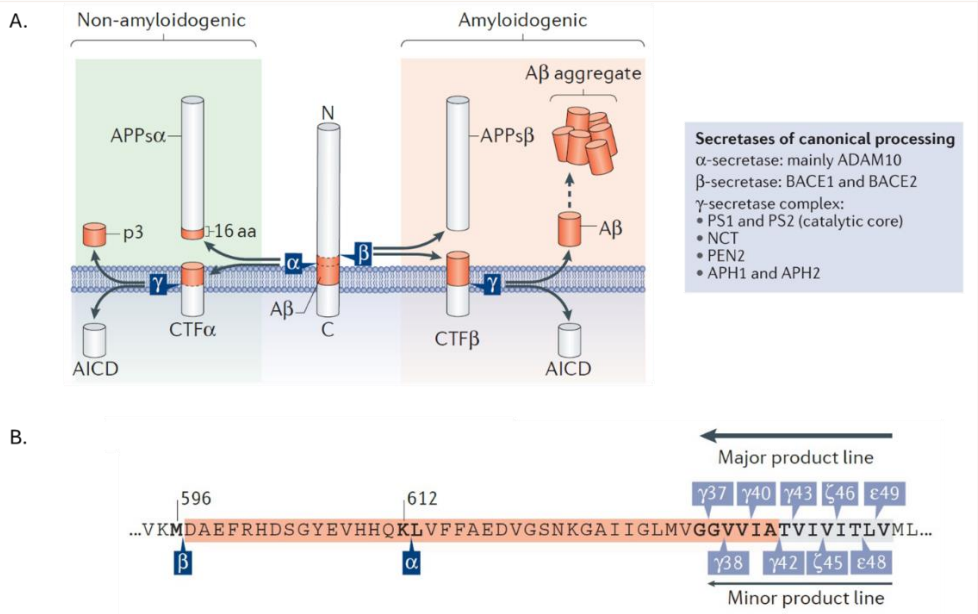

Figure 5. Amyloid Precursor Protein processing. Adapted from Müller et al. 2024 Nature. **A.** Illustration of the APP two mains processing pathways, the non-amyloidogenic and the amyloidogenic, leading to Aβ monomer formation. Detail regarding subunits or the secretases can be found in the right blue square. **B.** Aβ sequence, the cleavage sites of the different secretases are indicated in blue.

The γ-secretase is composed of different subunits, the presenilin 1 or 2, the catalytic core of the enzymatic complex, and three different membrane proteins, nicastrin [34], Aph-1 and Aph-2 , and Pen-2 [35]. The cleavage of CTFα will result in the liberation of AICD and the p3 fragment which may play a trophic function in neurons, but could also aggregate as amyloid-β based on recent findings suggesting its presence in senile plaques of post-mortem AD patients [36], and its capacity of oligomerization and fibrillation in in vitro conditions [37]. On the other hand, cleavage of CTFβ will produce different isoforms of amyloid peptide, initiating with an endoproteolytic cut at the ε-site (resulting in

the liberation of AICD) and proceeding through consecutive exoproteolytic cuts towards the N-terminus [38], allowing the production of Aβ isoforms, with two mains ones: Aβ40 and Aβ42.

3.1.3. The amyloid-β peptide

Aβ peptide is a 4kDa fragment of APP and it has been identified as the key component of amyloid plaques. The γ-secretase complex will cleave the C99 to produce a 37 to 49 amino acid residue peptide. Under physiological conditions, Aβ40 is the main isoform produced, while in AD, due to several factors, the production is shifted to Aβ42. Aβ monomers produced will aggregate into various types of assemblies, from Aβ oligomers to protofibrils, amyloid fibrils and amyloid plaques. Studies with NMR-models (Nuclear Magnetic resonance) allowed to elucidate the structure of Aβ peptide, with different conformation states in Aβ40 and Aβ42. In Aβ40, the primary structure is α-helical from amino acids 15 to 36. In contrast, the C-terminus of Aβ42 is more hydrophobic than that of Aβ40, which induces a shift from an α-helical to a β-sheet structure. This transition is crucial for peptide aggregation. Aβ42 adopts a double-horseshoe-shaped cross-β sheet structure with maximally buried hydrophobic side chains and a β-strand conformation, making it more neurotoxic and more likely to oligomerize into fibrils.

3.1.4. Aβ oligomers and mechanism of toxicity

Amyloid fibrils are large, insoluble structures that aggregate into amyloid plaques, which are histological markers of Alzheimer's disease. In contrast, Aβ oligomers are soluble and can spread throughout the

brain, as Aβ monomers. The size distribution of Aβ oligomers is heterogeneous. It is widely admitted that under relatively physiological conditions in vitro, a soluble high-molecular-weight species of approximately 100–200 kDa predominantly accumulates. Aβ monomers can form a range of higher-order assemblies, from low-molecular-weight oligomers such as dimers, trimers, tetramers, and pentamers, to midrange molecular weight oligomers like hexamers, nonamers, and dodecamers, and ultimately protofibrils and fibrils [39].

Aβ oligomers play an important role in amyloid-induced cytotoxicity, possibly more than plaques themselves. The binding of Aβ oligomers to various receptors has been proposed as a cause for neuronal toxicity.

- Aβ oligomers interact with N-methyl-D-aspartic acid receptor (NMDAR) and α subunit containing nicotinic acetylcholine receptor (α7nAChR), both of which are ion channel receptors at postsynaptic terminals [40]. By directly or indirectly binding to NMDAR, Aβ oligomers can induce dysregulation of calcium balance, leading to neuronal death and synaptic dysfunction. The α7nAChR receptor has a high binding affinity to Aβ, and in vitro studies have shown higher toxicity in cells expressing α7nAChR [41]. It also has been proven that this receptor can mediate Aβ-tau induced phosphorylation by affecting the ERK and JNK pathways [42].
- The Aβ-binding p75 neurotrophin receptor (p75NRT) can also bind Aβ oligomers in human neuroblastoma cells in vitro

cultures, activating their intracellular signaling to induce apoptosis. By activating caspases 3 and 8, these cells produce reactive oxygen species and experience oxidative stress [43], leading to neuronal death.

- The low-density lipoprotein receptor-related protein (LRP), also known as apolipoprotein E receptor (APOER), may play a crucial role in AD pathogenesis. Its roles in the brain are multiple: expressed in the BBB, LRP1 receptors export Aβ in the blood. Deficiency in LRP has been reported in AD cases, decreasing Aβ efflux and favorizing accumulation in brain parenchyma.
- It has been proven that Aβ oligomers also express high binding affinity to two immune globin receptors, FccRIIb and PirB [44]. This interaction may play neuropathic roles similar to p75NRT signaling.

Others studies suggest that specifics oligomers as hexamers of Aβ are stable and play a nucleation role, promoting fibrils formation and elongation by recruiting soluble Aβ monomers [45].

3.1.5. Mechanisms of Aβ clearance and degradation

Aβ peptide accumulation is physiologically counterbalanced by different mechanisms, including proteolytic degradation, cell-mediated clearance, active transport through the blood-brain barrier and deposition into insoluble aggregates.

The principal Aβ peptidase is neprilysin (NEP). This type 2 membrane glycoprotein is located in the intraluminal/extracellular space of

neurons where Aβ monomers are normally secreted. The Aβ proteolysis function of NEP was discovered in APP transgenic mice overexpressing NEP, where amyloid aggregation was undetectable [46]. Cathepsin D, an aspartyl protease found in lysosomes and endosomes, has been identified as a key enzyme responsible for degrading Aβ in brain homogenates. Its expression level in the brain was found to be altered in AD. Several other enzymes are studied as endothelin covering enzymes 1 and 2, matrix metalloproteases MMP2 and MMP9, and insulin-degrading enzyme, showing all to degrade Aβ monomers *in vitro*, moreover there is lack of evidence in human and further studies are needed.

In addition to degradation processes, Aβ is transported through the BBB, from the brain to the blood, and on the opposite from the blood to the brain (see Figure 6). The BBB is formed by endothelial cells attached by tight junctions, closely surrounded by pericytes and enclosed by the basement membrane, with all around astrocytic endfeet surrounding the endothelial cells and providing biochemical support. Aβ can bind to several chaperones, such as apoE, which will help transport and clearance of Aβ. The exchanges of soluble Aβ at the BBB regulate amyloid quantity in the brain and thus influence the oligomerization rate of Aβ. Amyloid deposition in the brain is sus critically influenced by this efflux mechanism. This transport has been reported to be regulated by two main receptors, the RAGE receptor [47] and the low-density lipoprotein receptor-related protein 1 (LRP1) [48].

- LRP1 is a signaling receptor and multifunctional scavenger, member of the LDL receptor family. LRP1 is responsible for the efflux of soluble Aβ to the blood plasma. LRP1 is ubiquitously expressed by the cells, but highly concentrated in the brain. As a major endothelial surface receptor, LRP1 binds Aβ monomers at the abluminal side of the endothelial cells and assist the transcytosis of amyloid through the cell to release soluble Aβ and soluble-LRP1 (sLRP1) to the luminal side in blood [49]. sLRP1 can bind plasma Aβ [50] helping the systematic clearance of amyloid. LRP1 expression in brain capillary endothelium is reduced in AD. This down regulation will reduce Aβ clearance and promote brain focal accumulations.
- RAGE is a multiligand receptor in the immunoglobulin family, binding multiple ligands, including Aβ. RAGE is mainly expressed on the luminal surface of brain vessels [47]. RAGE mediates a continuous influx of circulating Aβ into the central nervous system (CNS). In the AD brain, RAGE expression was shown to be increased in cerebral vessels. The interaction between RAGE and Aβ contributes to the development of Alzheimer's neurovascular disorder by facilitating the transcytosis of circulating Aβ across the blood-brain barrier and triggering inflammatory responses in the endothelium.
- The clearance of Aβ may also rely on the entry of some anti-Aβ antibodies (IgG) into the brain. IgGs with a pK close to 7.4 are transported into the brain from the cerebral circulation through a

saturable mechanism across the BBB. Additionally, they can enter the brain by passive diffusion at sites where the BBB is deficient. Once in the brain, anti-Aβ antibodies can disrupt the formation of Aβ aggregates and solubilize Aβ deposits. The anti-Aβ antibody/Aβ immune complexes can be cleared by Fc-dependent activation of microglia, followed by phagocytosis of Aβ deposits, and by Fc-independent mechanisms. Furthermore, anti-Aβ antibody/Aβ immune complexes are rapidly transported across the BBB via the neonatal Fc receptor for IgG (FcRn) present in the adult brain endothelium [51]. Although the mechanism of FcRn-dependent transcytosis of IgG is unclear, it is suggested that FcRn mediates Aβ transcytosis across the BBB after anti-Aβ antibody/Aβ immune complexes are internalized at the abluminal surface of the brain endothelium.

Aβ can also cross the BBB through exosomes, which are small extracellular vesicles involved in intercellular communication. Exosomes can encapsulate Aβ peptides and facilitate their transport across the BBB, contributing to the spread of amyloid pathology in Alzheimer's disease. These vesicles originate from multivesicular bodies within cells and are released into the extracellular environment, where they can be taken up by other cells. This vesicular transport mechanism allows exosomes to bypass the restrictive nature of the BBB. Research has shown that exosomes containing Aβ can cross the BBB, promoting the dissemination of Aβ plaques. Exosomes from Alzheimer's patients

contain toxic Aβ oligomers are capable of crossing the BBB, leading to neuronal uptake and further propagation of amyloid pathology[52].

Microglia represent another clearance mechanism for Aβ, with an LRP1-mediated endocytosis pathway, further degraded in the lysosomal pathway [49]. Astrocytes close to amyloid plaques express LRPs and can internalize Aβ for degradation participating in the amyloid balance in the brain.

These various mechanisms indicate the potential for Aβ to cross the BBB in both directions and subsequently to either populate the brain with Aβ forms from the periphery, or for neural Aβ to leak from the brain and to be detected in blood plasma. Consequently, the detection of amyloid in plasma holds promise as a candidate for the development of diagnostic and monitoring tools for Alzheimer's disease.

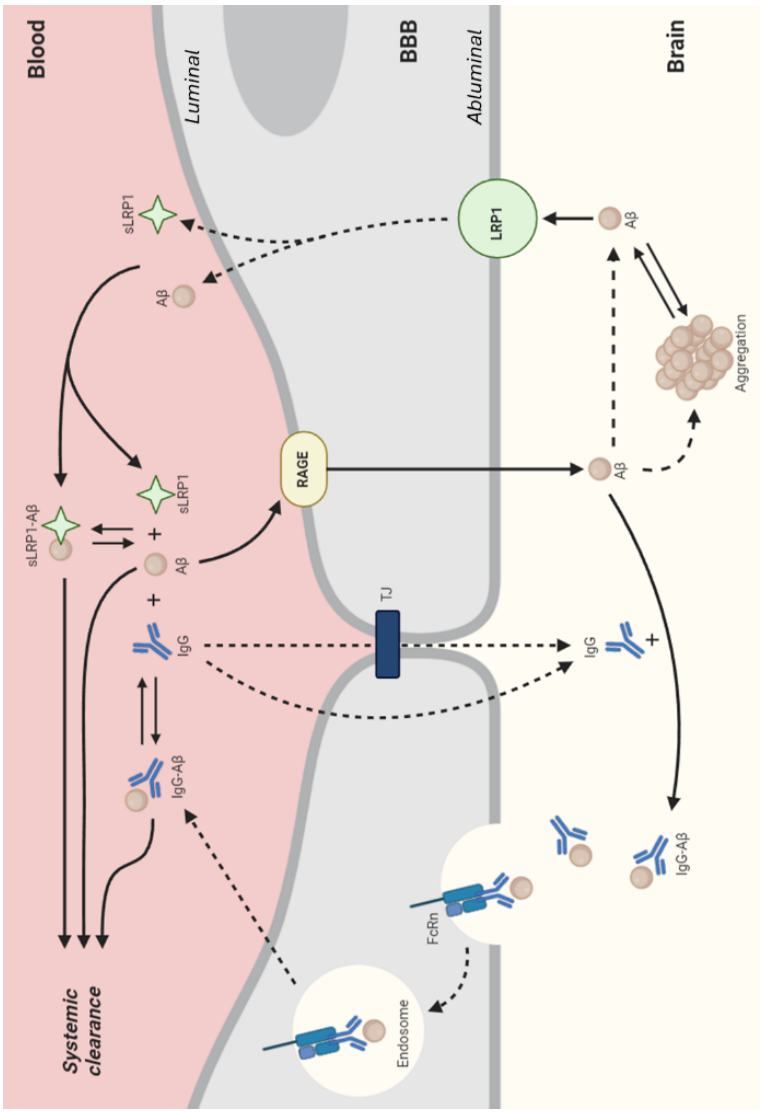

Figure 6. Illustration of the main hypothesis for Ab trafficking mechanisms through the blood brain barrier. Efflux mechanisms to the blood include active transport with LRP1 receptors and classic transcytosis mechanisms mediated by IgG. Influx transport to the CSF is mainly achieve by interaction with RAGE receptor, or by transcytosis.

3.2. Tau protein

3.2.1. Generalities

Tau protein is the second main protein involved in AD pathogenesis and associated tauopathies, whereas amyloid plaques are only found in AD. Tauopathies can be classified into two types: primary tauopathies, were tau pathological lesions are the first to appear an are causal lesion of the disease, and secondary tauopathies, as AD, where the first lesion appearing is different than tau, as Aβ deposits in AD which appears in the disease story before tau protein deposit, but where both of the typical lesions are needed to develop the disease. The primary tauopathies include the fronto-temporal dementia (FTLD), progressive supranuclear palsy (PSP) and corticobasal degeneration (CBD). Tau is a microtubule-binding protein predominantly localized to axons and neurons under physiological conditions. pTau accumulates inside neurons, leading to lesions described as NFTs. In AD, different types of NFTs are present, including pretangles, intracellular tangles, and extraneuronal (or ghost) tangles [53]. Pretangles represent a pre-accumulation state in the neuron, while ghost tangles result from the death of neurons containing NFTs.

3.2.2. Tau protein structure and physiological functions

Tau protein structure

Tau protein is expressed mainly in the CNS in human from a single *MAPT* gene localized on chromosome 17. This protein belongs to the family protein that, upon ordered assembly, forms structured

microtubules in neurons. The *MAPT* gene comprises 16 exons. Six different isoforms, ranging from 352 to 441 amino acids in length, can be expressed from *MAPT* gene. The tau sequence will differ depending on the presence or absence of inserts of 29 or 58 amino acids (encoded by exons 2 and 3) in the N-terminal part, and by the 31 amino acids microtubule-binding repeat (MTBR), encoded by exon 10, in the C-terminal half. The exons 9 to 12 encode these four microtubule-binding repeats. The inclusion of exon 10 will lead to three 4R isoforms, and by exclusion of exon 10 three 3R isoforms. Tau expression is developmentally regulated, such as in adult brain all six isoforms are expressed, whereas in fetal brain only shorter form (0N3R) is expressed. In the brain of healthy adults, there is approximatively equal amounts of 3R and 4R tau isoforms [54]. In AD and FTLD there is an equal ratio 3R:4R, while in other tauopathies the ratio is imbalanced with predominately 4R tau inclusions in PSP and CBD. All isoforms' structures are described in Figure 7.

The tau protein molecule is divided into four primary domains, each characterized by distinct biochemical properties. The N-terminal region (amino acids 1-150) contains two alternatively spliced N-terminal inserts. The MTBR domain is essential for the interaction and stabilization of microtubules within neurons. Despite being intrinsically disordered, tau can fold through intramolecular interactions among its variously charged domains. Interactions between the C-terminal region and the MTBR domain, as well as the N-terminal region, have been described, resulting in a "paperclip" truncated form of tau protein,

thereby maintaining tau in a soluble form within the cytoplasm, limiting oligomerization processus at the soluble level (see Figure 7) [55]. Notably, this association between N and C-terminus parts of tau is reduced upon tau binding to microtubules. When bound to microtubules, the N-terminal region of tau is exposed and extends outward. This specific region is involved in regulating microtubule

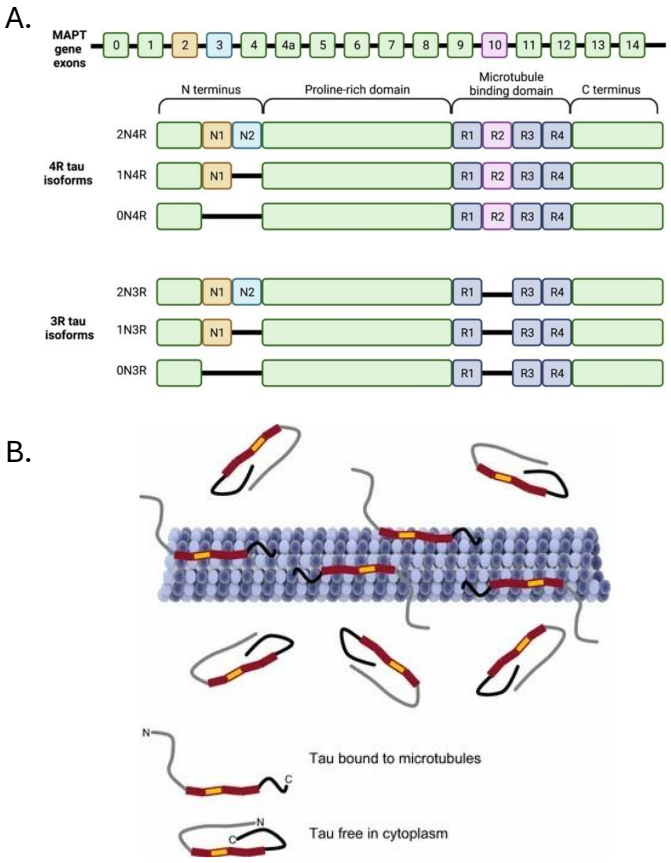

Figure 7. Illustration of MAPT and tau basic structure and conformations. A. Simplified sequence of tau protein isoforms. In AD, tau 3R and 4R isoforms are present. **B**. Structural implication of tau's capacity to bind to microtubule. When the conformation shifts to a "clipped form" due to post-translational modification (phosphorylation, ubiquitination), tau protein cannot bind to microtubule and is released in the neuron cytoplasm.

dynamics, influencing the attachment or spacing between microtubules and other cellular components. It has also been implicated in a signaling cascade that inhibits axonal transport in neurons.

The proline-rich domain is associated with the regulation of microtubule assembly and actin binding [56], highlighting the significance of this region in neuronal cell signaling, nuclear function, and the maintenance of the neuronal cytoskeleton. The MTBR domain also interacts with other proteins, including actin, α-synuclein, apolipoprotein E, and presenilin 1. These interactions highlight the potential critical functions of tau in maintaining healthy synapses and could be particularly important during development and in tauopathies, especially since these associations may be disrupted by increased tau phosphorylation.

Post-translational modifications of tau

There is a range of post-translational modifications that can occur in tau protein, including phosphorylation, isomerization, glycation, nitration, addition of β-linked N-acetylglucosamide, acetylation, oxidation, polyamination and ubiquitination [57].

Tau phosphorylation is the most commonly described post-translational modification of tau. There are 85 phosphorylation sites within the tau sequence, comprising 45 serine, 35 threonine, and 5 tyrosine residues. Phosphorylation significantly impacts tau's physiological functions. For instance, phosphorylation at Ser262, Ser293, Ser324, and Ser356 reduces tau's binding affinity to

microtubules [54]. Most phosphorylation events result in the detachment of tau from microtubules, thereby diminishing microtubule stability. Detached tau can then undergo self-aggregation, forming oligomers and higher-order aggregates, which lead to the formation of neurofibrillary tangles within neurons. Phosphorylation events could lead to destabilization of the “paperclip” confirmation of soluble tau, resulting in the formation of tau oligomers despite mechanisms of oligomerization being still elusive [58]. Phosphorylation events cause tau to be mislocalized from axons to somatodendritic compartments, thereby compromising axonal integrity and leading to synaptic dysfunction [59]. Moreover, there is evidence suggesting that increased tau phosphorylation induces neurodegeneration through mechanisms other than microtubule destabilization or the accumulation of toxic oligomeric/aggregated tau species in the cytoplasm. Phosphorylation events can also interfere with tau's intracellular degradation pathway, shielding tau from proteasomal degradation. Additionally, tau phosphorylation disrupts various signaling pathways by diminishing its interactions with the cytoplasmic membrane and DNA. Hyperphosphorylation of tau protein is a hallmark of tauopathies, including Alzheimer's disease (AD). Each year, new specific phosphorylation sites are identified that are unique to particular tauopathies, underscoring the potential use of phosphorylated tau species as biomarkers for these diseases. Tau phosphorylation at threonine 181 and 217 in the cerebrospinal fluid or plasma have shown

their potential as a biomarker for predicting the extent of dementia [60, 61].

Tau acetylation is mediated by the cAMP-response element binding protein (CREB)-binding protein CBP) in neurons. Tau also has an intrinsic acetyltransferase activity, which catalyzes auto-acetylation (mediated by cys291 and cys322 residues). Several studies have study the impact and role of acetylation of tau, suggesting that auto-acetylation processes of tau facilitate the fragmentation of tau and enhances its autophagic degradation [62]. The acetylation of specific residues has also been discovered in non-AD human brains, at lysine residues 259, 290, 321 and 353, located all in the microtubule binding domain. Acetylation on those specific sites prevent phosphorylation events and keep tau stable bind to microtubules. Conversely, acetylation on this lysine residues was shown to be decreased in AD brains. Acetylation could also be a trigger for tau aggregation, since several shared acetylation sites have been discovered in AD, PSP and FTLD brains [63], especially on lysine 280, which is shown to inhibit proteasome-mediated tau degradation, leading to accumulation of highly phosphorylated tau [64].

Ubiquitin is an 76-amino acid protein that can be transferred to lysine residues through three different enzyme cascade steps: ubiquitin activation, conjugation and ligation by E1, E2 and E3 ligase (CHIP) enzymes [65]. A polyubiquitination chain can be formed when another ubiquitin protein is conjugated to any of the seven lysines in the N-

terminal part of the first ubiquitin via its C-terminal GG amino acids. The tau protein contains 44 lysine residues, most of which are located in the proline-rich domain and the MTBR domain. Several of these sites have been studied extensively, with some being detected in human AD brains. To date, Lys-48 branching site is the most common form of tau ubiquitination, hypothesized to promote the formation of insoluble inclusions, and promoting proteasome degradation [66]. Another common branching site is Lys-63, which promotes autophagy. Several studies have shown that ubiquitination in AD occurs after phosphorylation events and promotes tau aggregation [67, 68]. E3 ligase CHIP has been proposed as a ligase of phosphorylated tau. CHIP mediates tau ubiquitination at sites K267, K290, K343 and K353, as well as specific sites on pTau: K257, K259, K274, K281, K321, K375 and K385. CHIP ubiquitinates these sites only after tau protein phosphorylation by glycogen synthase kinase-3β. Despite evidence that ubiquitination is involved in tau pathology, there is no direct evidence of tau ubiquitination causing neurotoxicity. Hyperphosphorylated tau and oligomers are describe as the most neurotoxic forms of tau [69]. Given that tau ubiquitination promotes soluble pTau aggregation into insoluble forms (NFTs), and that NFTs are less neurotoxic than tau oligomers, ubiquitination could likely protect neurons from neurotoxicity [58].

Tau functions in the synapses

As described before, in the axon, the tau protein functions as a cytoskeletal protein involved in microtubule stabilization and axonal transport. However, tau is also present in synapses, where it appears to be involved in neuronal signaling and synaptic plasticity. This conclusion is based on findings that reducing tau expression in vitro in mouse hippocampal neurons results in the loss of synapses [70], suggesting a critical role of tau in maintaining synaptic integrity. Conversely, there is evidence that tau protein, particularly phosphorylated tau, accumulates at both presynaptic and postsynaptic levels in AD brains. The appearance of synaptic tau correlates with the onset of cognitive decline [71], and the presence of phosphorylated tau oligomers in synapses is associated with neuronal injury and dementia. One current hypothesis is that the axonal damage observed in AD pathology may be linked to the loss of presynaptic terminals, leading to a retrograde "dying back effect" on neurons. Several studies have shown that tau interacts with various presynaptic proteins, such as synaptophysin, synapsin 1, synaptotagmin, synaptogyrin-3, syntaxin-1B, α-synuclein, and β-synuclein. Through these interactions, tau has the ability to cluster synaptic vesicles, particularly with synaptogyrin-3, thereby reducing the efficiency of synaptic vesicle release. Consequently, tau protein is a key player in the regulation of synaptic vesicle trafficking [72].

Tau clearance mechanisms

Tau regulation and degradation in the neuron are mainly mediated by the 20S proteasome and the 26S proteasome activity. Degradation by 20S proteasome does not required ubiquitination of tau, while degradation buy 26S proteasome is restricted to ubiquitinated tau on site Lys-48. Ubiquitination on site Lys-63 also promotes tau destruction by autophagosomes in the cell. Neurons can also internalize tau by direct biding to FcγRII/III receptors at the neuron plasma membrane, which might target tau to lysosomes for intracellular degradation.

Tau proteins can also be degraded by microglial cells, which, through phagocytosis process, internalize soluble tau monomers and oligomers for degradation [73]. The illustration of potentials tau clearance main mechanism can be found in Figure 8.

The are also evidence that tau can cross the blood brain barrier through different mechanisms. While specific carriers for tau have not been conclusively identified, analogous mechanisms for other proteins suggest the potential for carrier-mediated transport. Tau protein may bind to specific receptors in the surface of BBB endothelial cells, as LRP1 receptor, to cross the BBB by transcytosis [74]. After binding, the protein-receptor complex is internalized via endocytosis, and vesicles containing tau then traverses the cytoplasm of the endothelial cell to blood plasma exocytosis. One of the main hypotheses for tau crossing BBB direct leaking of tau in blood plasma due to BBB disruptions reported in AD pathology and other various neuropathological

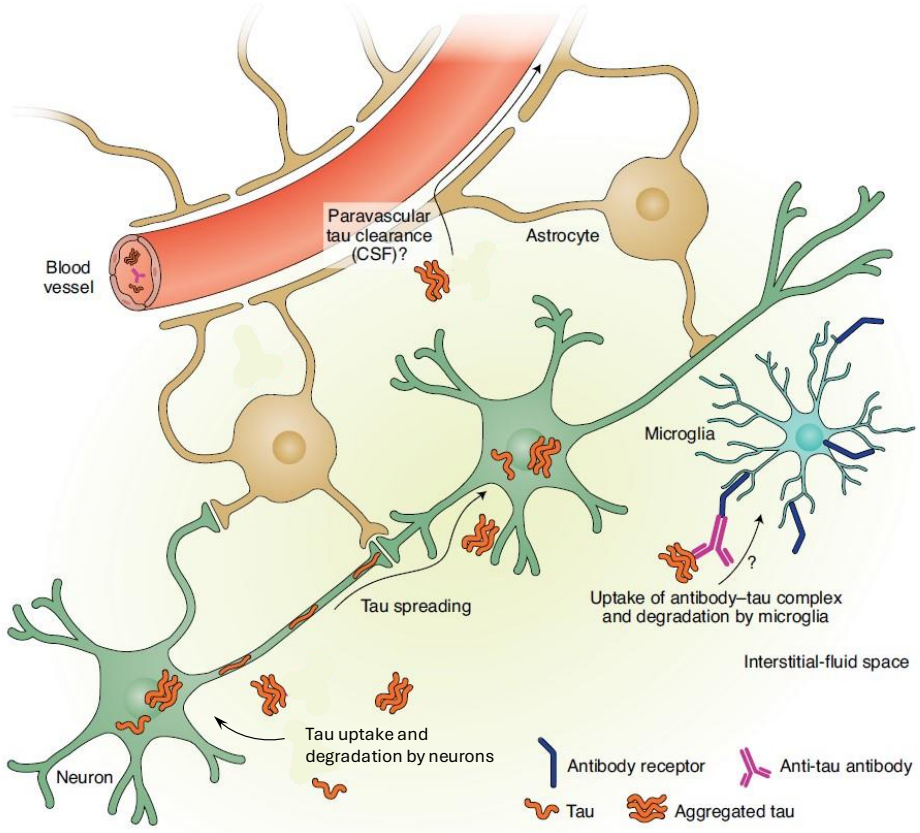

Figure 8. Illustration of potnetials tau clearance mechanisms. Adapted from Galasko, Nature Aging (2021). Once released into the extracellular space, tau could be re-integrated by neurons for degradation by proteasomes and spread also to healthy neurons for disease progression. Microglia could internalize directly of with specific receptors soluble tau for degradation, and the BBB through passive and active transport could clear tau species to the blood stream.

conditions. Inflammatory processes, oxidative stress and neurodegeneration can all contribute to BBB breakdown in AD, facilitating tau spreading into blood plasma [75]. The clearance of tau protein could also be linked to exosome mediated transport. Exosomes are small extracellular vesicles that can encapsulate proteins like tau and facilitate their transport in brain parenchyma, and across the BBB

[52]. Tau proteins can be packaged into exosomes, which can then be taken up by endothelial cells of the BBB through endocytosis or pass through transient openings in the BBB.

Given these multiple potential pathways for tau to cross the BBB and enter the bloodstream, it is likely that tau and pTau levels in blood plasma could reflect the pathological processes occurring in the brain.

3.2.3. Tau toxicity mechanisms

Tau protein and mainly post-translational modified forms of tau are neurotoxic in several ways.

As described previously, the accumulation of pTau in the synapses will interfere with synaptosome trafficking, contributing to synapse loss. Tau phosphorylation process occurring during AD and other tauopathies will also interfere with its connection to the microtubule, destabilizing axon structure, leading to neurodegeneration.

Tau protein has also been described to be implicated in the disruption of the fast axonal transport (FAT) mechanism. Axonal transport occurs along the axonal microtubules and is mediated by two primary families of molecular motors: kinesins and dyneins [76]. Kinesin-1, the most prevalent form within the kinesin superfamily, is responsible for anterograde FAT, whereas dynein, a large multi-subunit motor complex, facilitates retrograde transport along the axon. The regulation of normal FAT involves a complex system of post-transcriptional modifications of the motor complexes and the specific composition of various motor protein subunits [77]. Increased levels of pTau proteins interfere with

kinesins, inhibiting anterograde FAT in in vitro neuronal cultures, underline possible mechanism of neurotoxicity occurring during AD pathogenesis.

3.3. Role of the APOE in AD pathology

The APOE ε4 allele is the strongest genetic risk factor for sporadic Alzheimer's disease (AD), while the APOE ε2 allele provides the most protection. These alleles, located on chromosome 19, code for apolipoprotein E (APOE), a secreted glycoprotein involved in lipid transport. APOE binds cholesterol and phospholipids via its C-terminal domain and interacts with receptors through its N-terminal domain. In the brain, APOE transports lipids in HDL-like particles, while in the blood, it is involved in LDL-like particles. The primary APOE receptors, LRP1 and APOE receptor 2, are also receptors for amyloid-β (Aβ).

Humans have three APOE isoforms (APOE ε2, APOE ε3, and APOE ε4), differing by two amino acid residues and encoded by three distinct alleles. Individuals carry two alleles, either in homozygous or heterozygous form. Post-mortem neuropathological analyses show that APOE ε4 carriers have a higher Aβ plaque burden and more severe cerebral amyloid angiopathy, while APOE ε2 carriers have a lower Aβ plaque burden compared to APOE ε3 homozygotes. APOE ε4 is also linked to more severe tau pathology, as measured by Braak neurofibrillary tangle staging, while APOE ε2 is associated with less severe tau pathology. In the healthy brain, APOE is predominantly expressed and secreted by astrocytes, with lower levels produced by

microglia. In the AD brain, APOE directly interacts with both soluble and insoluble Aβ. APOE ε4 promotes Aβ aggregation into oligomers and fibrils and reduces its clearance from interstitial fluid, which can lead to Aβ plaque deposition.

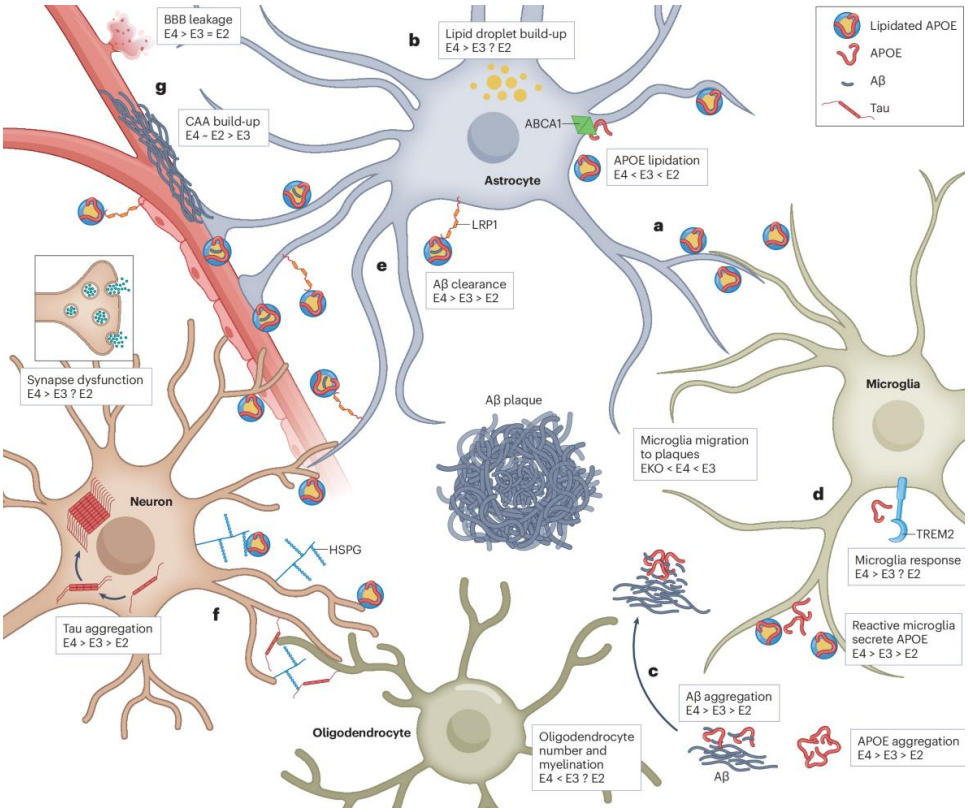

Figure 9. Roles of APOE in Alzheimer's disease pathophysiology. APOE 4 will promote synaptic dysfunction, reduce Aβ clearance, and promote Aβ aggregation. APOE4 also disturbs microglial response and oligodendrocyte number and myelinization process. Microglial activation could promote tau aggregation. Lipid transport in the brain is also disrupt with APOE4 isoform. (Rosemary J. et al. Nature Reviews neurology 2024)

In contrast, the link between APOE and tau pathology is less clear. No direct interaction between APOE and tau (a primarily intraneuronal and axonal protein) has been demonstrated in vivo. However, studies in

transgenic mice expressing the P301S mutant form of tau, either in the absence of APOE or with human APOE isoforms, show that APOE affects tau pathology indirectly. Specifically, APOE ε4 exacerbates tau-induced neurodegeneration and brain atrophy compared to APOE ε3, while APOE ε2 is protective. These effects are mediated indirectly through APOE's influence on microglia, rather than by direct interaction with tau.

3.4. Role of extracellular vesicles in AD pathology

Generalities about extracellular vesicles

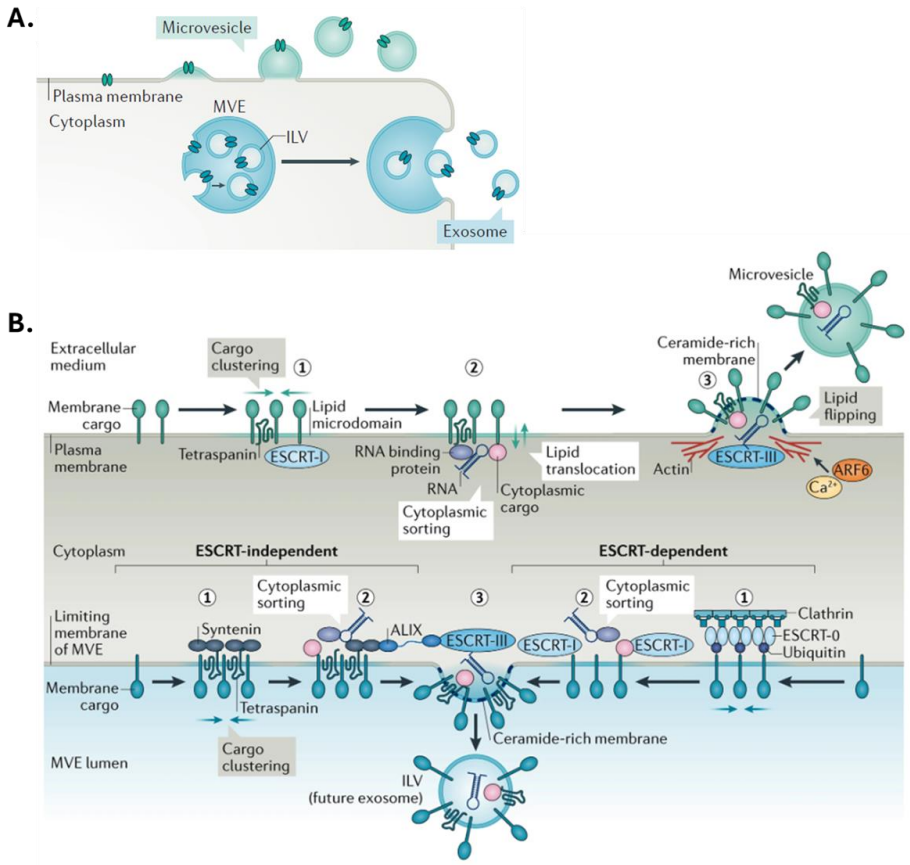

Figure 10. Origin Differences Between Microvesicles and Exosomes. A. Microvesicles are formed by the budding of the plasma membrane, whereas exosomes are formed by the invagination of the membrane of multivesicular endosomes (MVE), creating intraluminal vesicles (ILVs). ILVs are released into the extracellular compartment when the MVE membrane fuses with the plasma membrane, thereby named exosomes. **B.** Lipids and membrane-associated proteins cluster in specific microdomains at the plasma membrane for microvesicles (top) and the limiting membrane of MVE for exosomes (bottom). These microdomains recruit cytosolic proteins and RNA species for sorting into extracellular vesicles. Membrane budding and fission occur at the plasma membrane (microvesicles) or into the MVE lumen (exosomes), with exosomes maintaining the topology of plasma membrane proteins. Exosome biogenesis involves ESCRT proteins, while microvesicle formation includes unique lipid-flipping events. Common machineries include ESCRT components and ceramide generation by sphingomyelinase. (Adapted from Van Niel et al. Nature R.M.C.B 2018).

All cells are capable of generating various types of membrane vesicles, collectively known as extracellular vesicles (EVs). These secreted vesicles can be broadly classified into two main categories: exosomes and microvesicles. Exosomes are membrane vesicles, typically 30-100 nm in diameter, that are primarily formed via the endosomal pathway within cells. During the late endosomal stage, multivesicular endosome (MVE) undergo inward budding of their membranes, leading to the formation of intraluminal vesicles (ILVs) (see Figure 10. A). Exosomes are subsequently secreted upon the fusion of MVE with the plasma membrane [78]. Microvesicles, on the other hand, are generally larger vesicles, ranging from 50-1000 nm in diameter, and originate from the outward budding of the plasma membrane [79]. The biogenesis and secretion of EVs are regulated by various cargo proteins incorporated within their lipid bilayer membranes. For example, in exosome biogenesis, membrane cargoes proteins in the MVE membrane will cluster to form lipidic microdomains, and the activation of the endosomal sorting complex required for transport (ESCRT) machinery in the cytosol will drive membrane shaping and scission to deliver ILVs into MVE (Figure 10. B) [80]. The same mechanism has been reported at the cell membrane level, in the formation of microvesicles. Exosomes can also be formed through an ESCRT independent manner mediated by tetraspanins, mainly CD63, which have been reported to have enriched on exosome surface, associated to sphingolipid ceramide membrane enrichment. Tetraspanins CD81 and CD9 also have been reported to be involved in exosomes biogenesis and sorting in the cell. These

tetraspasnins will form clusters on the membranes with other tetraspanins and with different transmembrane proteins and cytosolic proteins, forming microdomains on the cells and cytosolic compartments membranes. In association, activation of neutral type II sphingomyelinase will hydrolyze sphingomyelin to ceramide, enriching locally membrane in ceramides. All these events will lead to membrane budding and exosomes formation [78, 81].

MVE are primarily targeted for lysosomal fusion within the cell, facilitating the degradation of proteins. However, mechanisms exist that prevent lysosomal fusion, thereby enabling the fusion of MVE with the plasma membrane and the subsequent release of exosomes into the extracellular compartment. Lysosomes are typically characterized as organelles with heterogeneous size and content, enriched in lysosomal membrane proteins (LMPs) and soluble lysosomal hydrolases. LMPs are predominantly expressed in the lysosomal membrane and serve various functions, including acidification of the lysosomal lumen, protein import for the cytosol, and membrane fusion with intracellular vesicles such as MVE [81]. The primary LMPs include lysosome-associated membrane protein 1 (LAMP1, LAMP2), lysosome integral membrane protein 2 (LIMP2) and CD63. The sorting of MVE to lysosome is associated with these LMPs and their ubiquitination, facilitating membrane fusion. This fusion release ILVs into the acidic lumen of lysosomes, where there are degraded [82]. The balance between secretion and degradation of ILVs is supposedly linked to the sorting machinery of MVE.

Amyloid beta and extracellular vesicles

As described above, the processing of APP can occur at the plasma membrane or within endosomal compartments. The β-cleavage of APP primarily occurs in early endosomes, with studies demonstrating colocalization of sAPPβ, APP, BACE-1 (β-secretase), and γ-secretase with early endosomal markers (Rab5) [83, 84]. This indicates that the complete molecular machinery necessary for Aβ production is present at the endosomal level. Furthermore, there is evidence that Aβ42 accumulates in MVE and can be subsequently released into the extracellular space via exosomes. This suggests that APP cleavage within endosomal compartments could be a principal mechanism for the propagation of amyloid lesions. Post-mortem observations of AD brains have shown significant accumulation of Aβ42 within MVE in both presynaptic and, more notably, postsynaptic compartments [83]. This accumulation is associated with abnormal synaptic morphology, indicating that intracellular Aβ42 accumulation is an active process contributing to synaptic loss observed in AD pathogenesis.

ILVs could also bind Aβ peptides through different ways. The cellular prion protein, a glycosylphosphatidylinositol-anchored surface protein is highly expressed in exosomes [85]. By interacting with the N-terminus sequence of Aβ, it can bind Aβ oligomers and accelerate fibrillization of amyloid, reducing the neurotoxic effects of Aβ oligomers and promoting Aβ plaques formation. Tetraspanines (e.g. CD9, CD63, CD8) have also been described to stabilize and regulate the γ-secretase complex in

tetraspanin-enriched microdomains (TEMs). CD9 and CD81 deficient mouse model shown inhibition of the γ-secretase activity and reduced Aβ levels [86], but no direct effect to β-secretase was observed. These TEMs where observed in late endosomal compartments, underling the importance of endocytic pathway to APP cleavage and Aβ production [87].

Tau and extracellular vesicles

Tau protein, particularly in its hyperphosphorylated form, accumulates in neurons during AD pathogenesis. The localization of tau deposition evolves with cognitive decline, affecting different brain regions at various stages, as described by Braak et al. in 2006 [88]. Initially, tau accumulates in the entorhinal cortex (Braak stages I-II), progresses to limbic regions (Braak stages III-IV), and finally spreads to cortical areas (Braak stages V-VI). Although not fully understood, there is increasing evidence suggesting that tau propagates through the brain in a prion-like manner, with exosome-mediated secretion of tau potentially playing a crucial role in this process. Tau and pTau181 have been detected in exosomes present in the CSF of AD patients, with pTau181 concentrations increasing significantly at Braak stages III, IV, and V. Recent studies have highlighted the potential role of EVs in tau dissemination. When tau-containing EVs, isolated from human AD brains, were injected into the hippocampi of wild-type mice, there was a marked increase in pTau deposition in the hippocampus. In contrast, injection of free tau isolated from the same human AD brains did not

result in pTau development in the mice hippocampus. These findings suggest that EVs exhibit higher transmissibility of tau compared to free tau [89]. Moreover, oligomeric forms of tau have been detected in EVs isolated from human AD brains and CSF, which can induce tau aggregation in cultured cells expressing tau (N2a cells) [90]. This cell-to-cell transfer of tau and oligomeric tau is proposed to be partially mediated by EVs. However, further investigations are necessary to confirm whether this represents a primary or secondary mechanism of tau spread.

Extracellular vesicles and blood brain barrier interface

Extracellular vesicles, characterized by their lipid bilayer membranes, possess the capability to traverse the BBB bidirectionally between the bloodstream and the brain parenchyma. Although there is no direct evidence of EVs crossing the BBB in vivo in humans, multiple in vitro and in vivo studies involving mice and zebrafish suggest the presence of active mechanisms facilitating this bidirectional transport across the BBB. Recently, various transcytosis mechanisms have been identified, which may constitute the primary routes for EVs to cross an intact BBB.

In vitro studies using human brain microvascular endothelial cell monolayers cultured in transwell inserts with human embryonic kidney 293T cells have demonstrated that macropinocytosis is one of the mechanisms involved in EVs trafficking across the BBB. Inhibition of macropinocytosis with specific blockers (cytochalasin D and EIPA)

resulted in a 75% reduction in EV uptake compared to untreated conditions [91]. Additionally, the inhibition of clathrin-dependent endocytosis with chlorpromazine in separate studies showed a 60% decrease in EVs trafficking, highlighting another potential mechanism for EVs crossing [92]. Other mechanisms, such as lipid raft/caveolae-dependent endocytosis, have been reported in the literature, although findings have been less consistent across studies.

Multiple pathways may contribute to the translocation of EVs across the BBB. Importantly, as describe above EVs have been shown to carry amyloid-beta and tau proteins, which are key biomarkers of neurodegenerative diseases such as AD. This suggests that EVs derived from the CNS can be present in blood plasma. Therefore, EVs not only play a crucial role in intercellular communication within the brain but could also serve as potential carriers of pathological proteins across the BBB, providing a possible use of plasmatic EVs derived from the brain as a peripheral biomarker for neurodegenerative disease.

4. Manifestations and diagnosis of AD

AD is characterized by progressive cognitive impairment resulting from the accumulation of amyloid-beta and tau proteins in the brain, leading to neurodegeneration. It is essential to differentiate the staging of AD's biological changes from the severity of its clinical symptoms. Over the past two decades, advancements in techniques for detecting amyloid-beta and tau accumulation have revealed that pathological lesions can appear over decades before the onset of cognitive impairment [93]. Moreover, these pathological lesions do not manifest simultaneously, with amyloid-beta lesions typically preceding tau

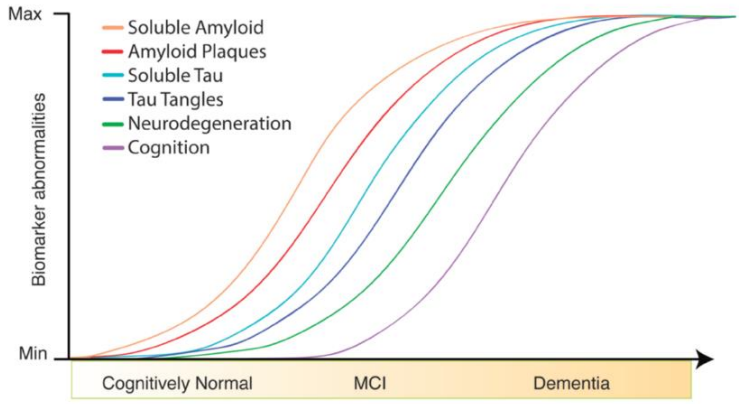

Figure 11. Biomarkers dynamics of AD depending on the cognitive decline. Leuzy et al. 2018. *The sequence of biomarker abnormalities is thought to begin with Aβ (with CSF Aβ1-42 changes appearing before PET), followed by tau (with CSF pTau alterations occurring before PET), and finally neurodegeneration (indicated by changes in CSF t-tau, MRI, and [^{18}F]FDG PET), which eventually leads to cognitive decline.*

pathology [94] (see Figure 11). The first variations are observed in the CSF with pathological changes in soluble amyloid, preceding the deposition of insoluble amyloid (typically detected by PET scans). This is followed

by changes in soluble tau and pTau in the CSF and tau deposition. Most of these variations occur while patients are still cognitively normal. By the time cognitive decline begins (ranging from mild cognitive impairment to later stages of dementia), patients already show signs of neurodegeneration. Consequently, there is a critical need to understand the dynamics between these biomarkers and cognitive decline to effectively incorporate plasma-based biomarker detection into this continuum. This understanding will enhance the ability to diagnose and monitor AD progression more accurately and at earlier stages.

4.1. Alzheimer's disease biological staging

In 2011, the National Institute on Aging and Alzheimer's Association redefined the staging of AD based on biological changes and cognitive decline. Continued scientific progress in biomarker detection necessitated an update to these criteria in 2018 and finally in June 2024 [95]. The biological profiling of AD now relies on the Amyloid-Tau-Neurodegeneration (ATN) framework, which categorizes patients based on the presence of amyloid pathology (A), tau pathology (T), and signs of neurodegeneration (N). Various biomarker profiles within this framework are illustrated in Figure 12.

AT(N) profiles	Biomarker category	
A- T- (N)-	Normal AD biomarkers	
A+ T- (N)-	Alzheimer's pathologic change	Alzheimer's continuum
A+ T+ (N)-	Alzheimer's disease	
A+ T+ (N)+	Alzheimer's disease	
A+ T- (N)+	Alzheimer's disease and concomitant suspected non-Alzheimer's pathologic change	
A- T+ (N)-	Non-AD pathologic change	
A- T- (N)+	Non-AD pathologic change	
A- T+ (N)+	Non-AD pathologic change	

Figure 12. A: Aggregated Aβ or associated pathologic state: CSF Aβ42, or Aβ42/40 ratio, amyloid PET; **T**: aggregated tau (neurofibrillary tangles) or associated pathologic state: CSF pTau, Tau PET; (**N**): neurodegeneration or neuronal injury: anatomic MRI, FDG PET, CSF total tau (NIA guidelines 2018).

Biological staging with CSF biomarkers measurement

Several cerebrospinal fluid (CSF) biomarkers are utilized in clinical settings for AD diagnosis. Amyloid pathology can be detected in the CSF by measuring the levels of soluble Aβ42 or the Aβ42/40 ratio using enzyme immunoassays (ELISA), or improved techniques developed on the same basis. Using the Lumipulse system (a fully automated chemiluminescent enzyme immunoassay, developed by Fujirebio Europe NV, Gent, Belgium), a pathological variation is indicated when CSF Aβ42 levels are [<437 pg/ml] [96]. However, this threshold can vary slightly depending on the detection technique employed by different hospital laboratories. For instance, when measured using the Meso Scale Discovery immunoassay (an electrochemiluminescence

immunoassay, ECLIA), the CSF Aβ42 threshold is [<495.9 pg/ml] and the Aβ42/40 ratio is [<0.09] [97]. The use of Aβ42/40 ratio is considered more sensitive for identifying AD patients compared to Aβ42 alone. Numerous studies have validated the use of CSF Aβ measurements for AD diagnosis, and this biomarker is now widely implemented in routine clinical practice, with careful consideration given to the threshold values used, which vary depending on the quantification technique. Patients with values higher than these thresholds are therefore categorized as A+ (amyloid pathology positive).

In the same idea, total tau and pTau can also be measured in the CSF. Validated thresholds for clinical practice are also available depending on the quantification technique. As an example, when measured by Lumipulse, AD threshold for total tau is [>381 pg/ml] and for pTau181 [>61 pg/ml][96]. Patients with measurements higher than these values are considered as T+ (tau pathology positive).

Biological staging with amyloid PET and tau PET

Before the last decades, it was impossible to visualize tau and Aβ pathology only using histologic dyes or immunohistochemical methods with postmortem tissues. The histological staging of amyloid plaques was established in 2002 by Thal and al. [98], staging Aβ deposits on a scale from I to V (**stage I**. lobes: frontal, parietal, temporal or occipital neocortex); **stage II-III**. in addition to I, entorhinal regions, insular cortex, cingulate gyrus, amygdala and later subcortical regions as the caudate nucleus, putamen, claustrum, thalamus, hypothalamus; and **stage IV-**

V. amyloid deposition extend to brainstem nuclei and cerebellum; see Figure 13. A). The histological deposition timeline of NFTs was established in 2006 by Braak and al. [88], staging NFTs deposits from I to VI (**stage I-II**. deposits in trans entorhinal region and extended to entorhinal region; **stage III-IV**. lesions extended to neocortex of the fusiform, lingual gyri and neocortical association areas; and **stage V-VI**. Lesions extended in frontal, superolateral, occipital regions and the striate area; see Figure 13. B).

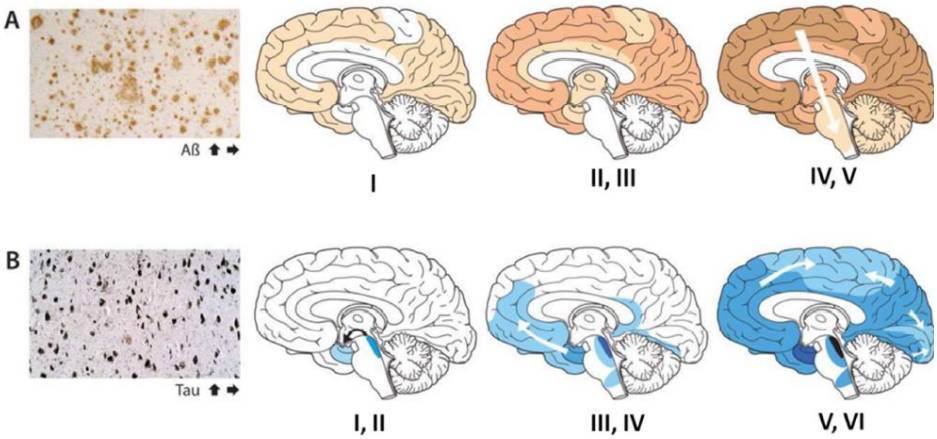

Figure 13. Schematic representation of the spatiotemporal evolution of AD main lesions according to Braak and Thal. A. Amyloid deposits progression; **B.** NFTs deposits progression. Adapted from Jouanne and al. 2017, EJMECH. DOI: 10.1016/j.ejmech.2017.07.070.

Insoluble amyloid plaques can be now detected using advanced brain imaging techniques. Positron emission tomography (PET) with radiotracers specific for amyloid deposits has significantly enhanced the diagnosis of amyloid pathology. This method allows for the visualization of insoluble amyloid deposition in the brain parenchyma,

whereas CSF measurements can only detect soluble forms. The first radiotracer developed for this purpose was ^{11}C-Pittsburgh Compound-B (^{11}C-PIB) in 2004 [99]. Subsequently, ^{18}F-labeled compounds such as ^{18}F-florbetaben, ^{18}F-florbetapir, and ^{18}F-flutemetamol were introduced [100].

All of these radiotracers have demonstrated an increased signal in the brains of AD patients compared to cognitively normal (CN) participants (see Figure 14) [101], specially within the lateral temporal cortex, inferior parietal lobe, dorso-lateral and orbito-medial regions of the prefrontal cortex, posterior cingulate cortex, insula and occipital lobe [102]. The quantification of the amyloid PET signal is expressed on the centiloid scale, a common quantitative output for beta-amyloid imaging that facilitates data comparison across sites using different radiotracers. For example, recent work by Hanseeuw et al. in 2020 at the Cliniques Universitaires Saint-Luc (Brussels, Belgium) established a threshold of centiloid 26 (≥26 considered positive) to predict long-term progression to dementia in patients with memory complaints [103].

Despite the efficacy of amyloid PET in identifying AD patients, the brain areas where amyloid deposition is detected show poor correlation with clinical symptoms and brain atrophy observed via MRI. Amyloid deposition often precedes the onset of cognitive symptoms by many years, making it a valuable early marker for Alzheimer's disease. However, this early presence of amyloid does not always correspond with the severity or presence of clinical symptoms, which complicates

its use as a sole diagnostic tool. Furthermore, brain atrophy observed through MRI, particularly in regions such as the hippocampus, is more directly correlated with cognitive decline and disease progression.

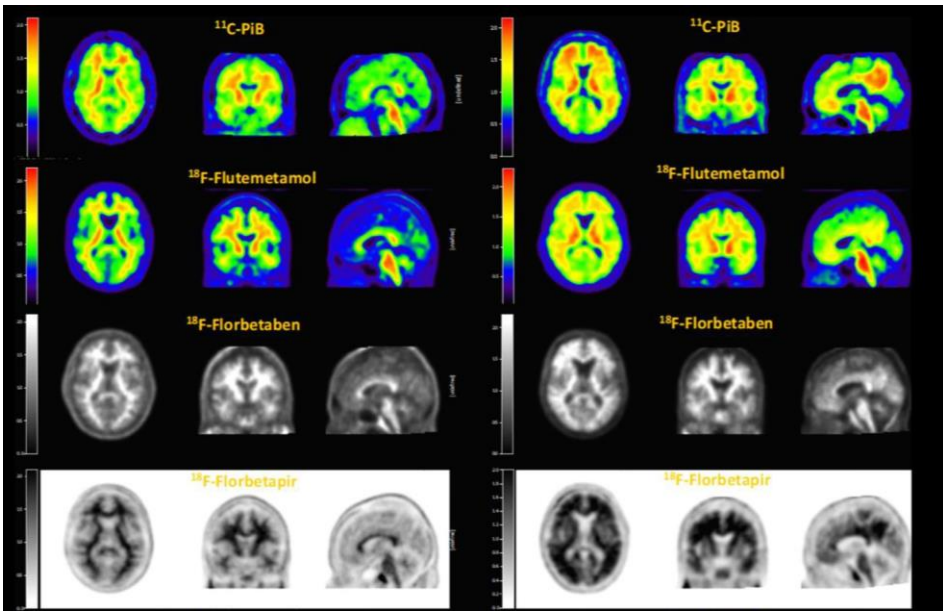

Figure 14. The images depict PET scans from different patients using the five most commonly utilized amyloid tracers. The left column displays Aβ-negative subjects (all approximately 0 Centiloid), while the right column features Aβ-positive subjects (all approximately 50 Centiloid).

The first FDA-approved radiotracer for amyloid PET diagnosis was 18F-florbetapir in 2012. This approval was soon followed by the approval of other radiotracers such as 11C-PIB and 18F-flutemetamol, broadening the tools available for clinicians to detect amyloid plaques. Amyloid PET is currently utilized by numerous clinical centers equipped with PET imaging facilities. Despite its advantages, the technique remains expensive and is not easily accessible to all patients and

hospitals, posing a significant barrier to widespread use. The high cost and limited availability restrict the use of amyloid PET primarily to research settings and specialized clinical centers [104].

Before the last decade, it was impossible to visualize tau pathology only using histologic dyes or immunohistochemical methods with postmortem tissues. Insoluble tau (NFTs) can also be now detected using PET imaging, but remains in the research field, with no radiotracer approved for clinical practice. At the contrary to amyloid pathology, which is mainly present in AD patients, tau brain deposition is a common shared feature with other tauopathies (FTLD, PSP, CBD and LBD). The spatial distribution of tau deposition is strongly associated with the clinical phenotype of tauopathies and is different for each of them. The in vivo visualization of such deposits would be useful for both differential diagnosis, disease severity and evaluation of tau spreading through brain areas for clinical staging. The first PET ligand detecting NFTs was the 18F-FDDNP (floroethyl(methyl)amino-2-naphthyl)ethylidene) back in 2002 [105], but it was also detecting at the same time Aβ deposits, remaining unspecific for differential diagnosis of tauopathies, or staging the disease. Over the years other markers where developed, derived from quinolone compound (18F-THK-523, 18F-THK-5105 and 18F-THK-5117 [106]) which were found specific for NFTs, without concomitant Aβ signal, but studies revealed high white matter retention which severely confounded quantification of gray matter signal, limiting the clinical use of such components [107]. Next generation tau tracers were developed with higher specificity for tau AD lesions, with low nonspecific binding.

For example, the 18F-MK-6240 (see Figure 15) is one of these next-gen tau radiotracers, showing good ability to detect tau accumulation in asymptomatic and symptomatic AD, following Braak stages [108]. Despite promising results, these next-gen tracers need further investigation before clinical use.

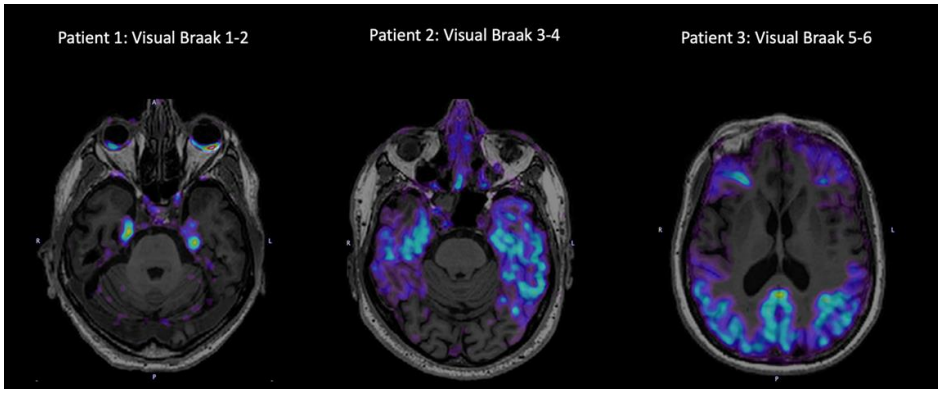

Figure 15. Images of ^{18}F-MK-6240 PET signals in AD patients. Patient 1 presented only visual deposition of radiotracer in the entorhinal region, patient 2 presented extended signal to fusiform and neocortical association areas, and patient 3 signals in most of the brain, especially in the occipital and frontal areas.

The 2024 revision of clinical criteria for AD diagnosis [95] recommends excluding neurodegeneration signs (N) from the biological staging of AD pathology. The classical imaging technique for visualizing neurodegeneration is MRI, which allows for the identification of cortical atrophy in the brain. However, as previously described, signs of brain atrophy appear only in the late stages of the disease and are not specific to AD. This limitation reduces the utility of MRI as an early diagnostic tool.

4.2. Alzheimer's disease clinical staging

Cognitive impairment is the core symptom of AD and can be classified into different stages based on the degree of cognitive decline and the impact on daily functioning. AD is considered a continuum (see

Figure 16), beginning with the preclinical stage. This stage encompasses asymptomatic individuals who exhibit biomarker evidence suggestive of AD, indicating a risk of progression to AD dementia. It also includes biomarker-positive individuals who demonstrate subtle cognitive decline but do not yet meet the criteria for Mild Cognitive Impairment (MCI) [109].

The preclinical stage is particularly crucial for the development of early biomarkers, as neurodegenerative signs are minimal at this point. Early detection within this window is essential for potential future treatments aimed at preventing the progression of the disease. Early biomarkers can provide insights into the disease process long before significant cognitive impairments manifest, allowing for intervention and potentially altering the disease trajectory.

The subsequent stage is MCI, where AD patients exhibit evidence of cognitive decline compared to previous evaluations. This impairment must affect at least one cognitive domain, such as memory, executive function, or language. The most common sign of MCI, particularly in those who subsequently progress to AD dementia, is impairment in episodic memory, which is the ability to learn and retain new

information. Patients with MCI maintain their independence in functional abilities and are not considered demented [110].

The final stage is dementia due to AD, which is further categorized into three levels: mild, moderate, and severe AD, based on the degree of cognitive and functional loss. At this stage, patients experience progressive loss of independence, deterioration in verbal communication, and significant changes in physical abilities, including walking, sitting, and eventually swallowing.

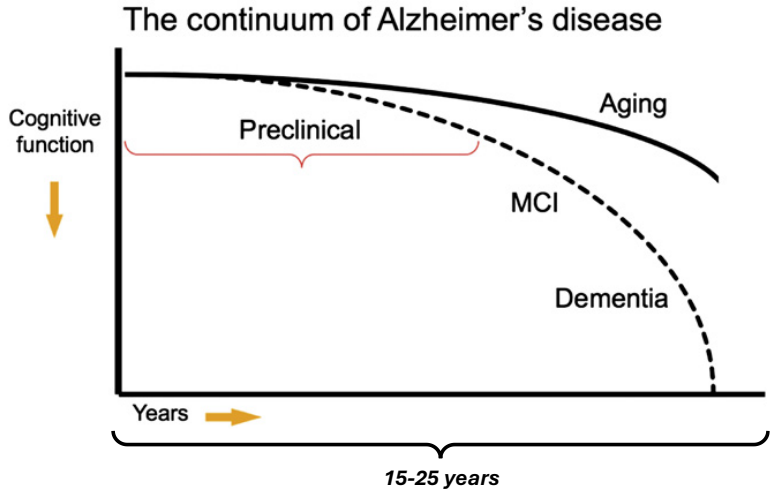

Figure 16. Schematic representation of normal cognitive decline compared to AD patients. Adapted from Sperling et al. 2011. At the preclinical stage (red) the cognitive functions are not impaired in comparison to the general population.

Staging of AD dementia can be performed using various cognitive and dependency assessments. Tests such as the Free and Cued Selective Reminding Test assess both immediate and delayed recall, while the Mini-Mental State Examination (MMSE) and the Montreal Cognitive Assessment (MoCA) are practical tools for evaluating cognitive

impairment during consultations. Using only one test is usually insufficient to diagnose dementia; a combination of different tests evaluating each cognitive domain is needed to characterize the type of impairment, guiding the neurologist's diagnosis toward a specific underlying disease. For example, in frontotemporal dementia, tasks like verbal fluency or the Wisconsin Card Sorting Test are typically impaired, whereas these functions are usually preserved in the classic AD pattern, which instead shows impairments in memory tasks. Scoring each item assessed by the neuropsychologist is crucial for identifying the type of disease, determining the severity at diagnosis, and tracking disease progression over the long term. Follow-up evaluations are often conducted with shorter tests, such as the MMSE or MoCA, with dementia typically indicated by an MMSE score of ≤24 or a MoCA score of <26 [111].

5. The place of plasma biomarkers in AD diagnosis

The lack of easy and accessible diagnostic tools for AD diagnosis has long been a significant challenge. Plasma measurement of AD core biomarkers is emerging as a promising approach for early diagnosis. Compared to CSF collection, blood drawing is a simple and less invasive procedure, making it more feasible for widespread use. This advancement opens up the possibility of implementing AD blood analysis in routine general practice, whereas lumbar puncture remains limited to well-trained physicians in specialized centers.

Historically, the use of blood-based biomarkers for diagnosing neurodegenerative diseases was constrained by the very low concentration of brain-derived proteins in plasma, which are surrounded by high quantities of other circulating proteins. For example, classical AD biomarkers such as Aβ42 and phosphorylated tau are approximately 100 times more concentrated in CSF than in plasma. However, recent advancements in precise quantification techniques have made it possible to measure amyloid and tau in plasma with high accuracy. The Single Molecule Array (Simoa™, Quanterix®) technology, for instance, allows for the measurement of Aβ42 with a lower limit of quantification of 0.142 pg/mL [112]. In clinical practice, AD diagnosis often occurs late in the disease progression (see Figure 17), typically when patients consult a neurologist due to memory complaints, marking the onset of MCI. At this stage, significant neurodegeneration has already occurred, making it too late to prevent the progression of the disease effectively. The development of blood-based biomarkers offers a more accessible and potentially earlier diagnosis of AD, which could

be crucial in initiating interventions before significant neurodegeneration sets in.

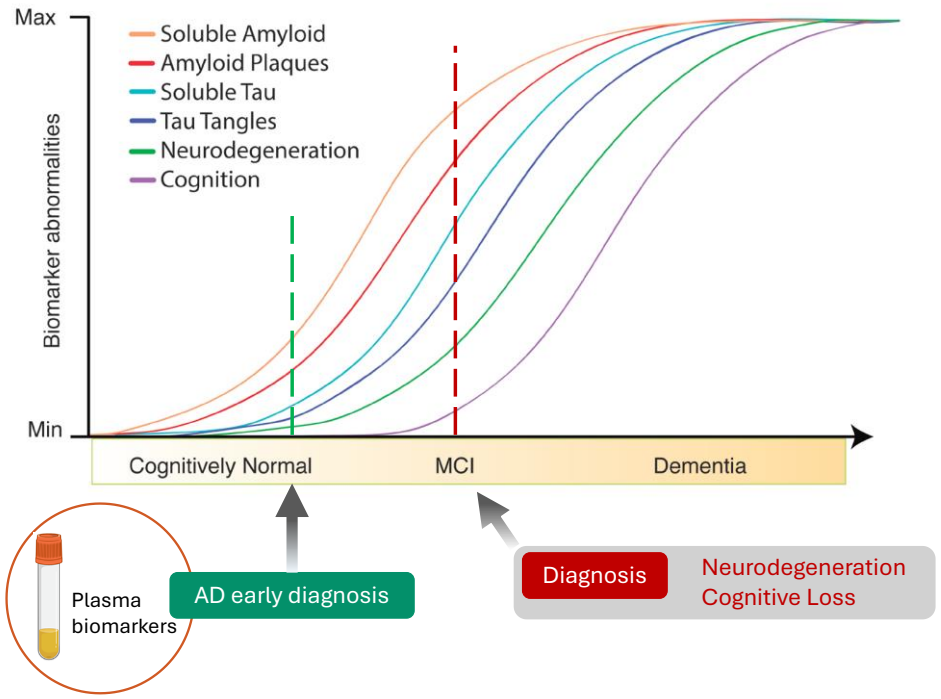

Figure 17. Potential application window of plasma biomarkers in AD biomarkers spectrum. Adapted from Leuzy et al. 2018. The current AD diagnosis occurs when neurodegeneration is already present (red line). The application of non-invasive plasma biomarkers could detect AD pathological modification at a preclinical stage (green line).

PET and CSF biomarkers for the Aβ pathway are already FDA-approved to assist in diagnosing AD and are widely used in clinical research. However, these biomarkers are not routinely incorporated into the clinical care of most patients presenting with memory and cognitive issues. The use of amyloid PET in routine practice remains limited due to its high cost, lack of insurance coverage, and limited availability. While CSF biomarker tests show high concordance with amyloid PET, their use is similarly restricted because many healthcare providers do not

perform lumbar punctures, and some patients view the procedure as invasive or at risk.

Currently, amyloid PET or CSF biomarker tests are typically reserved for cases where a full diagnostic workup has been completed and only when the results are expected to influence patient management, creating a high threshold for their use and significantly limiting their application. The need for blood-based biomarkers is becoming increasingly urgent, given the large number of cases that will require prompt evaluation and treatment as new therapies emerge.

Many patients with mild cognitive impairment have not been tested for AD pathology, largely due to the assumption that a more definitive diagnosis would not alter their clinical management. However, with the introduction of therapies specifically targeting AD pathophysiology that require confirmation of AD pathology before treatment, the demand for rapid and accurate diagnoses will increase, especially as early intervention becomes critical in preventing disease progression.

Several studies are ongoing to validate the use of plasma-based biomarkers exploring amyloid pathology, tau pathology, but also other biomarkers like neuro-inflammatory markers or neurodegenerative markers. In clinical diagnosis, accuracy, defined as the ability of a test to discriminate between those with and without the disease, is the most important consideration. Diagnostic accuracy can be measured by sensitivity and specificity, overall accuracy, positive and negative predictive values, likelihood ratios, the area under the receiver operating

characteristics curve (AUC), the Youden index, and the diagnostic odds ratio. In most published studies, the commonly reported metrics on blood-based biomarkers in AD are the AUC, sensitivity, and specificity.

The plasma ratio of Aβ42/40 was among the first biomarkers explored in plasma to monitor AD pathology. Initially identified in CSF, the Aβ42/40 ratio has been found to correlate more closely with amyloid pathology than Aβ42 alone. This is attributed to the normalization effect provided by Aβ40, which adjusts for interindividual differences in the production of Aβ peptides in the brain [113]. Similar trends were later observed in plasma. In individuals with amyloid pathology, CSF Aβ42/40 reductions can reach approximately 50%, while plasma Aβ42/40 reductions are more modest, typically only 10%–15%. This reduced effect size in plasma may stem from peripheral production of Aβ unrelated to AD pathology, which dilutes brain-derived Aβ and limits the dynamic range of the measurement. Research has also shown that the Aβ ratio is a more reliable predictor of tau status, as measured by tau PET, than of amyloid status. Although earlier studies employed tau radiotracers such as 18F-THK-523 and 18F-THK-5105, our study uniquely utilizes the radiotracer 18F-MK-6240, which offers novel insights in a population with preclinical amyloid pathology.

Tau, particularly phosphorylated tau isoforms, show greater promise than amyloid for detecting AD pathology in plasma, especially in prodromal stages. Due to challenges in measuring low-abundance

analytes within the complex plasma matrix, consistent data on plasma pTau isoforms have only emerged in recent years, fueling rapid advancements in this field. Similar to findings in CSF, pTau isoform levels rise early in the disease process and increase with AD progression, reflecting worsening neurofibrillary tangle (NFT) pathology as seen on tau PET or in neuropathological assessments [114]. Studies suggest that plasma pTau231 changes may precede those of pTau217 and pTau181, extending observations from CSF [115]. Neuroimaging studies have validated that plasma pTau isoforms reliably predict both brain amyloid PET and tau PET status.

Several assays, such as immunoassays on the Meso Scale Discovery (MSD) and Simoa platforms, have been developed to measure pTau isoforms in blood with analytical sensitivities below the pg/mL range. Additionally, a liquid chromatography–MS/MS approach, similar to that used for plasma Aβ42/40, was introduced in 2020. Comparative studies have shown that Simoa pTau assays have largely consistent clinical and analytical performance, correlating strongly with each other. Notably, pTau isoforms are less abundant than amyloid peptides in plasma, with pTau181 and pTau231 showing comparable levels, while pTau217 is present at lower concentrations. The currently available tests are listed in Table 1.

Manufacturer	Plasma biomarker measured	Assay platform	Assay development and analytical validation	Year of development	Status		In vivo used status
					RUO	CTUA	
C2N/Precivity	Aβ42/40	IP-LC-MS/MS	Kirmess et al.	2021		X	granted Breakthrough Device designation by FDA in 2019
Quanterix	Aβ42/40	Simoa	Song et al.	2016	X		
Araclon/Abtest-Al	Aβ42/40	immunoassay	Pérez-Grijalba et al.	2019		X	
Eli Lilly	pTau181	MSD,Simoa	Bayoumy et al.	2021	X	X	
Quanterix	pTau181	Simoa	Karikari et al. ; Bayoumy et al.	2020			granted Breakthrough Device designation by FDA in 2022
Fujirebio	pTau181	Lumipulse	Janelidze et al.	2023	X		
Eli Lilly	pTau217	MSD, Simoa	Bayoumy et al.	2021	X	X	
Janssen	pTau217	Simoa	Triana-Baltzer et al.	2021	X		
Adx	pTau217	Simoa	Bayoumy et al.	2021	X		

Table 1. Summary of commercially available plasma tests for AD biomarkers measurement. Not all existing tests are listed above, only the most common ones. Abbreviations: RUO = Research Use Only, CTUA = Clinical Trial Use Application.

Ongoing research is crucial to validate plasma biomarkers for AD diagnosis and establish precise diagnostic thresholds. Additionally, fundamental research should focus on identifying novel biomarkers that reflect AD pathophysiology with enhanced sensitivity and specificity. Advances in biomarker discovery hold potential to develop blood-based tests that improve diagnostic accuracy and provide valuable insights into disease progression and treatment responses. Incorporating validated plasma biomarkers into clinical practice could transform AD diagnosis and management, enabling early interventions and potentially altering disease progression.

In this study, the primary advancement lies in the use of the tau-specific radiotracer 18F-MK-6240 within a preclinical population also characterized by amyloid pathology through amyloid PET imaging. While most plasma tests cited above were validated in clinically impaired populations with a known AD diagnosis, it is crucial to assess whether these tests are relevant in preclinical AD participants. This study's innovative approach enables the exploration of plasma biomarkers at a preclinical stage using highly specific PET radiotracers for both amyloid and tau detection. By applying 18F-MK-6240 in a carefully selected population, the study aims to detect in blood plasma amyloid and tau variations in the earliest stages of AD progression, validating their use as prescreening tools. The findings from this study could provide essential insights into the temporal and mechanistic relationship between amyloid and tau pathologies, contributing significantly to our understanding of early AD pathology. By clarifying these early

pathological processes, this research may inform the development of more precise diagnostic approaches, allowing for earlier and more accurate detection of AD. Such advancements could ultimately support the development of targeted therapeutic strategies, improving the potential for early interventions that alter the trajectory of the disease.

OBJECTIVES

Objectives

The development of tools for early diagnosis of AD and the identification of new biomarkers have become central to AD research, particularly following the FDA's approval of anti-amyloid therapies in recent years. The main objectives of this research are: (A) to establish a plasma biobank in the AD field through a collaboration between Cliniques Universitaires Saint-Luc (CUSL) and UCLouvain, (B) to identify accurate biomarkers for early AD diagnosis and establish precise diagnostic thresholds for clinical application, and (C) to discover new biomarkers through fundamental research, focusing on the potential role of EVs in AD and their presence in blood plasma.

Plasma samples have been collected since 2020 at the CUSL Memory Center. This PhD project represents the first project at UCLouvain to create an extensive biobank dedicated to AD research, currently housing over 550 samples from AD patients and cognitively unimpaired volunteers. This plasma biomarker study is cross-sectional and is conducted alongside the study "Tau and Amyloid PET Imaging in Normal Aging, Early Alzheimer's Disease, and Related Syndromes" (UCL-2016-121), also performed at CUSL. This parallel study allows for amyloid and tau PET imaging data to be obtained from up to 140 participants. This specific population is then completely characterized for AD biomarkers and is precious for preclinical AD diagnosis, allowing the identification of preclinical AD patients, which are cognitively unimpaired but with AD biological changes (A+, T+), population at interest for the development of early blood-based AD diagnosis.

Objectives

The primary objective of this study is to quantify AD biomarkers in the plasma samples of our cohorts and identify the most promising candidates for clinical use. The quantification of plasma biomarkers has been facilitated by the recent acquisition of the Single Molecule Array (Simoa™) technology at UCLouvain, this advanced technology enabling precise measurement of low-abundance biomarkers, enhancing the reliability of early AD diagnosis. We measured with high accuracy different AD biomarker: Aβ42, Aβ40, total-tau and pTau 180. We aimed to (i) identify the best to distinguish AD patients from healthy cognitively normal volunteers, (ii) to predict the amyloid status of the participant or the tauopathy presence (evaluated either by CSF measurement or PET-CT imaging), (iii) to establish diagnostic thresholds for the best candidates identified.

The secondary objective of this work was to research new biomarkers for early AD diagnosis. We focused our work on EVs, seeing their implication in AD development and dissemination, we hypothesized their presence in plasma and their potential use as AD biomarkers. We aimed here to (i) rationalize the presence of AD core biomarkers in EVs using in vitro models expressing amyloid and tau, (ii) to isolate neurally derived EVs from the plasma of our participants and see whether their quantity and/or content could be used as an AD biomarker.

PART I

PLASMA BIOMARKERS: SOLUBLE AMYLOID AND TAU

To address the primary objective of our study, we employed Single Molecule Array (SIMOA) technology to analyze plasma samples from our cohort, quantifying the concentrations of Aβ42, Aβ40, total tau, and pTau 181. Among all biomarkers assessed, the Aβ42/40 ratio and pTau 181 alone exhibited the most significant differences between cognitively normal (CN) individuals and patients diagnosed with AD based on cerebrospinal fluid measurements or PET amyloid imaging.

We determined various thresholds for the plasma Aβ42/40 ratio and pTau 181 concentration to optimize the sensitivity and specificity for distinguishing AD patients from CN participants. These thresholds were applied in subsequent post-test calculations to evaluate their potential clinical utility, considering the pre-test probability of brain amyloidosis prevalence at ages 60 and 80 in the CN population. We assessed the effectiveness of using plasma Aβ42/40 ratio and pTau 181 thresholds individually and in combination.

The results pertaining to the Aβ42/40 ratio are detailed in the following published paper, while findings for pTau 181 are discussed in an unpublished manuscript.

Definition of a threshold on the plasma Aβ42/Aβ40 ratio measured by single-molecule array to predict the amyloid status of individuals without dementia

Emilien Boyer[1,2,] †, Lise Colmant[1,2,3,*] †, Thomas Gerard[1,2], Kristel Sleegers[4], Renaud Lhommel[2], Adrian Ivanoiu[1,2], Philippe Lefèvre[1,3], Pascal Kienlen-Campard[1] and Bernard Hanseeuw[1,2,5]*

[1] Institute of Neuroscience, UCLouvain, Brussels, Belgium
[2] Neurology Department, Cliniques Universitaires Saint-Luc, Brussels, Belgium
[3] Institute of Information and Communication Technologies, Electronics and Applied Mathematics, UCLouvain, Louvain-la-Neuve, Belgium
[4] Complex Genetics of Alzheimer's Disease Group, VIB-UAntwerp Center for Molecular Neurology, University of Antwerp, Belgium
[5] WELBIO department, WEL Research Institute, avenue Pasteur, 6, 1300 Wavre, Belgium
* Correspondence: LC: lise.colmant@uclouvain.be; EB: emilien.boyer@uclouvain.be
† These authors contributed equally to this work

Int. J. Mol. Sci. 2024, *25*(2), 1173; https://doi.org/10.3390/ijms25021173

Submission received: 15 December 2023 / Revised: 15 January 2024 / Accepted: 16 January 2024 / Published: 18 January 2024

Abstract: Alzheimer's disease (AD) is characterized by amyloid beta (Aβ) plaques and hyperphosphorylated tau in the brain. Aβ plaques precede cognitive impairments and can be detected through amyloid-positron emission tomography (PET) or in cerebrospinal fluid (CSF). Assessing the plasma Aβ42/Aβ40 ratio seems promising for non-invasive and cost-effective detection of brain Aβ accumulation. This approach involves some challenges, including the accuracy of blood-based biomarker measurements and the establishment of clear, standardized thresholds to categorize the risk of developing brain amyloid pathology. Plasma Aβ42/Aβ40 ratio was measured in 277 volunteers without dementia, 70 AD patients and 18 non-AD patients using single-molecule array. Patients (n=88) and some volunteers (n=66) were subject to evaluation of amyloid status by CSF Aβ quantification or PET analysis. Thresholds of plasma Aβ42/Aβ40 ratio were determined based on a Gaussian mixture model, a decision tree, and the Youden's index. The 0.0472 threshold, the one with the highest sensitivity, was retained for general population without dementia screening, and the 0.0450 threshold was retained for research and clinical trials recruitment, aiming to minimize the need for CSF or PET analyses to identify amyloid-positive individuals. These findings offer a promising step towards a cost-effective method for identifying individuals at risk of developing AD.

Keywords: Alzheimer's disease; plasma amyloid; SIMOA; plasma Aβ42/Aβ40 ratio; amyloid prediction; biomarkers; Alzheimer's disease screening.

1. Introduction

Alzheimer's disease (AD) is the most common cause of dementia [116]. AD is characterized by the abnormal accumulation of amyloid beta (Aβ) peptides in the brain, and the aggregation of hyperphosphorylated tau deposits in neurons, forming neurofibrillary tangles. Aβ peptides are naturally released in the brain by the proteolytic cleavage of the amyloid-β precursor protein (APP) [117]. In AD, there is an imbalance between production and clearance of Aβ which leads to Aβ accumulation in brain parenchyma. Longer isoforms of Aβ (e.g. Aβ42 or Aβ43) have intrinsic nucleation properties [118], leading to the formation of toxic oligomers which can further promote aggregation and fibrillization [119] to eventually form plaques in the brain [120]. The formation of toxic oligomers containing long forms of Aβ (Aβ42 or Aβ43) or fibrils typically containing Aβ42 results in decreased concentrations of soluble monomeric Aβ42 circulating in cerebrospinal fluid (CSF) [121]. The shorter and more abundant soluble Aβ40 form is less prone to aggregation, and its concentration in biofluids is assumed to distinguish high and low β-amyloid producers. The CSF soluble Aβ42/Aβ40 ratio decreases in AD, and the ratio may be more relevant to the diagnosis of AD than soluble Aβ42 or Aβ40 levels alone [122], because it normalizes the soluble Aβ42 concentration to intra-individual Aβ production reflected by soluble Aβ40 concentration.

Positron emission tomography (PET) imaging studies showed that Aβ plaques precede the formation of tau neurofibrillary tangles and

cognitive decline [123]. Individuals with abnormal amyloid deposits and no cognitive impairment can be characterized as having preclinical AD [124]. These clinically normal individuals with abnormal amyloid deposits have a higher risk to develop cognitive decline than individuals without amyloid deposition [125]. Determining amyloid status in clinically normal individuals thus allows identification of a population at risk to develop AD. Amyloid status (positive or negative) is currently determined by measuring Aβ42 in the CSF or by PET-based radiotracers detecting amyloid deposits in the brain parenchyma. However, their widespread use is restricted because they are invasive (CSF sampling) or expensive (PET).

Blood biomarkers including Aβ measurement have attracted growing interest [126]. They have long been inaccessible due to the low concentration of AD biomarkers (e.g. soluble Aβ42) in the blood and technical limitations due to the detection threshold of the tests classically used (enzyme-linked immunosorbent assay, ELISA) to monitor them in the CSF. Indeed, the concentrations of Aβ are 50–100 times lower in the plasma than in the CSF [127]. The recent emergence of novel technologies that allow protein detection in the femtomolar range (typically around or below 1 pg/ml) has sparked clinical interest in blood biomarkers. The low concentrations of plasma Aβ can now be quantified by approaches initially described as single-molecule enzyme-linked assay (or digital ELISA) and now often referred to as single-molecular array (SIMOA) [128, 129]. Single-molecule analysis can be achieved using paramagnetic beads coupled with specific antibodies,

enabling the binding of a single specific target (antigen) to one bead at low concentrations. These beads can then be loaded onto an array to measure the signal of a single antigen/antibody complex in the detection step. This approach has also been developed for multiplex (e.g. Aβ42/Aβ40) assays, allowing the measurement of different biomarkers in the same sample.

Because Aβ deposition in the brain is the earliest pathological signature of AD, measuring the soluble Aβ42/Aβ40 ratio appears promising to detect AD [130], even at preclinical stages. Blood measurement of Aβ has the advantage of being minimally invasive compared to lumbar puncture, and less expensive than PET-imaging. Several studies have already shown that a decrease in the plasma soluble Aβ42/Aβ40 ratio was an indicator of brain amyloidosis [131-134] and could predict cognitive decline [135, 136]. Existing tools include mass spectrometry and SIMOA assays (Quanterix®), with SIMOA being easier to implement in clinical research settings.

Even though accurate measurement of the plasma soluble Aβ42/Aβ40 ratio has been reported as a potential tool for the detection of early AD stages, no cut-off value of this ratio has been clearly established in the literature to define amyloid status (positive or negative). The aim of the present study was to determine a threshold of the plasma soluble Aβ42/Aβ40 ratio measured by SIMOA in order to use this plasmatic measure as a screening tool for amyloid pathology, and to identify individuals at risk to develop AD before dementia. Individuals

with plasma soluble Aβ42/Aβ40 ratios within the normal range would be characterized as free of amyloid pathology, and individuals with abnormal biomarker values would be recommended toward further confirmatory examination, including CSF biomarker assessments or PET imaging. This screening tool also holds promise for potential utilization in forthcoming treatments for AD, such as Lecanemab or Donanemab, both of which have demonstrated improved efficacy in mitigating cognitive decline in patients with prodromal AD or mild AD dementia [137, 138]. The plasma soluble Aβ42/Aβ40 ratio could be used to measure the outcome of these treatments on amyloid pathology.

2. Results

2.1. Participants

We recruited 277 volunteers in Belgium, aged over 50 years and without known cognitive impairment, through local advertisements. All volunteers were without dementia. We also enrolled 88 patients from the Memory Clinic at Saint-Luc University Hospital, all of whom had reported memory complaints during a prior consultation. Patients had been clinically diagnosed with AD (n=70) or non-AD (n=18) neurodegenerative diseases. Demographic characteristics of the participants are presented in Table 1.

AD patients were significantly older than volunteers ($p<0.0001$) and non-AD patients ($p=0.017$). Age was not different between volunteers and non-AD patients. As expected, Mini-Mental State Examination

(MMSE) scores were higher among volunteers than AD ($p<0.0001$) and non-AD patients ($p<0.0001$); MMSE scores were also higher among non-AD patients compared to AD patients ($p=0.0011$). As expected, there were more apolipoprotein E (*APOE)* ε4 carriers among AD patients than volunteers ($p<0.0001$), and among AD than non-AD patients ($p=0.0006$). Indeed, the ε4 allele of the *APOE* gene increases the risk to develop AD [139-141]. The *APOE* ε4 status was not different between non-AD patients and volunteers. The gender repartition was not different between groups. Among AD patients, 23 individuals had dementia; among non-AD patients, 2 individuals had dementia.

Table 1. Demographic characteristics of volunteers and patients. SD: standard deviation

	Volunteers	AD patients	Non-AD patients
n	277	70	18
Age: mean (SD)	66.5 (7.78)	71.1 (8.05)	65.6 (9.55)
MMSE: mean (SD)	28.5 (1.27)	24.1 (4.59)	26.4 (2.12)
APOE: n ε4-/n ε4+ (% ε4-/% ε4+)*	192/83 (70%/30%)	21/40 (34%/66%)	14/2 (87.5%/12.5%)
Gender: male/female	98/179	32/38	7/11

**APOE*: 2 missing among volunteers, 9 missing among AD patients, 2 missing among non-AD patients; ε4- = ε4 noncarriers, ε4+ = ε4 carriers.

2.2. Amyloid status

2.2.1 Amyloid status of all individuals

The cohort of 88 patients, along with a subset of volunteers (n=73), underwent CSF analysis or an amyloid PET scan for validation of their amyloid status. The final analysis included only individuals with a maximum time delay of 2 years between the blood test and CSF/PET amyloid status measurement, unless the CSF/PET amyloid measurement was done before the blood test and gave an amyloid positive result. The final sample comprised 66 volunteers, 69 AD patients, and 16 non-AD patients.

Amyloid PET or CSF analysis classified 74 participants as amyloid positive (Aβ+) and 77 participants as amyloid negative (Aβ-) (Table 2). Aβ+ individuals were significantly older than Aβ- individuals ($p=0.03$). Gender repartition did not differ between these two groups. As expected, MMSE scores were significantly lower for Aβ+ participants than Aβ- ($p<0.0001$), and there were more ε4 carriers among Aβ+ participants than Aβ- ($p<0.0001$). Table 2 also shows the clinical diagnosis of participants (volunteers, AD, or non-AD patients), and the way that amyloid was measured (CSF, [^{18}F]flutemetamol PET, or [^{11}C]Pittsburg Compound B ([11C]PIB) PET).

Table 2. Characteristics of all participants with confirmed amyloid status through CSF/PET analysis, and of participants without dementia with confirmed amyloid status. SD: standard deviation.

	All participants		Non-demented participants	
	CSF/PET Aβ+	**CSF/PET Aβ-**	**CSF/PET Aβ+**	**CSF/PET Aβ-**
n	74	77	53	73
Age: mean (SD)	70.8 (8.11)	67.8 (8.67)	70.9 (7.32)	67.5 (8.63)
MMSE: mean (SD)	24.6 (4.57)	27.8 (2.15)	27.06 (1.62)	28.15 (1.54)
APOE: n ε4- / n ε4+*	20/47	49/23	15/36	48/21
(% ε4-/% ε4+)	(30%/70%)	(68%/32%)	(30%/70%)	(70%/30%)
Gender: male/female	33/41	35/42	24/29	32/41
Non-demented/demented	53/21	73/4	–	–
Volunteers	13	53	13	53
AD patients	60	9	39	7
Non-AD patients	1	15	1	13
Measure of amyloid:				
CSF	54	24	37	21
[18F]flutemetamol PET	17	51	15	51
[11C]PIB PET	3	2	1	1

**APOE*: All participants: 7 *APOE* missing among Aβ+, 5 *APOE* missing among Aβ-; Without demented patients: 2 *APOE* missing among Aβ+, 4 *APOE* missing among Aβ-. ε4- = ε4 noncarriers, ε4+ = ε4 carriers.

2.2.2 Amyloid status of individuals without dementia

As we focused on the evaluation of the amyloid status of individuals without dementia, the sensitivity and specificity of tests were evaluated on this subgroup of individuals. The characteristics of Aβ+ and Aβ- individuals without dementia are described in Table 2.

Aβ+ individuals without dementia were significantly older than Aβ- ($p=0.017$). Gender repartition did not differ between two groups. As expected, MMSE scores were significantly lower for Aβ+ participants than Aβ- ($p=0.0002$) and there were more ε4 carriers among Aβ+ participants than Aβ- ($p<0.0001$). Table 2 also shows the clinical diagnosis of participants (volunteers, AD, or non-AD patients), and the way that amyloid was measured (CSF, [18F]flutemetamol PET, or [11C]PiB PET).

2.2.3 Distribution of the plasma Aβ42/Aβ40 ratio

The distribution of the plasma soluble Aβ42/Aβ40 ratio was represented for the different populations (Fig. 1). By considering all individuals (volunteers, AD, and non-AD patients), the plasma Aβ42/Aβ40 ratio was lower for volunteers than AD patients ($p<0.0001$), and lower for AD than non-AD patients ($p=0.033$) (Fig. 1A). To determine the sensitivity and specificity of the plasmatic test for different thresholds, only individuals with a known CSF/PET amyloid status were considered (Fig. 1B). The plasma Aβ42/Aβ40 ratio was lower for Aβ+ than Aβ- individuals ($p<0.0001$). Finally, we restricted the analysis to

individuals without dementia (Fig. 1C). The plasma Aβ42/Aβ40 ratio stayed lower for Aβ+ than Aβ- individuals without dementia (p=0.0002).

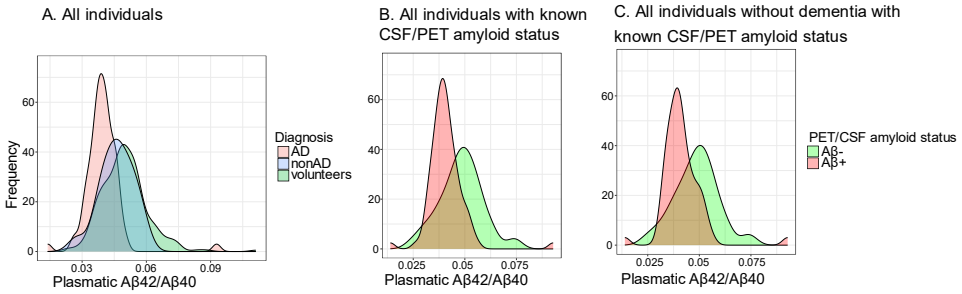

Figure 1. A. Distribution of the plasma soluble Aβ42/Aβ40 ratio among all participants based on their clinical status; **B.** among all participants with known amyloid status; and **C.** among participants without dementia and with known amyloid status.

2.3 Determination of the thresholds

The threshold for plasma soluble Aβ42/Aβ40 ratio, to classify individuals as plasmatic Aβ+ or Aβ-, was determined using three methods: an unsupervised learning method (Gaussian mixture model, GMM), a supervised learning method (decision tree), and the Youden's index calculated on the Receiver Operating Characteristic (ROC) curve. The unsupervised method was applied to all participants, including those with no amyloid measure done using CSF or PET. The supervised method included only participants with a known amyloid status using CSF or PET. The ROC curve was estimated on individuals with a known amyloid status and without dementia.

2.3.1 GMM-based classification of plasma Aβ

All participants (volunteers, AD, and non-AD patients) were included in the GMM analysis, except for 8 individuals (2.2%) whose plasma soluble Aβ42/Aβ40 values were outliers. The GMM was modeled with two components, as our aim was to classify the participants into two groups (plasmatic Aβ+ or Aβ-) (Fig. 2). The intersection of the two gaussians was localized at 0.0472; participants with a plasma soluble Aβ42/Aβ40 ratio ≤0.0472 were classified as plasmatic Aβ+, and those with a ratio >0.0472 were classified as plasmatic Aβ-.

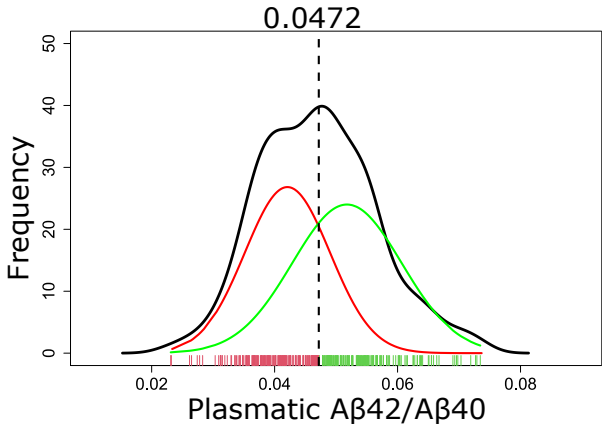

Figure 2. The full distribution of the plasma soluble Aβ42/Aβ40 ratio is shown in black. This distribution was then approximated as two gaussians, represented in red (plasmatic Aβ+) and green (plasmatic Aβ-). Each tick on the x-axis represents one individual. The threshold at the intersection of the two gaussians is 0.0472.

Using this threshold, 95.7% of AD patients were accurately categorized as plasmatic Aβ+ (Table 3), suggesting the presence of amyloid pathology. This specific threshold aligns with the 95th percentile of AD patients. Conversely, 44.4% of non-AD patients were appropriately

classified as plasmatic Aβ-, suggesting the absence of amyloid pathology. Finally, 58.5 % of the volunteers were classified as plasmatic Aβ-, suggesting the absence of amyloid pathology. The true amyloid status of volunteers remains unknown, but it is possible that some volunteers would have amyloid brain deposits, corresponding to individuals with preclinical AD.

Table 3. *Number of volunteers, AD, and non-AD patients classified as plasmatic Aβ+ or plasmatic Aβ- using the threshold of 0.0472, determined by GMM.*

	Volunteers	AD	Non-AD
Plasmatic Aβ+	115	67	10
Plasmatic Aβ-	162	3	8

Among the volunteers who were ε4-carriers, 49.4% (41/83) were classified as plasmatic Aβ+; among the volunteers who were ε4-noncarriers 38.5% (74/192) were classified as plasmatic Aβ+. The difference in the proportion of plasmatic Aβ+ and plasmatic Aβ- volunteers was not significantly different between ε4-carriers and noncarriers ($p = 0.12$).

Sensitivity and specificity of the plasma soluble Aβ42/Aβ40 ratio were evaluated using a subgroup of participants with known amyloid status. Table 4 shows the number of participants classified as plasmatic Aβ+ or plasmatic Aβ- according to their CSF or PET amyloid status, using the 0.0472 threshold, determined by GMM. Sensitivity was 87.8% and specificity was 55.8%.

Table 4. Number of participants classified as plasmatic Aβ+ or plasmatic Aβ- based on the plasma soluble Aβ42/Aβ40 ratio, using the 0.0472 threshold determined by GMM, and according to their amyloid status determined by CSF or PET analysis.

All individuals	CSF/PET Aβ+	CSF/PET Aβ-
Plasmatic Aβ+	65	34
Plasmatic Aβ-	9	43

Since our focus lies in ascertaining the amyloid status of individuals without documented cognitive impairment, we conducted an evaluation of the test's sensitivity and specificity for classifying participants without dementia (Table 5), using the same threshold value of 0.0472. The sensitivity was 83%, and the specificity was 57.5%.

Table 5. Number of participants without dementia classified as plasmatic Aβ+ or plasmatic Aβ- based on the plasma soluble Aβ42/Aβ40 ratio, using the 0.0472 threshold determined by GMM, and according to their amyloid status determined by CSF or PET analysis.

Non-demented individuals	CSF/PET Aβ+	CSF/PET Aβ-
Plasmatic Aβ+	44	31
Plasmatic Aβ-	9	42

2.3.2 Decision tree

A decision tree was used as second independent method to determine the threshold on the plasma soluble Aβ42/Aβ40 ratio. A decision tree with one split was trained on one feature, the plasma soluble Aβ42/Aβ40 ratio. The threshold determined by the decision tree was 0.0465 (Fig. 3) and yielded a sensitivity of 86.5% and specificity of 58.4% (Table 6).

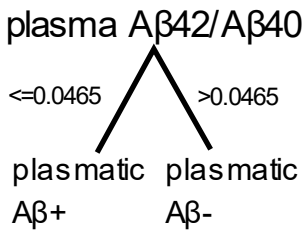

Figure 3. Result of the decision tree. Participants were classified as plasmatic Aβ+ if their plasma soluble Aβ42/Aβ40 ratio was ≤0.0465, and as plasmatic Aβ- otherwise.

Table 6. Number of participants classified as plasmatic Aβ+ or plasmatic Aβ- based on the plasma soluble Aβ42/Aβ40 ratio, using a threshold of 0.0465, as determined by decision tree, and according to their amyloid status determined by CSF or PET analysis.

All individuals	CSF/PET Aβ+	CSF/PET Aβ-
Plasmatic Aβ+	64	32
Plasmatic Aβ-	10	45

Subsequently, individuals without dementia were analyzed to determine whether those classified as plasmatic Aβ+ were indeed Aβ+ and those classified plasmatic Aβ- were indeed Aβ- (Table 7). For participants without dementia, the threshold value of 0.0465 yielded a sensitivity of 81.1% and a specificity of 60.3%.

Table 7. Number of participants without dementia classified as plasmatic Aβ+ or plasmatic Aβ- based on the plasma soluble Aβ42/Aβ40 ratio, using a threshold of 0.0465 as determined by decision tree, and according to their amyloid status determined by CSF or PET analysis.

Non-demented individuals	CSF/PET Aβ+	CSF/PET Aβ-
Plasmatic Aβ+	43	29
Plasmatic Aβ-	10	44

2.3.3 ROC curve

We plotted a ROC curve using only individuals without dementia for whom the amyloid status was defined by CSF or PET examination (Fig. 4). The area under the curve (AUC) was 0.728 (95% confidence interval (CI): 0.642–0.815). Youden's index was calculated to maximize the sum of sensitivity and specificity and corresponded to a cutoff value of 0.0450. At the Youden's index, sensitivity was 75.4% and specificity 67.1%, for individuals without dementia.

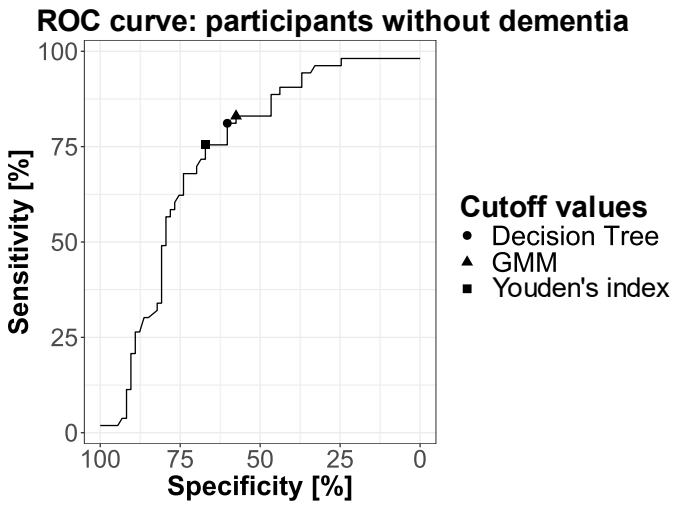

Figure 4. ROC curve representing the sensitivity and specificity of the plasma soluble Aβ42/Aβ40 ratio for different cutoff values, calculated on participants without dementia. The cutoff values obtained by GMM (0.0472) and decision tree (0.0465) are indicated on the curve, as well as the Youden's index (0.0450).

2.4 Posttest probabilities

Two cutoff values were retained: the one giving the best sensitivity (0.0472) and the one giving the best specificity (0.0450). The posttest probabilities of having brain amyloidosis were calculated according to the plasma soluble Aβ42/Aβ40 ratio at these two cutoff values, at two different ages (60 and 80). The prevalence of amyloid pathology among the clinically normal population was 15.8% at 60 years old [142], corresponding to pretest odds of 0.187. The prevalence of amyloid pathology among the clinically normal population at 80 was 32.6% [142], corresponding to pretest odds of 0.484.

The threshold determined by GMM (0.0472) gave the best sensitivity. At this threshold, among the population without dementia, the sensitivity was 83.0%, specificity was 57.5%, LH+ was 1.95, and LH- was 0.29. At 60, if the plasmatic test gave a positive result, the posttest odds was 0.365, corresponding to a posttest probability of 26.8%; if the plasmatic test gave a negative result, the posttest odds was 0.055, corresponding to a posttest probability of 5.2%. At this same threshold, at 80, a positive plasmatic test gave a posttest probability of brain amyloidosis of 48.6%, and a negative plasmatic test gave a posttest probability of 12.5%.

The Youden's index (0.0450) gave a specificity of 67.1%, a sensitivity of 75.4%, LH+ of 2.30, and LH- of 0.36. With this threshold, at 60, if the plasmatic test gave a positive result, the posttest probability of having brain amyloidosis was 30.0%; if the plasmatic test gave a negative result, the posttest probability was 6.4%. At this same threshold, at 80, a

positive plasmatic test gave a probability of brain amyloidosis of 52.6%, and a negative plasmatic test of 15.0%.

3. Discussion

The present study confirmed that plasmatic measures of Aβ are useful for predicting cerebral Aβ deposition [129, 132, 134, 143, 144], as measured using either in CSF or by PET analysis. Several blood Aβ assay methods have been developed recently, including mass spectrometry. The performances of plasma Aβ42/40 assays in detecting cerebral amyloid pathology in early AD patients was recently compared [145]. SIMOA along with immunoprecipitation coupled to mass spectrometry (IPMS) appear to be the two whose sensitivity (detection level) is sufficiently good and which can be operated for large-scale sample assays [132, 134, 146]. We used SIMOA 3-Plex A assays, a promising technique, way easier to implement de routine and with a higher throughput for measurement over a wider sample range than mass spectrometry, although its performances have been reported to be more modest that IPMS to discriminate AD vs MCI groups [147].

Biomarker concentration values alone are of limited use for classifying individuals in a cohort and predicting their clinical status, as no clear threshold was available in the literature. The aim of this work was to determine a threshold to classify participants as amyloid positive or negative based on the plasma soluble Aβ42/Aβ40 ratio obtained by SIMOA [131]. We determined two different thresholds, according to the

context in which the plasmatic test would be used. The first threshold, which minimizes false negatives, is intended to be used as an AD exclusion tool; the second, which maximizes accuracy, is intended to be used to improve research enrollment in AD studies.

In this study, a threshold of 0.0472 was used for the plasma soluble Aβ42/Aβ40 ratio measured by SIMOA, with the specific aim of applying it as a screening test to exclude an AD diagnosis in clinical practice. This threshold yielded the best sensitivity (83.0%), and a specificity of 57.5%, when tested on adults without dementia. This threshold corresponds to the 95th percentile among AD patients. In clinical conditions, the selection of a cutoff value should prioritize sensitivity because missing any diagnosis is undesirable. The blood test would be the first examination performed, and more specific examinations would be ordered only if necessary. A sensitivity of 83.0% would reassure individuals with a negative plasma test that they are not at risk for developing AD. This threshold allows to decrease the probability of having brain amyloid deposit in case of negative result to 5% at 60, and to 12% at 80. Therefore, in case of negative blood test result, individuals can be reassured in the sixties, and quite reassured in the eighties. Conversely, the low specificity means that specific assessments, such as amyloid-PET scans or CSF analysis, will be necessary follow-up for positive cases.

The threshold of 0.0450, obtained by the Youden's index, improved specificity to 67.1% but reduced sensitivity to 75.4%. It gave the best

accuracy. A threshold with higher specificity could be useful for research applications, especially for enrollment in AD studies. It could be used to classify a large cohort of individuals without requiring PET imaging or CSF analysis. It could also be a helpful inclusion criterion in clinical trials studying amyloid in early stages of AD. Such prescreening for clinical trials recruitment would reduce the cost of clinical studies. To include one amyloid-positive individual aged 60 years old, an average of 6.3 amyloid-PET scans or CSF analyses are required given the known prevalence of amyloid positivity at this age in the general population (15.8%) [142]. In practice, using PET-scan for screening is not recommended. With the availability of a prescreening blood test, the frequency of amyloid-PET scans or CSF analyses could be substantially reduced by limiting the use of these examinations to at-risk individuals. Adults aged 60 years old with a positive blood test defined by our criteria have a 26.8% probability of cerebral amyloid deposit. Therefore, if we aim to recruit one amyloid-positive individual aged 60 years old in a clinical trial, we need to realize 3.73 PET amyloid-PET scans (or CSF analyses) among individuals with a positive blood test, which is half the number required without blood test (6.3 CSF/PET analysis).

The present findings expanded previous results on plasma amyloid measurements [129, 132, 134, 144], and defined thresholds for the plasma soluble Aβ42/Aβ40 ratio measured by SIMOA. Other authors have reported correlation between PET or CSF amyloid status and the plasma soluble Aβ42/Aβ40 ratio measured by SIMOA [129, 131, 148]. Verberk et al. showed that the plasma soluble Aβ42/Aβ40 ratio could

serve as a prescreening test of AD pathology, and that a lower plasma soluble Aβ42/Aβ40 ratio was associated with an increased risk of clinical progression to mild cognitive impairment or dementia [129]. These studies found that the best cutoff values to predict amyloid status varied from 0.038 [148] to 0.056 [149], without consensus. They focused on clinically unimpaired individuals as in our study. However, participants' mean age was higher than the present cohort in two of the studies (mean age: 77) [148, 149]and younger than our cohort in one study (mean age: 61) [129]. Additional studies investigating the effect of age on plasma soluble Aβ42/Aβ40 ratio should be carried out in the future. Our results confirmed a cutoff value between 0.038 and 0.056 on an independent cohort and extended it to a general population without dementia aged over 50. We retained a threshold of 0.0472 for exclusion of AD, and a threshold of 0.0450 for research applications.

A previous study evaluated plasma biomarkers measured by SIMOA against brain autopsy [150]. The plasma soluble Aβ42/Aβ40 ratio decreased with brain amyloid deposits, but with only modest accuracy (AUC = 0.60). Immunoprecipitation followed by spectrometry analysis also allowed to measure the plasma soluble Aβ42/Aβ40 ratio, and gave better sensitivity and specificity (AUC = 0.75–0.89) than immunoassays for plasma [130, 132, 143, 148, 151-154]. Although IPMS could appear as future gold standard, some hurdles remain for its implementation as a routine technique in comparison to SIMOA. Other commercially available ELISA kits (EUROIMMUN, Lübeck, Germany) are capable of measuring soluble amyloid in plasma and demonstrate similar

correlations to CSF when compared to SIMOA for Aβ42/40 ratio (AUC = 0.69–0.70) [145]. ELISA also exhibits comparable accuracy to SIMOA in detecting cerebral amyloidosis based on plasma amyloid levels (ELISA: AUC= 0.78, 95% CI 0.72–0.84; SIMOA: AUC=0.79, 95% CI 0.73–0.85) [155]. While the plasma Aβ42/40 threshold defined in the present study could be applied to assays performing similarly to SIMOA for quantifying plasma Aβ, it should be reconsidered for techniques that offer more precise measurement of different Aβ forms in plasma, such as IPMS [145].

The present study evaluated plasma soluble Aβ42/Aβ40 ratio, but not other AD blood biomarkers such as total-tau or neurofilament light chains, as our aim was to have a measure the brain amyloidosis. Blood-based biomarkers of phosphorylated tau (pTau231, pTau181, and pTau217) have recently become available on SIMOA. PTau181 and pTau231 showed good accuracy for predicting AD-related neuropathological changes, but it may reflect different brain processes, such as soluble tau pathology, and/or neural damage [150]. Plasma pTau231 has been shown to increase at early stages of AD but recent studies showed that pTau217 better captures the earliest cerebral changes related to AD [156]. Prior studies have also shown a relationship between plasma pTau181 and amyloid PET, even in clinically unimpaired participants [150, 157, 158]. Plasma pTau181 could be an accurate predictor of AD [157]. However, only the soluble Aβ42/Aβ40 ratio relates purely to brain amyloidosis without considering tau pathology. Given our objective to predict brain amyloidosis rather than brain tauopathy in AD,

our focus was solely on quantifying plasma amyloid levels. The associations between Aβ and pTau measured in plasma require further evaluation in future studies.

Not all plasma amyloid peptides come from the central nervous system, which could explain the limited ability of observing AD-related Aβ pathology in plasma. The key components of Aβ-processing pathways are expressed in diverse extracerebral tissues, including the pancreas, appendix, gastrointestinal tract, and both male and female reproductive organs [159]. This suggests a potential peripheral Aβ production. Furthermore, compelling evidence links Aβ with the vascular system: higher plasma levels of Aβ have been associated with cerebral white matter lesions, cerebral microbleeds, hypertension, diabetes, and ischemic heart disease [131]. Aβ is also synthesized by the skeletal muscles, platelets, and vascular walls [160]. In addition, plasma proteins such as immunoglobulins, albumin, and complement are known to bind to and mask Aβ peptides [161]. Plasma Aβ is excreted by the kidneys, meaning that its level will rise in cases of renal dysfunction [162]. All these parameters influencing amyloid in plasma could explain the challenges in achieving high specificity and sensitivity in blood-based amyloid tests.

One limitation of the present study is that the thresholds defined were established in participants older than 50. Because amyloid pathology is rare before age 50 [163], we do not recommend to test individuals for plasmatic amyloid before this age. Furthermore, aging has been

reported to increase plasma Aβ in both humans [162], and nonhuman primates [164]. Additional studies are needed to determine a threshold for the plasma amyloid level on a population younger than 50 years old, and to evaluate whether the threshold should be adapted according to age.

Another limitation is that amyloid status was confirmed using two different methods, PET and CSF analysis. Although it would have been more consistent to use a single reference technique, it would have restricted the number of participants eligible for the study. Finally, soluble Aβ40 concentration was not measured in the CSF of our participants, in accordance with hospital protocols at the recruitment site. Given that the CSF soluble Aβ42/Aβ40 ratio enhances the accuracy of AD diagnosis by adjusting Aβ42 values based on whether the patient is a high or low amyloid producer (with a high or low quantity of Aβ40) [122], the absence of this measurement in our study may contribute to the fact that some patients received a clinical diagnosis of AD while being classified as Aβ- in CSF assessments.

4. Materials and Methods

4.1. Participants

We recruited 277 volunteers in Belgium, aged over 50 years and without known cognitive impairment. In order to validate the absence of cognitive impairment, volunteers completed the MMSE [111]. All volunteers had a MMSE ≥ 24/30 and were thus without dementia. All volunteers reported no recent illness or change in medical treatment during the last three months. The exclusion criteria were alcohol abuse, active cancer, major neurological condition like stroke or known neurodegenerative disorder. We also enrolled 88 patients from the Memory Clinic at Saint-Luc University Hospital, all of whom had reported memory complaints during a prior consultation and received a clinical diagnosis of AD (n=70), or non-AD neurodegenerative disease (n=18). The non-AD pathologies included: frontotemporal lobar degeneration, normal pressure hydrocephalus, microvascular disease, corticobasal degeneration, Lewy body dementia, or primary progressive aphasia.

The study was conducted in accordance with the Declaration of Helsinki and approved by the institution's Ethical Committee. All participants provided written informed consent (UCL-2022-473; UCL-2016-121; UCL-2018-119).

All participants (volunteers and patients) undertook a blood test in which deoxyribonucleic acid (DNA) and plasma were extracted. The plasma Aβ42/Aβ40 ratio was measured using SIMOA (Neurology 3 plex

A, Quanterix). The genetic risk for AD was estimated by genotyping the apolipoprotein E gene (*APOE*).

The cohort of 88 patients, along with a subset of volunteers (n=73), also underwent CSF analysis or an amyloid PET scan for validation of their amyloid status. The final analysis included only individuals with a maximum time delay of 2 years between the blood test and CSF/PET amyloid status measurement. The blood test could have been performed before or after the CSF/PET amyloid status measurement. Participants were excluded if more than 2 years had elapsed between the two exams, unless the CSF/PET amyloid measurement was done before the blood test and gave an amyloid positive result (n=21). Since none of the individuals in our cohort received anti-amyloid therapy, those who were previously identified as amyloid-positive will continue to retain their amyloid-positive status [165]. Six individuals were excluded who had a negative CSF/PET amyloid measurement done more than 2 years before the blood test, and four were excluded who had a blood test done more than 2 years before the CSF/PET amyloid status measurement. The final sample comprised 66 volunteers, 69 AD patients, and 16 non-AD patients.

Individuals were classified as amyloid positive (Aβ+) when the CSF amyloid measurement was lower than 438 pg/ml [96], or when the amyloid PET Centiloid score was higher than 26 [166]. Otherwise, they were categorized as amyloid-negative (Aβ-). Both volunteers and patients underwent an MMSE evaluation on the same day as the blood

test. They were classified as having dementia when their MMSE was below 24/30, and without dementia when MMSE was higher or equal to 24/30.

4.2. Blood drawing and plasma prepatation

A standard venipuncture procedure was performed using a 21 g needle and blood was collected in ethylenediaminetetraacetic acid (EDTA) polypropylene K2 tubes (K2E K2EDTA, Vacuette Tube, REF:455045). Immediately after collection, the tube was placed on ice and plasma isolation was performed within 2h. Blood was centrifuged at 2000 × g for 10 min at 4°C, and plasma was aliquoted by 500µl in cryotubes and stored at -80°C until further analysis.

4.3. APOE genotyping

DNA was extracted from blood samples. Participants were analyzed for *APOE* polymorphisms rs429358 (which is a [T/C] substitution on chr19:44908684 (GRCh38.p14) of the sequence GCTGGGCGCGGACATGGAGGACGTG[T/C]GCGGCCGCCTGGTGCAGT ACCGCGG), and rs7412 (which is a [C/T] substitution on chr19:44908822 of the sequence CCGCGATGCCGATGACCTGCAGAAG[C/T]GCCTGGCAGTGTACAGGCC GGGGC). Based on two single-nucleotide polymorphisms, alleles were assigned as ε2, ε3, or ε4. The *APOE* ε4 allele represents a major risk factor of AD [24–26]. We classified participants into two groups: “ε4 carriers” (ε3ε4, ε4ε4, and ε2ε4) and “ε4 noncarriers” (ε2ε2, ε2ε3 and

ε3ε3); ε4 carriers have a higher risk of developing AD compared to ε4 noncarriers.

4.4. Quantification of plasma Aβ40 and Aβ42

Quantification of soluble Aβ40 and Aβ42 was performed using the Neurology Plex A kit from Quanterix (Neurology 3 Plex A, REF:101995). Each plasma sample was thawed to room temperature for 1h before processing for SIMOA. This assay relies on distinct antibodies for capturing and detecting amyloid-β species (Aβ42, Aβ40). The capture antibody (6E10) recognizes the N-terminal region of both species (amino acids 4 to 10), while the detection antibodies are specific to the C-terminal ends of Aβ42 and Aβ40 to reveal them. Aβ42 and Aβ40 were simultaneously measured following the manufacturer's instructions. The same experimenter and same duration of experiment were used for all assay runs.

4.5. CSF analysis

Aβ42 measurements in CSF were done with Lumipulse® (G β-Amyloid 1-42, REF: 230336) in the Biology Lab of the Saint-Luc University Hospital, Brussels, Belgium. Participants were classified as Aβ+ when CSF Aβ42 was below 438 pg/ml, and Aβ- otherwise [96].

4.6. Amyloid PET-CT acquisition and computing

Two amyloid PET-radiotracers were used in this study: [18F]flutemetamol and [11C]Pittsburg Compound B ([11C]PiB). An anatomical 3D-T1 MRI was acquired for each participant on a 3T MRI (GE Signa Premier).

For both radiotracers, semi-quantitative PET data were computed using PNEURO software (v4.1) (PMOD LLC Technologies, Zurich, Switzerland) following the previously developed Centiloid pipeline [53] to return a Centiloid value for each participant. A threshold of Centiloid = 26 was used to discriminate participants considered Aβ+ (Centiloid > 26) and Aβ- (Centiloid <=26). This threshold was previously shown to be the most useful for classifying patients that would progress to dementia from those who would remain clinically stable six years after PET imaging [103].

4.6.1. [18F]flutemetamol PET-CT

Ninety minutes after [18F]flutemetamol (GE Healthcare, Chicago IL) intravenous injection (target activity 185 ± 5 MBq), a 30-min list-mode PET/CT acquisition was performed on a Philips Gemini TF (Philips Healthcare, Amsterdam Netherlands). The images were reconstructed as a dynamic scan of 6 × 5 minutes frames with 2 mm isometric voxels including attenuation, scatter and decay corrections, and time-of-flight information using the manufacturer's standard reconstruction algorithm. No partial volume correction was applied to the data.

4.6.2. [11C]PiB PET-CT

Forty minutes after [11C]PiB intravenous injection (target activity 500MBq), a 20 min list-mode PET/CT acquisition was performed on a Philips Vereos digital PET (Philips Healthcare, Amsterdam, Netherlands). Images were reconstructed in 4 x 5 minutes frames with 2 mm isometric voxels using the manufacturer's reconstruction algorithm which includes attenuation, scatter, and decay corrections, and time-of-flight information.

4.7. Basic characteristics

4.7.1. Characteristics of volunteers and patients

Baseline characteristics were compared between volunteers and patients, using Chi-square tests for gender and *APOE* ε4 status, and ANOVA for age and MMSE, with posthoc t-tests and Holms correction for multiple testing where appropriate.

4.7.2. Characteristics of participants with amyloid measured through CSF or PET analysis

A subgroup of volunteers and patients benefited from an amyloid measurement through either amyloid PET or CSF analysis, and were classified as Aβ+ or Aβ-. The subgroup of volunteers to whom we proposed PET or CSF analysis was enriched in *APOE* ε4 carriers, matching the frequency of ε4 carriage observed in AD patients. We compared characteristics of Aβ+ and Aβ- individuals, using t-tests for

age and MMSE, and Chi-squared tests for *APOE* ε4 status and gender repartition. We also compared characteristics of Aβ+ and Aβ- individuals without dementia, using the same tests.

4.7.3 Distribution of the plasma Aβ42/Aβ40 ratio

We represented the distribution of the plasma Aβ42/Aβ40 ratio for the different populations (all individuals, all individuals with a CSF/PET known amyloid status, all individuals without dementia with a CSF/PET known amyloid status). We visually verified with qq-plots that all distributions were well normally distributed. The plasma Aβ42/Aβ40 ratio was compared between volunteers, AD, and non-AD patients with ANOVA; and between Aβ+ and Aβ- individuals with t-tests.

4.8. Determination of the thresholds

The threshold for plasma Aβ42/Aβ40 ratio, to classify individuals as plasmatic Aβ+ or Aβ-, was determined using three methods: an unsupervised learning method (GMM), a supervised learning method (decision tree), and the Youden's index calculated on the ROC curve.

4.8.1 Gaussian mixture model (GMM)

A GMM was applied on the distribution of the plasma Aβ42/Aβ40 ratio of all participants (277 volunteers, 70 AD patients, and 18 non-AD patients) to approximate the distribution as two gaussians. The GMM analysis was implemented in R (version 4.2.1) using the mclust package (version 6.0.0) [167]. First, outliers were removed from the plasma

Aβ42/Aβ40 distribution of all participants (n=8, 2.2%). Outliers were defined according to the interquartile range (IQR) criterion; values were excluded if they fell above $q_{0.75}$ + 1.5 IQR, or below $q_{0.25}$ - 1.5 IQR, where $q_{0.75}$ and $q_{0.25}$ corresponded to first and third quartile respectively, and IQR was the difference between the third and first quartile.

The plasma Aβ42/Aβ40 distribution, without outliers, was then modeled using a two-component GMM with unequal variance. The threshold value of the Aβ42/Aβ40 ratio, used to categorize participants, corresponds to the point of intersection between the two Gaussian distributions. Participants with plasma Aβ42/Aβ40 ratio below the threshold were considered plasmatic Aβ+ and those with a ratio above the threshold were considered plasmatic Aβ-.

The plasmatic amyloid classification of participants was then compared across clinical diagnoses (AD, non-AD, and volunteers). Among the volunteers, plasmatic amyloid classification was also compared between ε4-carriers and noncarriers using a Chi-squared test.

We also evaluated the sensitivity and specificity of the plasma test using the 151 participants (66 volunteers, 69 AD patients, and 16 non-AD patients) for whom amyloid status was determined by PET or CSF analysis. Finally, as we were specifically interested in the ability of the plasmatic measure to determine the amyloid status of individuals before dementia, we evaluated the sensitivity and specificity of the test based only on participants without dementia (n=126) with a known amyloid status.

4.8.2 Decision tree

The 151 participants with a known amyloid status were classified by a supervised algorithm. A decision tree was trained in MATLAB using the Classification Learner app, with a maximum of one split to classify individuals as plasmatic Aβ+ or plasmatic Aβ- based on one feature: the plasma Aβ42/Aβ40 ratio. We trained the model using all data. The decision tree split nodes were based on the Gini diversity index. This decision tree provided a classification threshold. The sensitivity and specificity of this method were estimated.

Finally, sensitivity and specificity of the test were evaluated based only on individuals without dementia with a known amyloid status.

4.8.3 ROC curve

We generated the ROC curve for the 126 non-demented individuals with confirmed amyloid status, with R (version 4.2.1). In this analysis, we exclusively considered individuals without dementia to assess the plasma Aβ42/Aβ40 ratio capability to accurately discriminate amyloid status as a screening tool among individuals before dementia. We computed the AUC and its 95% confidence interval. We determined the Youden's index. We evaluated the sensitivity and specificity of test at this cutoff value.

4.9 Posttest probabilities

Finally, posttest probabilities resulting in a positive or negative result of the plasma measurement were computed with R (version 4.2.1), with the likelihood ratio, for the cutoffs giving the best sensitivity or specificity for clinically normal adults aged 60 or 80. The prevalence of amyloid pathology in the clinically normal population at these two ages (15.8% at 60, 32.6% at 80) were used to estimate the pretest probabilities [142].

The likelihood ratio for a positive test result (LR+) was defined as the sensitivity divided by one minus the specificity (LH+ = Sn/(1-Sp)), and the likelihood ratio for a negative test result (LR-) as one minus the sensitivity divided by the specificity (LH- = (1-Sn)/Sp). Then, the pretest odds were calculated as the pretest probability divided by one minus the pretest probability. Posttest odds were obtained by multiplying the pretest odds by the likelihood ratio. Finally, posttest odds were converted into the posttest probability.

5. Conclusions

The present findings build upon and refine previous work on plasma amyloid measurements. More specifically, this study established two plasma Aβ42/Aβ40 ratio thresholds measured by SIMOA, evaluated on a population without dementia aged over 50. The first threshold was 0.0472, offering higher sensitivity to minimize the risk of missing AD cases. In cases with positive results, individuals would benefit from additional exams such as PET or CSF analysis to confirm their amyloid

status. The second threshold, 0.0450, may be more suitable for research and clinical trial recruitment to streamline processes and reduce costs. The significance of this threshold lies in its potential to facilitate early detection of amyloid pathology. These findings offer a promising step towards more accessible and cost-effective methods for identifying individuals at risk of developing AD, with potential implications for early intervention and clinical trial recruitment.

Author Contributions: Conceptualization, L.C. and E.B.; methodology, L.C. and E.B.; software, L.C..; formal analysis, E.B., T.G., R.L. and K.S.; investigation, L.C., E.B., B.H., and A.I.; resources, B.H., P.K.C, and P.L.; data curation, L.C.; writing—original draft preparation, L.C. and E.B.; writing—review and editing, L.C., E.B., P.K.C, P.L., and B.H.; visualization, L.C. and E.B; supervision, B.H., P.K.C, and P.L.; funding acquisition, B.H. All authors have read and agreed to the published version of the manuscript.

Funding: L.C. was funded by Belgian Fund for Scientific Research (FNRS), grant number No. ASP40001844. B.H. was funded by FNRS, grant number CCL40010417, and by the FRFS-WELBIO, grant number 40010035. E.B was funded by Fondation Louvain and Fondation St Luc. P.K.C was funded by Queen Elisabeth Medical Foundation (FMRE AlzHex), F.R.S.-FNRS (FNRS J.0106.22), SAO-FRA Alzheimer Research Foundation (SAO-FRA 2018/0025) and UCLouvain Action de Recherche Concertée (ARC21/26-114).

Institutional Review Board Statement: The study was conducted in accordance with the Declaration of Helsinki, and approved by the Institutional Ethics

Committee of Clinics Saint-Luc University Hospital (UCL-2022-473; UCL-2016-121; UCL-2018-119).

Informed Consent Statement: Informed consent was obtained from all subjects involved in the study.

Data Availability Statement: All data collected in the context of this study will be made available in an anonymized form upon the publication of the article.

Acknowledgments: We thank all participants and the Stichting Alzheimer Onderzoek for their help in our study. We thank Esther Paître and Daniela Savina for their technical supports.

Conflicts of Interest: The authors declare no conflict of interest.

Combining Plasma pTau 181 and Aβ42/40 Ratio for Enhanced Alzheimer's Disease Diagnosis

1. Introduction

Finding efficient, costless, accessible and reliable tools for the preclinical diagnosis of Alzheimer's disease (AD) is a major challenge for early intervention in the disease. The recent approval by the Federal Drug Agency (FDA) of two immunotherapies targeting amyloid pathology, one core lesion of AD [137, 138], demonstrated and improved efficacy in mitigating cognitive decline in patients with early AD pathology (prodromal AD or mild AD dementia). The results obtained in all the recent clinical trials aimed at developing disease-modifying treatments indicate that early treatment offers the best guarantees of efficacy.

AD is primarily characterized by an abnormal accumulation of amyloid beta (Aβ) peptides into plaques in the brain, and the aggregation of hyperphosphorylated tau into neurofibrillary tangles (NFT) [168]. Those lesions are associated to neurotoxicity and neuroinflammation [169, 170], causing progressive neurodegeneration over the years. This pathological process is the leading cause of dementia worldwide. The main risk factor to develop late onset AD that accounts for more than 90% of AD cases (while early onset form represent less than 5% [171]) is advancing age. Considering that the population of individuals aged 80 years or older will double by 2050, reaching over 426 million people

(source: WHO report on Aging ang Health, 2022), AD is poised to become an ever-increasing socioeconomic burden, with very substantial implications for healthcare costs.

Advancements in AD diagnostic methodologies have significantly improved diagnostic precision. The detection of tau protein and its phosphorylated forms is instrumental to the biological diagnosis of AD and essential for disease staging. Current clinical diagnostics for AD rely on the quantification of Aβ peptides and tau/pTau proteins in cerebrospinal fluid (CSF) and the visualization of amyloid and tau deposition in the brain using positron emission tomography (PET) with specific radiotracers. The potential of plasma-based biomarkers is an emerging research field as a less invasive and more accessible alternative for AD diagnosis. Plasma biomarkers, especially pTau 181 which is a validated standard for CSF measurement in AD diagnosis, have shown great promise in distinguishing AD from cognitively normal (CN) individuals. The utilization of pTau 181 is particularly pertinent due to its direct correlation with tau pathology, which is intimately linked with neurodegeneration and cognitive decline in AD.

The objective of this study was to establish a diagnostic threshold for plasma pTau 181 that could readily discriminate AD patients from non-AD CN individuals and predict tau PET positivity and amyloid PET positivity. We also aimed to compare the performance of pTau181 to the plasma ratio Aβ42/40 for predicting tau deposition and amyloid deposition in the brain, as evaluated by PET scanner, and to determine

whether combining their measurements could increase test accuracy. Additionally, we sought to investigate whether combining the pTau181 threshold with the Aβ42/40 ratio threshold could enhance the accuracy of diagnosing amyloid deposition based on plasma biomarkers.

2. Results

2.1. Participants

We enrolled 137 individuals aged over 50 at the Cliniques Universitaires Saint Luc (CUSL). Detailed cohort composition is presented in Table 1. Recruitment was carried out on a voluntary basis to recruit cognitively preserved participants, and through the memory clinic at CUSL to enlist participants with cognitive impairment attributable to AD. Each participant, both volunteers and patients, underwent comprehensive screening for AD biomarkers. We classified the participants for the presence of amyloid pathology (A+) and tau pathology (T+) based on the CSF measurements of amyloid β42, total-tau and pTau181 proteins, and for the A status amyloid PET was also used. The T status was established based on the CSF measurement, or the tau PET measurement. Most of the AD patients had previously undergone CSF quantification of Aβ42, total tau, and pTau181 during their clinical evaluations. An AD diagnosis was considered based on the following CSF biomarker thresholds: Aβ42 < 437 pg/ml, total tau > 381 pg/ml, and pTau181 > 61 pg/ml [96]. Patients with Aβ42 < 437pg/ml, total-tau > 381pg/ml and pTau181 > 61pg/ml, or ratio pTau181/Aβ42 > 1.12 were considered amyloid positive (A+) and tau positive (T+), the

other ones with normal values were considered amyloid and tau negative (A-, T-). For volunteers and cases with discordant CSF measurements (characterized by elevated amyloid with elevated total tau and pTau181), amyloid status was further assessed using [^{18}F]flutemetamol PET or [^{11}C]PIB PET imaging [100]. Amyloid PET signal was considered positive when centilloid was >26. Patients with positive amyloid PET were considered A+, the other ones were considered A-. Additionally, all participants underwent [^{18}F]MK-6240 PET imaging [108] to evaluate tau deposition in the brain. The evaluation of brain tau insoluble aggregates PET signal was done visually on Braak scaling. We considered as tau PET positive (T+) all participants with Braak stage from 1 to 6, participants without signal were considered tau PET negative (T-). Cognitive assessments for all participants were conducted within 6 months before or after blood sampling with at least one MMSE evaluation [111].

In the volunteers, we identified 14 participants with unimpaired cognitive function but with A+ status. According to the NIA 2018 guidelines, these individuals could be classified as preclinical AD patients. Along these participants, 8 were tau PET positive. In the patients recruited from the memory clinic, 56 participants had an A+ status. 5 patients recruited at the memory clinic were non-AD diagnosis in the clinical assessment: two patients were A-T+ with amyloid PET negative result and total-tau / pTau181 CSF increased, one diagnosed with FTLD, one with CBD and one with LBD. The patient with LBD was A+

based on CSF measurement. The patient with FTLD was tau PET + and A-, and the patient with CBD was A-T-.

Among all the participants, 70 participants were A+ based on CSF measurement or amyloid PET, and 67 were A-. The A+ group was significantly older than the A- (student's t-test, $p=0.0027$), and their MMSE was also significantly lower (student's t-test, $p < 0.0001$). Among all the participants, 64 had a [^{18}F]MK-6240 tau PET positive result (Braak stage 1 to 6), 59 had an A+ status (A+T+), and 5 an A- status. On the other hand, 73 participants were tau PET negative, out of which 62 with A- status (A-T-) and 11 with A+ status.

The non-demented group comprised A- cognitively normal (CN) volunteers (n=65), A+ CN volunteers (A+, CN; n=14), A+T+ patients with MMSE > 24 (n=27) and the 3 patients diagnosed with LBD, FTLD and CBD. They were also split into A+ (n=41) and A- (n=66) groups, based on CSF measurement / amyloid PET results. The A+ group was significantly older than A- participants (student's t-test, $p = 0009$), and the MMSE of the A+ participants was also significantly lower (student's t-test, $p = 0.0001$). In the non-demented group, 35 participants had a [^{18}F]MK-6240 tau PET positive result (Braak stage 1 to 6), with 31 with A+ status (A+T+), and 4 with A- status. On the other hand, 71 participants were tau PET negative, with 62 with A- status (A-T-) and 9 with A+ status.

Table 1. Cohort's characteristics. *Some participants had both CSF measurement and amyloid PET.

	All participants		Non-demented participants	
	CSF/PET A+	**CSF/PET A-**	**CSF/PET A+**	**CSF/PET A-**
n	70	67	41	66
Age: mean (SD)	70.7 (10.38)	65.70 (8.54)	71.4 (8.40)	65.6 (8.54)
MMSE: mean (SD)	24.5 (4.20)	28.5 (1.45)	27.5 (1.60)	28.6 (1.30)
APOE: n ε4-/n ε4+	23/47	38/29	12/26	38/31
(% ε4-/% ε4+)	(33%/67%)	(57%/43%)	(29%/71%)	(58%/42%)
Gender: male/female	37/33	31/36	22/19	31/35
Non-demented /demented	41/29	66/1	–	–
Volunteers	14	63	14	63
Patients	56	4	27	3
*Measure of Aβ:**				
CSF	57	14	29	14
[18F]flutemetamol PET / [11C] PIB PET	32	56	25	55
Measure of tau:				
[F]MK-6240 PET +/-	59/11	5/62	31/9	4/62

2.2. Plasma p-181 is elevated in A+T+ participants

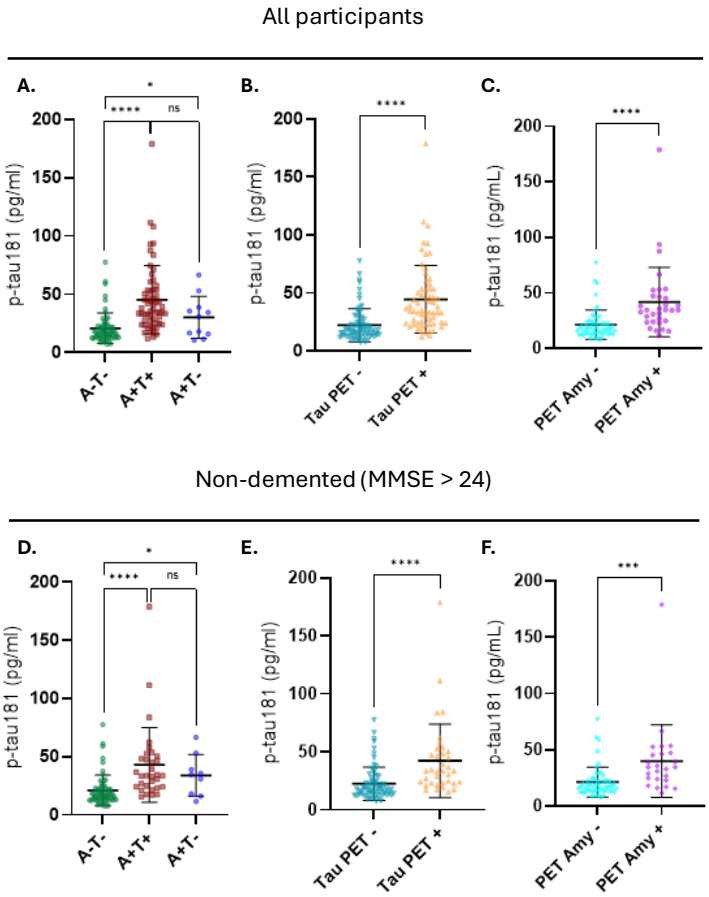

Figure 1. Quantifications of pTau181 circulating in plasma by Simoa (PTAU181 Assay V2.1). In all participants: **A.** pTau181 is significantly increased in A+T+ participants (n=59, Student's t-test, p<0.0001) and in A+T- participants (n=11, Mann-Whitney test, p=0.05) compared to A-T- participants (n=62). **B.** pTau181 is significantly increased in participants with a tau PET positive signal (n=64, Student's t-test, p<0.0001) compared to tau PET negative participants (n=73). **C.** pTau181 is significantly increased in amyloid PET positive participants (n=32, Student's t-test, p<0.0001) compared to amyloid PET negative participants (n=56). In the non-demented group: **D.** pTau181 is significantly increased in A+T+ participants (n=31, Student's t-test, p<0.0001) and in A+T- participants (n=9, Mann-Whitney test, p=0.05). **E.** pTau181 is significantly increased in tau PET positive participants (n=35, Student's t-test, p<0.0001) and **F.** in amyloid PET positive participants (n=25, Student's t-test, p<0.0001).

Initially, we aimed to determine whether plasma pTau181 concentration, measured using the Single Molecule Array (Simoa), is variating in A+T+ and A+T- participants, patients with tau PET positivity and patients with amyloid PET positivity. In all the participants, we observed a significant increase in plasma pTau181 concentration among A+T+ participants (Figure 1A, $P<0.0001$), in participants with a positive MK-6240 Tau PET signal (Figure 1B, $P<0.0001$) and in patients with amyloid PET positive signal (Figure 1C, $P<0.0001$). We could also find a small significant increase of plasma pTau 181 in patients with A+T- status (Figure 1A, $P=0.05$), meaning a that increase in pTau181 could not only be linked to tau deposition but also to amyloid deposition alone in the brain.

Given that the primary objective of this research was to assess the potential of plasma pTau181 to identify A+T+ and tau PET + at a preclinical or prodromal stage, we focused our analysis on non-demented participants. In the non-demented group, A+T+ participants also exhibited a significant increase in plasma pTau181 (Figure 1D, $P<0.0001$), and non-demented participants with a positive tau PET signal demonstrated elevated plasma pTau181 concentrations as well (Figure 1E, $P<0.0001$). Non-demented participants with amyloid PET positive signal also had increased plasma pTau181 values (Figure 1F, $P<0.0001$). We could also find a significant increase of plasma pTau181 in A+T- patients (Figure 1D, $P=0.05$).

2.3. Plasma pTau181 strongly correlate to Braak stage

Next, we aimed to evaluate whether plasma pTau181 concentration changes with the progression of tauopathy in the brain parenchyma. We assessed brain tau deposition using the [^{18}F]MK-6240 tau radiotracer via PET imaging, and Braak staging was performed visually in accordance with the standard classification from 0 to 6 established by Braak et al. in 2006 (REF). Plasma pTau181 concentration exhibited a strong correlation with Braak stage (Figure 2A, simple linear regression, r=0.46, P<0.001), with increased levels observed in conjunction with higher brain tau deposition (Braak stages 5-6). Given that tau deposition in the brain is closely associated with cognitive decline, we further investigated whether plasma pTau181 levels vary

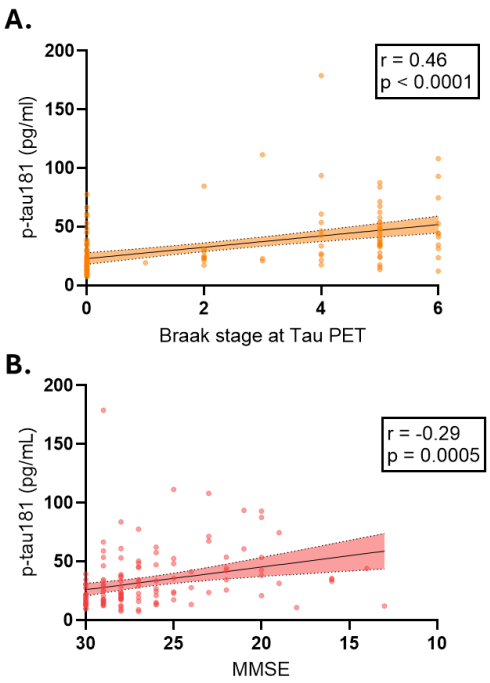

Figure 2. Plasma pTau181 variations upon Braak stage and MMSE score. Statistical Analysis: Pearson correlation and simple linear regression were conducted, with 95% confidence intervals displayed for each curve. ANCOVA was performed to assess the confounding effects of age, biological sex, and APOE status. **A.** Plasma pTau181 strongly correlate to tau-PET Braak stage (adjusted p-value < 0.0001); **B.** and negatively correlated to MMSE score (adjusted p-value = 0.0021).

with cognitive impairment, as measured by the Mini-Mental State Examination (MMSE) score. In our cohort, plasma pTau181 was negatively correlated with MMSE scores (Figure 2B, simple linear regression, r=-0.26, P=0.0021), with higher levels observed in patients with more advanced cognitive impairment (MMSE < 24).

2.4. ROC analysis

As demonstrated in Figure 1, plasma pTau181 levels are elevated in A+T+ participants and in non-demented A+T+ participants compared to A-T- CN participants. Given that the Aβ42/40 ratio was available for all participants from our previous study, our aim was to determine whether plasma pTau181, the Aβ42/40 ratio, or their combination could: (1) indicate A+T+ status, (2) provide information about their respective pathology detected by PET, or (3) inform about the PET status of the other pathology. The following sections will present all the results regarding these points.

ROC analysis of plasma pTau181

We conducted several Receiver Operating Characteristic (ROC) analyses to determine if plasma pTau181 is an effective biomarker for predicting (i) amyloid status as evaluated by amyloid PET, (ii) [^{18}F]MK-6240 tau-PET positivity, and (iii) A+T+ status evaluated with CSF and PET measurements.

First, we assessed plasma pTau181 as a biomarker in the entire cohort (Figure 3A). ROC analysis for predicting A+T+ status yielded an

area under the curve (AUC) of 0.84. The Youden's index indicated a threshold of pTau181 > 22.60 pg/ml, with a sensitivity of 84.75% (95% CI [73.48-91.76%]) and a specificity of 75.81% (95% CI [63.85-84.75%]). For predicting tau PET positivity, the AUC was 0.81, with a Youden's index threshold of pTau181 > 22.54 pg/ml, resulting in a sensitivity of 84.38% (95% CI [73.57-91.29%]) and a specificity of 71.23% (95% CI [59.99-80.35%]). Lastly, to predict amyloid PET positivity, the AUC was 0.81, with a Youden's index threshold of pTau181 > 23.44 pg/ml, yielding a sensitivity of 81.25% (95% CI [64.69-91.11%]) and a specificity of 76.79% (95% CI [64.23-85.90%]).

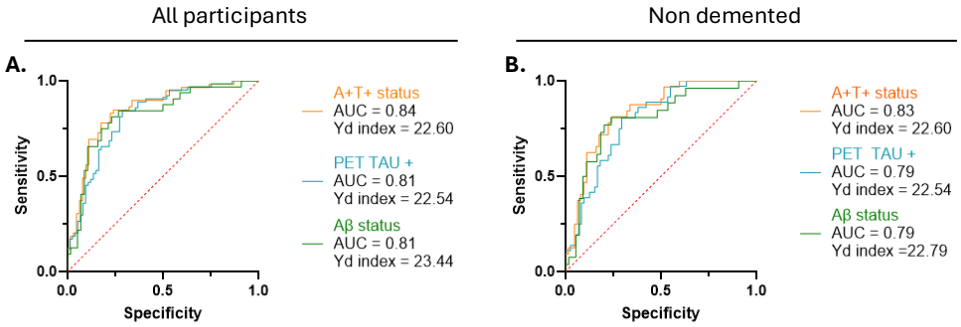

Figure 3. ROC curves representing the sensitivity and specificity of the plasma pTau181 for different cut-off values, calculated on all the participants (**A.**) and on participants without dementia (**B.**). The best cutoff values for each outcome (A+T+ status, [^{18}F]MK-6240 tau PET positivity and amyloid status (evaluated with CSF measurement or amyloid PET) were calculated with the Youden's index.

Subsequently, we performed the same analysis on the subgroup of non-demented participants to evaluate the capability of plasma pTau181 to predict these outcomes in the general population (Figure 3B). ROC analysis for diagnosing A+T+ status in this subgroup produced an AUC of 0.84 and a threshold of pTau181 > 22.60 pg/ml, with a sensitivity of 81.25% (95% CI [64.69-91.11%]) and a specificity of 75.81%

(95% CI [63.85-84.75%]). To identify tau PET-positive participants, the AUC was 0.79, with a Youden's index threshold of pTau181 > 22.54 pg/ml, resulting in a sensitivity of 80.56% (95% CI [64.91-90.22%]) and a specificity of 70.42% (95% CI [58.98-79.77%]). Finally, to predict amyloid PET positivity, the AUC was 0.79, with a Youden's index threshold of pTau181 > 22.79 pg/ml, yielding a sensitivity of 80.77% (95% CI [62.12-83%]) and a specificity of 75.93% (95% CI [63.05-85.36%]).

ROC analysis of ratio Aβ42/40

We aimed to investigate whether the Aβ42/40 ratio could predict A+T+ status, tau PET positivity, and amyloid PET positivity. Plasma amyloid concentrations were quantified using the Simoa platform (Neurology Plex A, Quanterix), allowing simultaneous measurement of Aβ42 and Aβ40 levels. We opted to use the Aβ42/40 ratio instead of direct Aβ measurements, as this ratio demonstrated the highest significance in distinguishing A+T+ from A-T- participants (see Figure 4A).

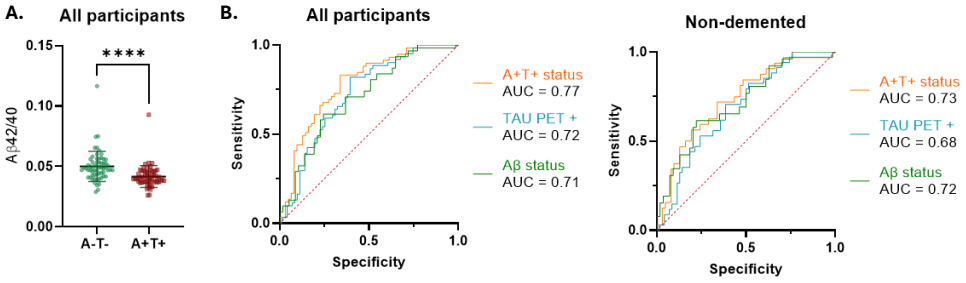

Figure 4. Plasma amyloid measurement in all the participants of the cohort, using Simoa. A. Comparison of plasma ratio Aβ42/40 between A-T- and A+T+ participants. Significant decrease of ratio Aβ42/40 is present in A+T+ participants (student's t-test, p <0.0001); **B.** ROC curves analysis for ratio Aβ42/40 to predict A+T+ status, tau PET positivity and amyloid status, in all the participants and in the non-demented participants.

To evaluate the diagnostic utility of the Aβ42/40 ratio in predicting A+T+ status, tau PET positivity, and amyloid PET positivity, we performed ROC curve analyses. The AUC for A+T+ status prediction was 0.77 (Figure 4B) in all the participants. In comparison, pTau181 alone yielded a higher AUC of 0.84 (Figure 3A), indicating that the Aβ42/40 ratio alone was less effective for AD diagnosis. Surprisingly, the Aβ42/40 ratio was also less effective for predicting amyloid status than plasma pTau181, with AUCs of 0.71 and 0.81, respectively. In the non-demented subgroup, we found similar results with an AUC of 0.73 for predicting A+T+ status, 0.68 for predicting tau PET positivity, and 0.72 for predicting amyloid PET positivity, which all performed less than plasma pTau181 alone in the same non-demented group (Figure 3B).

ROC analysis of combined plasma pTau181 and ratio Aβ42/40

We then explored whether combining the Aβ42/40 ratio with pTau181 could enhance diagnostic among all participants and the non-demented subgroup (Figure 5).

This combination improved both the sensitivity and specificity of several tests. For all participants, the AUC for A+T+ status prediction increased to 0.86 (Figure 5A), compared to 0.84 when using only plasma pTau181 (Figure 3A). The prediction of amyloid PET positivity was not improved by adding ratio Aβ42/40 measurement, with an AUC of 0.82 (Figure 4A), compared to 0.81 for pTau181 alone (Figure 3A) and 0.71 for the Aβ42/40 ratio alone (Figure 4B). In the non-demented participants, the combination of plasma pTau181 and the Aβ42/40 ratio also

enhanced the diagnostic performance, with an AUC of 0.82 for amyloid PET positivity prediction (Figure 5B), whereas for pTau181 alone AUC was 0.79. However, there was no significant improvement in the prediction of tau PET status or A+T+ status, with the AUC remaining unchanged when compared to the use of plasma pTau181 alone.

2.5. Influence of covariables sex, age and APOE

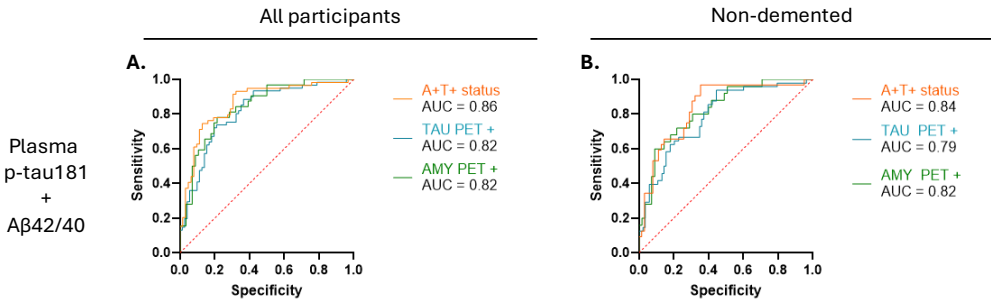

Figure 5. ROC curves representing the sensitivity and specificity of the plasma pTau 181 and ratio Aβ42/40 combination to predict AD status, [^{18}F]MK-6240 tau PET positivity and amyloid status. A. In all the participants, the best AUC was found to predict A+T+ status (AUC = 0.86); and **B.** in the non-demented participants, the best AUC was also to predict A+T+ status (AUC = 0.84).

We next examined the influence of biological sex, age, and APOE genotype on plasma pTau181, either combined with or without the Aβ42/40 ratio, to predict amyloid status, A+T+ status, and tau PET positivity. The results of the multivariable ROC analysis are presented in Table 2.

For predicting A+T+ status, the inclusion of covariates such as sex, age, and APOE did not improve the AUC, with the best performance still

observed when plasma pTau181 and the Aβ42/40 ratio were used together (Figure 5A, B).

Table 2. ROC estimates for pTau181 with additional variables. Table summarize Area Uder Curve (AUC); AUC 95% confidence intervals; AUC standard error; Log Likelihood ratio test p-value; sensitivity and specificity for correct classification of the participants (cutoff log = 0.5).

ROC Estimates for plasma p-tau181 with additional Covariates (Aβ42/40, sex, age and APOEε4 +/-)							
Outcome		Biomarker	AUC (95%CI)	Std. Error	*LRT p-value*	Sensitivity	Specificity
A+T+ status	All participants n = 133	p-tau181 + age + sex + *APOE*	0.83 (0.76,0.90)	0.037	*<0.0001*	0.80	0.74
		p-tau181 + Aβ42/40 + age + sex + *APOE*	0.85 (0.78,0.92)	0.034	*<0.0001*	0.82	0.77
	Non-demented n = 103	p-tau181 + age + sex + *APOE*	0.83 (0.76,0.92)	0.040	*<0.0001*	0.74	0.75
		p-tau181 + Aβ42/40 + age + sex + *APOE*	0.84 (0.77,0.92)	0.040	*<0.0001*	0.78	0.82
Tau PET positivity	All participants n = 133	p-tau181 + age + sex + *APOE*	0.81 (0.73,0.88)	0.038	*<0.0001*	0.80	0.70
		p-tau181 + Aβ42/40 + age + sex + *APOE*	0.81 (0.74,0.90)	0.037	*<0.0001*	0.76	0.73
	Non-demented n = 103	p-tau181 + age + sex + *APOE*	0.79 (0.71,0.88)	0.044	*<0.0001*	0.71	0.74
		p-tau181 + Aβ42/40 + age + sex + *APOE*	0.79 (0.71,0.89)	0.044	*<0.0001*	0.74	0.76
Amyloid PET positivity	All participants n = 88	p-tau181 + age + sex + *APOE*	0.85 (0.76,0.92)	0.042	*<0.0001*	0.78	0.72
		p-tau181 + Aβ42/40 + age + sex + *APOE*	0.87 (0.80,0.94)	0.038	*<0.0001*	0.80	0.74
	Non-demented n = 80	p-tau181 + age + sex + *APOE*	0.84 (0.75,0.93)	0.046	*<0.0001*	0.78	0.73
		p-tau181 + Aβ42/40 + age + sex + *APOE*	0.86 (0.74,0.91)	0.041	*<0.0001*	0.81	0.81

To predict tau PET positivity in all participants or specifically in the non-demented population, adding covariates to plasma pTau181 and the Aβ42/40 ratio did not enhance the AUC compared to using plasma biomarkers alone.

Finally, in predicting amyloid status, only the model incorporating plasma pTau181 along with age, sex, and APOE improved the AUC to 0.81, compared to an AUC of 0.78 when using plasma pTau181 alone in the non-demented population. However, this model performed equivalently to the one associating plasma pTau181 with the Aβ42/40 ratio (AUC = 0.81, Figure 6B).

2.5. CSF pTau181 outperforms plasma pTau181 in predicting Tau PET positivity

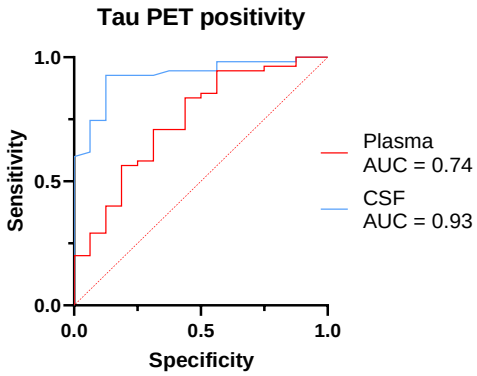

Figure 4. ROC curve analysis for the prediction of tau PET positivity using CSF and plasma pTau181. The cohort with available CSF data consists of 71 participants. Lumbar puncture was performed within a maximum of one year before the blood draw.

Among all our participants who underwent tau PET examination, the CSF measurement of pTau181 was available for 16 participants with tau PET negative results (Braak stage = 0), and 55 participants with tau PET positive results (visual Braak stage > 0). We performed ROC curves analysis for prediction of tau PET positivity in this population. The results can be found in Figure 4. For CSF pTau181,

the AUC equaled 0.93 (95%CI [0.86-0.99]), outperforming plasma pTau181 who for this same population gave an AUC equal to 0.74 (95%CI [0.60-0.88]).

2.6. Post test probabilities of pTau181 and Aβ42/40 combination

Based on the literature, in the general non-demented population, the prevalence of brain amyloidosis at 60 years of age is 15.8%, corresponding to pretest odds of 0.187; and at 80 years of age, it is 32.6%, corresponding to pretest odds of 0.484 [142].

In the non-demented population, the plasma pTau181 cutoff value for diagnosing amyloid status, determined using Youden's index, was 22.79 pg/ml, yielding a sensitivity of 81% and a specificity of 75.9%. The positive likelihood ratio (LH+) was 3.36, and the negative likelihood ratio (LH-) was 0.25. For the Aβ42/40 ratio, we used a cutoff of 0.045 for amyloid status diagnosis, also determined using Youden's index from a previous publication [172]. This threshold provided a sensitivity of 75.4%, a specificity of 67.1%, an LH+ of 2.30, and an LH- of 0.36.

At 60 years of age, if both plasma tests were positive (pTau181 > 24.91 pg/ml and Aβ42/40 ratio < 0.045), the posttest odds were 1.437, corresponding to a posttest probability of 59%. Conversely, if both plasma tests were negative (pTau181 < 24.91 pg/ml and Aβ42/40 ratio > 0.045), the posttest odds were 0.017, corresponding to a posttest probability of 2%.

At 80 years of age, if both plasma tests were positive, the posttest odds were 3.724, corresponding to a posttest probability of 79%. If both tests were negative, the posttest odds were 0.045, corresponding to a posttest probability of 4%. Detailed posttest probabilities are presented in Figure 6.

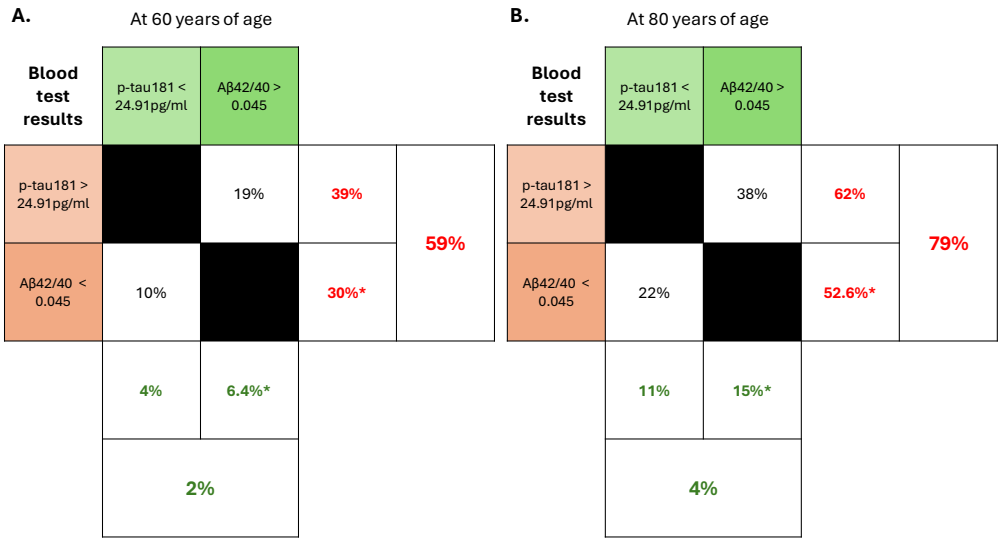

Figure 6. Posttest probability of brain amyloidosis in cognitively normal population when thresholds of plasma pTau181 and Aβ42/40 ratio are applied. A. Posttest probabilities at 60 years of age; **B.** Posttest probabilities at 80 years of age. *Data for application of ratio Aβ42/40 alone were extracted from previous study (Colmant et.al, 2023). Values in **black** represent posttest probabilities when one test was positive, and the other was negative. Values in **green** represent posttest probabilities when one or both tests were negative, and values in **red** represent posttest probabilities when one or both tests were positive.

3. Discussion

The present study confirmed that measuring plasma pTau181 is a useful tool for predicting A+T+ status (or AD status based on the NIA 2018 definition of AD), cerebral tau deposition, and brain amyloidosis, as with PET analysis and its accuracy is improved when combined to plasma ratio Aβ42/40.

In our study, CSF pTau181 demonstrated superior predictive accuracy for tau PET positivity compared to plasma pTau181. The subset of participants with available CSF measurements (n=71) was smaller than the overall cohort (n=137), with only 16 individuals being tau PET negative. Nonetheless, CSF pTau181 predicted tau PET positivity with an AUC of 0.93, whereas plasma pTau181 showed an AUC of 0.66. Similar findings have been reported in other studies; for instance, one study found that CSF pTau181 predicted brain tau deposition with an AUC of 0.91, significantly outperforming plasma pTau181 [173]. This consistency across studies supports the validity of our measurements and highlights that soluble pTau181 in the CSF correlates well with insoluble tau deposition in the brain parenchyma, while soluble plasma pTau181 is less indicative of tau deposition in the brain.

One of the main findings was that plasma pTau181 better predict brain amyloid deposition than plasma ratio Aβ42/40 in our cognitively preserved population. The AUC for pTau181 was 0.79, while for Aβ42/40 it was equal to 0.72. Associating both measurements improved significantly the predictive power with and AUC equal to 0.82, and the

association of covariates age, sex and *APOE* genotype improved test accuracy with AUC equal 0.86. Recent studies, such as Kwon et al. (2023), also evaluated the prediction of amyloid PET positivity using plasma pTau181 and other combinations of plasma biomarkers [174]. In this study, PET acquisition was performed with 18F-florbetaben instead of PIB or flutemetamol, but plasma biomarker quantification was conducted using Simoa SR-X, consistent with our methodology. Their cohort was similar to ours, with 52 A- and 48 A+ participants, but included only 5 non-demented A-T- participants and 3 non-demented A+T+ (or preclinical AD) participants. In contrast, our study enriched these specific populations with extensive PET screening of CN volunteers and included more *APOE ε4* participants to increase the probability of identifying non-demented A+T+ participants. Kwon et al. predicted PET amyloid positivity using ROC curve analysis and found an AUC of 0.85 for plasma pTau181 and an AUC of 0.66 for the Aβ42/40 ratio, both corrected for age and sex. These results are in line with our findings, demonstrating better predictive power of amyloid PET positivity using plasma pTau181 compared to the Aβ42/40 ratio. Similar results have been reported in other studies [175], reinforcing the well-established link between amyloid and tau in AD pathology and the idea that plasma pTau181 is a better predictor of brain amyloidosis than Aβ42/40. This unexpected result could be due to several factors. PIB and flutemetamol radiotracers used in PET detect only the insoluble form of amyloid. The amyloid measured in plasma represents the soluble form of amyloid and the current technique cannot measure intermediate

oligomeric forms of Aβ. One current hypothesis in the AD field is that insoluble plaques may act as protective structures aggregating soluble neurotoxic Aβ oligomers. By measuring only soluble Aβ42 and Aβ40, we miss the information about intermediate Aβ forms, which could be more sensitive for brain amyloid deposits prediction. Another possibility is that Amyloid Precursor Protein (APP) is expressed ubiquitously, leading to potential peripheral production of amyloid that could affect the Aβ pool circulating in blood plasma. In contrast, tau protein is exclusively produced in the brain. This may explain why pTau181 is more effective at predicting amyloid brain deposition compared to the soluble amyloid ratio. However, plasma amyloid is not as effective as plasma pTau181 in indicating brain amyloidosis, although the Aβ42/40 ratio performs better than amyloid isoforms alone. Winston et al. (2023) [176] found that plasma Aβ42 and Aβ40 alone (measured by mass spectrometry) had AUCs of 0.65 and 0.55, respectively, for predicting amyloid burden, while their ratio achieved an AUC of 0.80.

The prediction of tau PET positivity using the [^{18}F]MK-6240 radiotracer was a key outcome of our study. We found that the best predictive marker for tau PET positivity was plasma pTau181 alone, with an AUC of 0.79 in the non-demented population. Additional measurements of Aβ42/40 and adjustments for age, sex, and APOE status did not enhance the AUC. There are limited studies available on this specific radiotracer and plasma tau [173, 177]; one study reported an AUC of 0.967 but compared only 30 cognitively unimpaired young participants (mean age 23.0±2.1) with an Alzheimer's disease group of 32 participants [177]. Our

study extended the population to include individuals aged 50 and older, considering that the at-risk population for developing Alzheimer's disease is generally older [178]. This likely explains why our AUC was lower compared to other studies. Another recent study published in 2024 [173] also investigated plasma pTau181 but used the [^{18}F]-florbetapir radiotracer for tau PET acquisitions. Their population was similar to ours, including well-characterized CSF/PET cohorts with 33 non-demented A+T+, 67 mild cognitive impairment A+T+, and 14 demented A+T+ participants. They reported a similar AUC of 0.75 for predicting tau PET positivity, supporting the validity of our findings despite the different radiotracer used. Thus, our study demonstrates that plasma pTau181 is a reliable predictor of tau PET positivity in an older, non-demented population, corroborating the potential of plasma pTau181 as a biomarker for early Alzheimer's disease detection.

In our work, we did not study other forms of phosphorylated tau, primarily because on the Simoa SR-X, all pTau forms were available only on separate kits. We measured total tau alongside Aβ42 and Aβ40, but its concentration in plasma couldn't differentiate A+T+ participants from A-T-. Therefore, we decided not to include this measurement in the current study. We acknowledge that other phosphorylation sites for tau could be more accurate for AD diagnosis and could more accurately reflect tau-PET positivity. Plasma pTau231 and pTau217 have been recently compared to pTau181 for correlation with amyloid PET and tau-PET [173, 177, 179, 180]. Plasma pTau231 was found to correlate with tau PET status evaluated with [^{18}F]MK6240 similarly to plasma pTau181

levels [177, 180], and similar results were reported with the [^{18}F]flortaucipir radiotracer [173]. Regarding plasma pTau217, it showed an even higher correlation with tau PET imaging. Therriault et al. (2022) assessed plasma pTau biomarkers using the same radiotracer as in our study. Among the plasma pTau biomarkers, pTau217 exhibited the strongest correlation with tau deposition measured by PET [180]. Mendes et al. [173] conducted a similar study for plasma pTau217, calculating ROC curves for the prediction of tau-PET positivity. They found an AUC of 0.95 for pTau217, compared to an AUC of 0.75 for pTau181 and 0.78 for pTau231, concluding that the best predictor of tau-PET positivity was plasma pTau217. However, they did not include covariates for sex, age, or *APOE* genotype, and their study included participants across all cognitive stages of the disease, not just a non-demented population. Nevertheless, plasma pTau217 appears to outperform plasma pTau181 in both predictive power for tau-PET positivity and the identification of AD patients. Our study could benefit from the measurement of pTau217 for the evaluation of preclinical AD identification, building on previous works that validated plasma pTau217 as the current best candidate for identifying individuals with AD dementia.

The secondary objective of this research was to identify plasma pTau181 concentration thresholds that accurately distinguish Aβ+ from Aβ- patients in a CN population and to determine whether adding the Aβ42/40 ratio could modulate the post-test probability of brain amyloidosis. We utilized the Simoa pTau 181 Advantage V2.1 assay on

the SR-X (Quanterix), a promising technique for plasma biomarker quantification, allowing for the quantification of pTau181 with a lower limit of quantification (LLOQ) of approximately 2.87 pg/mL (Quanterix pTau181 Advantage V2.1 Kit Data Sheet). Our study identified a plasma pTau181 threshold of 22.79 pg/ml for distinguishing Aβ+ from Aβ- patients within a cognitively preserved population, achieving a sensitivity of 81% and a specificity of 75.9%. Post-test analysis for brain amyloidosis at ages 60 and 80 was completed using prior work on the plasma Aβ42/40 ratio [181], enabling calculations of combined test probabilities. At age 60, if both tests were negative, the post-test probability of brain amyloidosis was 2%. If both tests were positive (plasma pTau181 > 24.91 pg/ml and Aβ42/40 ratio < 0.045), the probability of brain amyloidosis was 59%, nearly four times higher than the general prevalence of brain amyloidosis without any testing, which stands at 15.8%. The combination of both tests maximized the positive and negative predictive values for brain amyloidosis. Using only plasma pTau181, the positive post-test prevalence was 39%, and the negative prevalence was 4%. At age 80, similar results were observed: when both tests were positive, the prevalence of brain amyloidosis was 79%, and when both were negative, it decreased from 32.6% in the general population to 4%. At both ages, scenarios with divergent blood test results yielded a brain amyloidosis probability close to that of the age-matched general population.

The use of such blood tests could be valuable in various aspects. Primarily, the thresholds calculated for the CN population could serve

as a preclinical screening tool for detecting Alzheimer's disease. With several anti-tau immunotherapies under development [182] and recent achievements in anti-amyloid immunotherapies [183-185], showing promising results in reducing pathological protein deposits and stabilizing cognitive decline, there is a growing body of scientific evidence emphasizing the importance of developing large-scale, suitable techniques for preclinical Alzheimer's disease diagnosis. The use of our plasma thresholds for pTau181 combined with the Aβ42/40 ratio could be applied to pharmacological studies for patient screening, allowing access to expensive screening tools to be reduced to only those at risk. Another application could be as a tool for general practitioners. When a patient presents with memory loss complaints and an MMSE score higher than 24, the blood test for pTau181 and Aβ42/40 ratio could be proposed instead of directly referring them to a specialist neurologist. If the patient tests negative for both markers, they could be reassured of not having a risk of Alzheimer's pathology, even in cases over 80 years old, considering the risk at that age would be only 4%. If both tests are positive, the physician could then refer the patient to specialized colleagues for further investigations, such as extensive neuropsychological evaluation, CSF biomarker measurements, and amyloid/tau PET imaging. Blood tests have the advantage of being non-invasive in comparison to lumbar puncture and less expensive than PET scans. Overall, the use of blood tests for the preclinical diagnosis of Alzheimer's disease could reduce the number of first-line consultations with neurologists for cognitive disorders, enabling only patients at

significant risk to be referred to specialists. Additionally, this approach would restrict the use of expensive tests to the most at-risk patients, thereby reducing the economic burden on hospitals.

4. Conclusion

In a non-demented population, plasma pTau181 was a better indicator of amyloid deposition in the brain than ratio Aβ42/40 alone, but their combination increased the prediction of amyloid PET positivity. The best candidate for tau deposit detection was plasma pTau181 and to diagnose AD status (A+T+) the best was to use the association of both markers.

For the diagnosis of preclinical Alzheimer's AD among a non-demented population, the use of the plasma pTau181 threshold of 22.79 pg/mL, combined with the threshold of 0.045 for the Aβ42/40 ratio, improved the diagnosis of brain amyloidosis and thus AD diagnosis, compared to using either biomarker alone. The post-test probability calculations effectively illustrate their potential use in the general CN population, especially for reassuring patients when both tests are negative.

PART II

EXTRACELLULAR VESICLES AS AD BIOMARKERS?

The search for reliable biomarkers for early diagnosis and disease progression monitoring is a critical area of research in AD. Among the various potential biomarkers, EVs have emerged as a promising tool in human AD research due to their potential involvement in AD pathogenesis and their ability to spread through the brain parenchyma.

Extracellular vesicles are small, membrane-bound particles released by cells into the extracellular space. They play a vital role in intercellular communication by transporting proteins, lipids, and nucleic acids between cells. This unique property makes EVs valuable for studying disease mechanisms and identifying biomarkers. In the context of Alzheimer's disease, EVs have been proposed to carry Aβ and tau proteins, which are hallmark pathological features of AD.

The involvement of EVs in AD pathogenesis is multifaceted. EVs could facilitate the spread of toxic Aβ and tau proteins between brain cells, contributing to the propagation of neurodegenerative processes. Moreover, the contents of EVs could reflect the pathological state of their parent cells, providing insights into disease mechanisms at a molecular level. These EVs can cross the blood-brain-barrier and be found in blood plasma. This makes EVs a valuable source of biomarkers for AD diagnosis and monitoring that could be detected in blood of patients.

In the following section of this research, our primary objective was to rationalize the use of EVs for Aβ and tau measurements by demonstrating in vitro that the content of EVs reflects key biomarkers of AD, including tau, phosphorylated tau (pTau), amyloid precursor protein (APP), and associated metabolites. We utilized the immortalized human neuroblastoma-derived cell line SH-Sy5y transfected with various plasmids to express human CTFβ (C99), human C42 (sequence of the Aβ42 peptide), human total-tau sequence, and human tau sequence mutated at position 301 to enhance phosphorylation. The content of cell lysates and EVs was then analyzed by western blotting.

Subsequently, we conducted a study on EVs derived from the brain (NDEVs) in the blood plasma of human participants, including those with AD and controls. Our aims were twofold: (i) to evaluate if quantifying the amount of NDEVs in plasma could serve as an AD biomarker comparable to soluble amyloid and tau, and (ii) to determine if the level of NDEVs could influence the quantity of amyloid and tau, given their potential role in amyloid secretion and tau propagation.

In vitro experiments: EVs content does reflect cellular AD pathology

1. Methods

Cell culture

SH-SY5Y cells (human neuroblastoma-derived cells) were cultured in DMEM/F-12 medium (Dulbecco's Modified Eagle Medium F-12 Nutrient Mixture) (ThermoFisher Scientific, #11039-021). Media was supplemented with 10% FBS (Fetal Bovine Serum Heat Inactivated) (Biowest, #S181H-500) and 1% penicillin/streptomycin (ThermoFisher Scientific, #15140-122).

Plasmids used for transfection

The plasmids used for expression of amyloid pathology were produced in the laboratory. Sequences of the plasmids can be found in supplementary data 1. We used a pcDNA3.4 backbone plasmid containing either the sequence of the precursor of Aβ, the CTFβ (C99), or the direct sequence of amyloid peptide β42. The plasmids contained a CMV (cytomegalovirus) promotor and a CMV enhancer.

The plasmids used for expression of tau pathology were bought from AddGene company. The backbone was a AAV.CBA.WPRE plasmid (dedicated use for AAV production) with a CBA (chicken β-actin) promoter and a CMV enhancer. Plasmids allowed the expression of full-length human wild type tau and P301L tau. The P301L sequence was

mutated on site 301, the proline present in WT tau is changed to a leucine. This mutation was identity as one of the causative mutations of fronto-temporal dementia. Mutation at this site promote phosphorylation and aggregation of tau (REF).

Cell transfection

The transfection of the cells took place 24 hours after seeding $2.2.10^6$ cells per Petri dish. Two transfection mixes were prepared, one containing Opti-MEM® I (ThermoFisher Scientific, #31985-062) and DNA, and the other containing Opti-MEM® I (ThermoFisher Scientific, #31985-062) and Lipo2000 (ThermoFisher Scientific, #11668-019). They were mixed and pre-incubated at room temperature for 15 minutes. 24 hours after transfection, the medium was replaced with serum-free medium (FBS). Cell lysates and media were collected 48 hours after transfection.

Cell lysate and EVs collection

Various successive centrifugations at cold temperature (4°C) were performed to collect the different components of the cell culture. The cells underwent an initial centrifugation at 300g for 10 minutes. The supernatant was collected and then centrifuged at 1000g for 10 minutes and finally at 10,000g for 30 minutes to eliminate dead cells and cell debris. The collected supernatant was ultracentrifuged at 100,000g for 60 minutes to collect the extracellular vesicles. Cells and EVs were lysed in a lysis buffer composed of 150 mM sodium chloride (NaCl), 50 mM Tris-base (pH 7.5), 2 mM EDTA, 1% Nonidet P-40, PhoSTOP 1X, and a

protease inhibitor (NP-40 buffer) and sonicated for 5 seconds. They were stored at -20°C for further experiments.

Western blotting

Cells lysate and EVs lysate were analyzed by Western blotting. The entirety of the EVs lysate was analyzed, while protein quantification by colorimetry using the Pierce™ BCA Protein Assay Kit (ThermoFisher Scientific) was performed beforehand on the cell lysates to load 30 µg of protein. A mixture of dithiothreitol (DTT, Merck Millipore, 0.05 M), LDS NuPage® Sample Buffer (ThermoFisher Scientific, #NP0007), and the desired amount of protein was prepared and heated for 10 minutes at 70°C. The samples and a SeeBlueTM Plus2 Prestained Protein Standard (ThermoFisher Scientific, #LC5925) were loaded and separated by SDS-PAGE electrophoresis on a NuPage™ 4-12% Bis-Tris Gel (ThermoFisher Scientific, #NP0335BOX). After 2 hours of migration at 80V in NuPAGE® MES SDS running buffer (ThermoFisher Scientific, #NP0002), the proteins were transferred onto a nitrocellulose membrane for 2 hours at 30V using NuPage® transfer buffer (ThermoFisher Scientific, #NP0006-1). Non-specific binding were blocked with 5% milk diluted in 1% PBS-Tween before incubating the membrane overnight at 4°C with the primary antibody. The following day, the membrane was washed with 0.1% PBS-Tween and incubated for 1 hour at room temperature with the secondary antibody conjugated to peroxidase. Protein detection was achieved using a chemiluminescent reaction with Western Lightning® Plus-ECL reagents (PerkinElmer, #NEL105001EA).

The primary antibodies used were diluted in 0.1% PBS-Tween: anti-Aβ W0-2 (1/1500, Sigma-Aldrich, #MABN10), anti-total-tau (1/1000, D1M9X, Cell Signaling, #46687) and anti-pTau PHF1 (1/100, provided by Peter Davies Lab, Queen's University, Canada). PHF1 antibody has been described to bind serine-396 and serine-404 phosphorylated sites (REF) The secondary antibodies, anti-mouse IgG (Sigma-Aldrich, #A0168-1ML) and anti-rabbit IgG (Sigma-Aldrich, A6154-1ML), were diluted 10,000 times in 0.1% PBS-Tween.

2. Results

EVs content reflects amyloid pathology at the cellular level

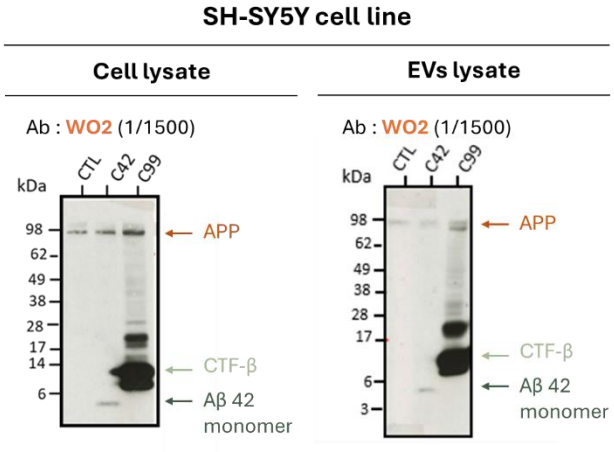

Figure 1. Western Blot of cell lysates and EVs lysates of SHSY5Y cells. Conditions tested: transfection with plasmids pcDNA3.4-C42, pcDNA3.4-C99 or non-transfected (CTL). Detection with WO2 antibody.

We compared the cellular and EV content isolated from the cell media of SH-SY5Y cells (Figure 1). The cells were transfected with either the pcDNA3.4-C42 or the pcDNA3.4-C99 plasmid 48 hours prior to collection. The WO2 antibody, which detects the N-terminal part of the Aβ sequence, was used to identify Aβ monomers, CTF-β, and full-length APP. Non-transfected SH-SY5Y cells served as the control. In both the cells and EVs, Aβ42 monomers at 4kDa were detected in cells transfected with C42. No Aβ assemblies were detected under these conditions. In cells transfected with C99, we detected CTF-β (14kDa) in both cell lysates and EVs. APP was detected in all conditions (98kDa) in both EVs and cell lysates, corresponding to the endogenous APP of SH-SY5Y cells.

EVs content reflect tau pathology occurring at the cellular level

We next investigated whether tau protein and its phosphorylated forms could be detected in EVs and whether this reflected the cellular content (Figure 2). Full-length tau (60kDa) was detected in both transfected conditions but not in the non-transfected control condition at the cellular level. PTau S396/404 was detected in both transfected conditions within the cells (60kDa). In EVs, total tau was detectable only in the condition transfected with tau301L but pTau S396/404 wasn't detected. Neither full-length tau nor phosphorylated tau at S396/404 was detected in the non-transfected EVs control condition.

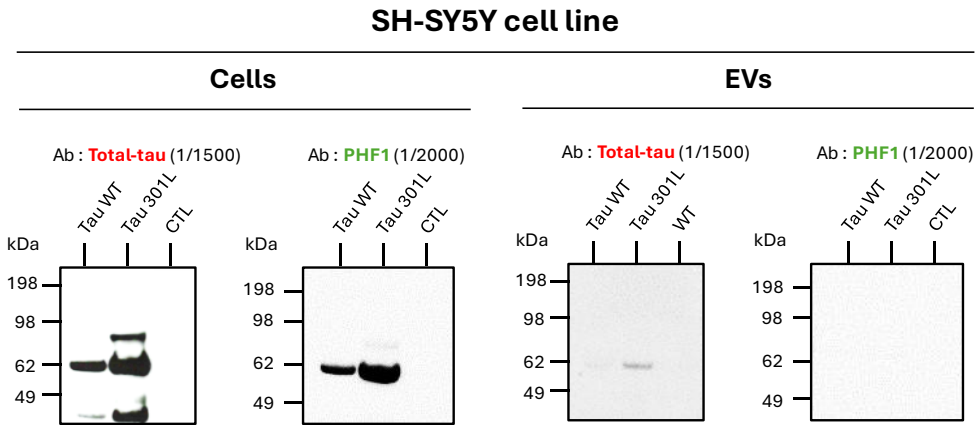

Figure 2. Cell lysate and EVs lysate analyzed by western blotting for tau pathology. Conditions tested: transfection with AAV.CBA.WPRE-tauWT or -tau301L. Detection of total-tau with antibody anti-total tau and anti phospho-tau PHF1.

3. Summary and perspectives

In summary, these experiments demonstrated that both amyloid and tau pathologies are present in EVs derived from cells expressing key biomarkers of AD. Although SH-SY5Y cells are not neurons per se, they provide an optimal balance between transfection efficiency and a model closely resembling human neurons in culture. Further experiments using induced pluripotent stem cell (iPSC) models could enhance these findings and allow for a deeper exploration of the role of EVs in biomarker trafficking and release. Nevertheless, our result allowed us to expect EVs content isolated from human blood sample to reflect AD pathology keys hallmarks, and to serve as biomarkers for AD. This objective is further explored in the next section of this chapter, presented as the second published paper of this thesis.

Comparison of plasma soluble and extracellular vesicles-associated biomarkers in Alzheimer's Disease patients and cognitively normal individuals

Emilien Boyer[1,2,3], Louise Deltenre[1], Marion Dourte[1], Lise Colmant[2,3], Esther Paître[1], Kristel Sleegers[5,6], Nuria Suelves[1], Bernard Hanseeuw[2,3,4], Pascal Kienlen-Campard[1]*

1. Aging and Dementia group, Cellular and Molecular Division (CEMO), Institute of Neuroscience, UCLouvain, 1200 Brussels, Belgium
2. Louvain Aging Lab, Institute of Neurosciences, UCLouvain, 1200 Brussels, Belgium
3. Neurology Department, Cliniques Universitaires Saint-Luc, 1200 Brussels, Belgium
4. WELBIO department, WEL Research Institute, avenue Pasteur, 6, 1300 Wavre, Belgium
5. Complex Genetics of Alzheimer's Disease Group, VIB-UAntwerp Center for Molecular Neurology, 2000 Antwerp, Belgium
6. Departement of Biomedical Sciences, VIB-UAntwerp, 2000 Antwerp, Belgium

Alzheimer's Res Ther. 2024; 16: 141.

Published online 2024 Jun 28. doi: 10.1186/s13195-024-01508-6

Abstract

BACKGROUND: Amyloid-β (Aβ) and tau are brain hallmarks of Alzheimer's disease (AD), also present in blood as soluble biomarkers or encapsulated in extracellular vesicles (EVs). Our goal was to assess how soluble plasma biomarkers of AD pathology correlate with the number and content of EVs.

METHODS: Single-molecule enzyme-linked assays were used to quantify Aβ42/40 and tau in plasma samples and neurally-derived EVs (NDEVs) from a cohort of *APOE* ε4– (n = 168) and *APOE* ε4+ (*n* = 68) cognitively normal individuals and AD patients (*n* = 55). The ratio of CD56 (Neuronal cell-adhesion molecule) to CD81 signal measured by ELISA-DELFIA was used for the relative quantification of NDEVs in plasma samples.

RESULTS: The soluble plasma Aβ42/40 ratio is decreased in AD patients compared to cognitively normal individuals. The amount and content (Aβ40, Aβ42, tau) of plasma NDEVs were similar between groups. Plasma NDEVs quantity remain consistent with aging and between AD and CN individuals. However, the quantity of soluble biomarkers was negatively correlated to NDEVs number in cognitively normal individuals, while in AD patients, this correlation is lost, suggesting a shift in the mechanism underpinning the production and the release of these biomarkers in pathological conditions.

CONCLUSION: Soluble plasma Aβ42/40 ratio is the most robust biomarker to discriminate between AD patients and CN individuals, as it normalizes for the number of NDEVs. Analysis of NDEVs and their content pointed toward peculiar mechanisms of Aβ release in AD. Further research on independent cohorts can confirm our findings and assess whether plasma Aβ and tau need correction by NDEVs for better AD risk identification in CN populations.

Keywords:

Alzheimer's disease, blood biomarkers, extracellular vesicles, Aβ42/40 ratio, tau, neurally-derived EVs.

1. Background

The prevalence of age-related neurodegenerative diseases is expected to increase globally in the coming decades, attributed to improved overall health conditions and increased life expectancy in many countries. Currently, around 50 million individuals are affected by dementia, a number projected to reach 130 million by 2050 [186]. Alzheimer's disease (AD) is the primary cause of senile dementia. Finding reliable, easily accessible, and cost-effective biomarkers is a major challenge for the accurate and early diagnosis of AD. Diagnostic techniques based on neuroimaging and fluidic biomarkers have made great strides over the last two decades. New tracers like the ^{18}F-Flortaucipir have been developed to accurately image tau pathology in the brain and are approved by the FDA [187]. However, the cost and

limited accessibility of PET imaging to clinical research centers prevent, for instance, large-scale screening of at-risk populations.

Regarding fluidic biomarkers, the analysis of amyloid-β peptide (Aβ42), tau, and phospho-tau (pTau) in cerebrospinal fluid (CSF) has long been the gold standard for AD diagnosis [188]. These biomarkers are also key actors of AD pathological process, and prime targets for the development of disease-modifying therapies. Monoclonal antibodies targeting aggregated Aβ, such as aducanumab and lecanemab, gained FDA approval in 2021 and 2023 [189, 190]. These emerging disease-modifying therapies might greatly benefit from screening techniques that are more accessible, less invasive than lumbar puncture and that would accurately inform about disease progression. While blood-based biomarkers hold promise, none is currently fully validated or clinically used for AD. The development of blood biomarkers faces certain challenges. For example, the low plasma concentrations of CNS-derived biomarkers require a robust and reliable technique for their detection that can be implemented for routine use. The development of ultrasensitive single molecule detection arrays [191] has set new standards for biomarker detection in plasma or serum, fueling the interest for the easily-accessible blood samples. Still, regardless of their sensitivity, these quantification techniques detect only soluble/monomeric forms of Aβ and tau, leaving aside other forms (e.g. aggregated or encapsulated in biological vesicles) that may be relevant for understanding the pathological processes. Other parameters can additionally act as confounding factors in biomarker quantification. Sex

seems to influence plasma amyloid, as evidenced by a lower Aβ42/40 ratio in males [192]. Age is also a factor, as older cognitively normal (CN) individuals show lower levels of soluble Aβ42 and Aβ42/40 ratio [192-194]. *APOE* status is associated with amyloid levels, with significantly lower Aβ42 levels in *APOE* ε4 carriers in CN individuals [192, 194]. Additionally, factors like body mass index, recently linked to plasma concentrations of Aβ42 and Aβ40, should be considered as potential influencers of Aβ levels in blood [195].

Recent investigations indicate that extracellular vesicles (EVs) are highly transmissible and play critical roles in the propagation of tau pathology [196]. Although EVs' precise role in AD pathogenesis remain elusive, they may facilitate the spreading of pathological factors like Aβ and tau seeds between cells [197, 198]. Other studies showed that EVs can be loaded with neurotoxic Aβ forms [199]. The processing of the Amyloid Precursor Protein (APP) occurs in late endosomal pathways, involved EV formation, which could be a potential source of Aβ release in the extracellular space [200, 201]. Neurally-derived EVs (NDEVs), detectable in plasma, can cross the blood-brain barrier. NDEVs appear thus as a promising tool to investigate brain changes during disease progression, with their content potentially reflecting AD pathogenesis more accurately than soluble blood biomarkers or providing complementary information [197]. The perfect marker for the detection or isolation of NDEVs (e.g. expressed exclusively on neurally-derived extracellular vesicles) does not exist. Two main markers are commonly employed: L1CAM and the neuronal cell adhesion molecule 1 (NCAM1).

A recent controversy appeared surrounding L1CAM and EVs [202]. By using size exclusion chromatography (SEC) like us to isolate EVs prior to analyzing plasma- and CSF-derived EVs, Norman et al., found that L1CAM did not co-elute with the EVs but instead eluted in fractions containing soluble proteins. This suggests that while it is possible for a small proportion of EVs in plasma to be L1CAM-positive, L1CAM is more abundant in a soluble form. We chose to use NCAM1, also known as CD56, to track NDEVs. It's worth noting that CD56 is not exclusively in neural cells but also in some other cell types, such as NK cells, that could in theory contaminate our NDEVs pool. Nevertheless, for the sake of clarity, we will continue to use the term "NDEVs" to refer to CD56-positive EVs.

Our aim in this study was to measure with high accuracy and sensitivity Aβ peptides, tau and EVs in plasma samples and evaluate how they correlate to the clinical status of cognitively normal or AD individuals. Furthermore, we aimed at determining whether the concentration of NDEVs present in the plasma can (i) reflect AD progression, (ii) modulate the levels of soluble biomarkers, and can be used as a potential diagnosis tool and as an indication of possible changes in the mode of Aβ production associated to AD pathogeny.

2. Methods

2.1. Participants and study settings

Participants were recruited at Cliniques Universitaires Saint Luc (CUSL), Brussels, and divided into two groups: cognitively normal (CN) and AD-diagnosed groups. CN subjects were recruited from healthy volunteers in the general population, while AD patients were recruited at the memory clinic of the CUSL (UCLouvain). Cognitively normal individuals had no evidence of cognitive impairment and had a Mini-Mental State Examination (MMSE) test superior or equal to 27. All volunteers with lower MMSE were excluded from the study. The MMSE is a widely used cognitive test that is employed as routine practice at the memory clinic of CUSL. As all AD patients had previously undergone MMSE assessments, we chose to perform MMSE tests in the CN population to facilitate result comparisons between the two groups. All participants also needed to be free of neurological and psychological troubles, previous history of stroke, brain lesions, or epileptic episodes. Patients with AD were recruited based on the results of their lumbar puncture for AD biomarkers and neuropsychological evaluations. Cognitive evaluation included: Free and Cued Selective Reminding Test (FCSRT), Wechsler MEM-III test, Baddeley forms test, Trail Making Test, Luria alternating series test, verbal fluency task, 64 items denomination task (LEXIS test), GREMOTs denomination test, Clock drawing test and the CERAD Constructional Praxis Recall. Criteria for AD diagnosis required cognitive impairment at least in the memory domain (amnestic

MCI or dementia) and an AD pattern on CSF biomarker analysis with: Aβ42 below 437 pg/ml, pTau 181 above 61 pg/ml and total-tau above 381 pg/ml [96]. Discordant AD cases (normal Aβ42 or normal tau) were excluded. This analysis was performed during the routine medical checkup. All participants with AD underwent another MMSE evaluation for cognitive status at the time of blood collection. The lower age limit for both groups was 50 years old.

2.2. Blood sampling and plasma preparation

A standard blood test procedure was performed. Blood was collected with a 21-gauge needle and transferred to EDTA polypropylene K2 tubes (Vacuette, #455045). Immediately after collection, the tube was placed on ice and plasma isolation was performed within 2h. Blood was centrifugated at 2000g for 10 min at 4°C, and plasma was aliquoted by 500µl in cryotubes and stored at –80°C until further analysis.

2.3. Apolipoprotien E (APOE) genotyping

DNA genotyping was performed at the VIB-UAntwerp Center for Molecular Neurology (UAntwerp, Belgium) on blood samples. Participants were monitored for *APOE* single-nucleotide polymorphisms (SNPs) rs429358 ([T/C] substitution on chromosome 19q13.32 of the sequence GCTGGGCGCGGACATGGAGGACGTG[T/C]GCGGCCGCCTGGTGCAGT ACCGCGG), and rs7412 ([C/T] substitution of the sequence CCGCGATGCCGATGACCTGCAGAAG

[C/T]GCCTGGCAGTGTACCAGGCCGGGGC). Based on the two SNPs, *APOE* alleles (ε2, ε3, or ε4) were assigned.

2.4. Soluble Aβ and tau quantification in plasma

Quantification of soluble Aβ40, Aβ42 and total-tau was performed using the Neurology Plex A kit from Quanterix(R) (Neurology 3 Plex A, #101995). Each plasma sample was thawed at room temperature for 1h before Simoa analysis in strict accordance with the manufacturer's protocol. All assay runs were carried out with same duration by the same experimenter.

2.5. EVs isolation form plasma samples

We used size exclusion chromatography (SEC) qEVs columns from Izon Science Limited © to isolate EVs from blood plasma (#ICO-70). As it is critical to remove any aggregated or macro-protein contaminants associated with the EVs, EVs were purified using SEC rather than classical ultracentrifugation procedures[203]. Aliquots of plasma were placed at RT for 30min prior to EVs isolation to allow plasma to thaw completely. The columns were placed at RT for 30min before isolation. Columns were washed once with 20ml of DPBS (ThermoFisher scientific, #14190250) before loading with 500µl of plasma. DPBS (500µl) was used to elute and collect fractions. Fractions 7 to 12 were considered as EVs-containing fractions (see below for EVs characterization). The final volume of the EVs fraction collected was 3ml. 6ml of DPBS were added to eliminate the protein fractions. The

column was subsequently washed with 1 ml of DPBS NaOH 0.5M – 16 ml DPBS 1x Triton 0.1% – 12 ml DPBS 1x – 2 ml of DPBS NaNa3 (0.05%), and finally stored at 4°C for further use. Isolated EVs were stored at 4°C for maximum 24h.

2.6. EVs characterization

Nanoparticle tracking, DELFIA-ELISA Europium, FACS and Dot Blot analyses were performed to characterize the isolated EVs. All validation steps were performed according to MISEV2018 guidelines [204] in n=3.Nanoparticle tracking analysis was used to determine the size distribution and concentration of isolated EVs. All samples were diluted 50 times in DPBS prior to analysis with the Particle Metrix ZetaView® analyzer.

2.6.1. DELFIA-ELISA Europium

Further characterization was achieved by DELFIA-ELISA Europium sandwich assays with three different EV markers as inclusion markers (CD81, CD9, and CD63) and human serum albumin (HSA) as an exclusion marker. ELISA was performed on freshly isolated EVs (same day). All EVs samples were plated in a 96-well plate (Greiner, #762071) at 100µl per well and incubated overnight at 4°C. The plate was then washed 3 times with 300µl of 1x DELFIA wash buffer (PerkinElmer, #4010-0010), blocked with PBS BSA 1% for 1h30 with gentle agitation and washed three times again with DELFIA wash buffer. Primary antibodies were added: anti-CD81 (BioLegend, TAPA-1, #349502), anti-

CD63 (BioRad, # MCA2142), anti-CD9 (R&D, # MAB1880), and anti-HSA (R&D, MAB1455) in PBS BSA 0.1% for 2h with gentle agitation. Plates were washed three times with DELFIA wash buffer and incubated with the secondary antibody (anti-mouse IgG1 biotin, PerkinElmer, #NEF823001EA) for 1h with gentle agitation. After three washes, streptavidin-europium conjugate (PerkinElmer, #1244-360) diluted 1/2500 in assay buffer (PerkinElmer, #1244-111) was added for 45 min, and then washed again six times. 100µl of enhancement solution (PerkinElmer, #1244-105) was added per well before reading the plate (Victor, Perkin Elmer). To note, the same technique was used for the quantification of NDEVs in plasma, but this time using as primary antibodies anti-CD81 (BioLegend, TAPA-1, #349502) and anti-CD56 (BioLegend, #318319). The relative NDEVs amount was calculated as the signal ratio CD56/CD81.

2.6.2. Identification of the NDEVs population by FACS analysis

The identification of the NDEVs population was done using CD56 (Neuronal cell adhesion molecule 1 or NCAM1) as a CNS marker. 500µl of plasma samples were incubated prior to EVs isolation with 6µl of CFSE-FITC (Life technologies ThermoFisher, #C34554A) for 1h30 at RT. EVs were isolated following the protocol described in section 2.5. After isolation, 200µl of EVs suspension was incubated overnight at 4°C with either anti-CD9-APC (R&D Biotech, #FAB1880R-100UG), anti-CD56-eFluor450 (ThermoFisher scientific, #48-0566-42) or both at the same time. FACS analysis was performed the next morning on NovoCyte

Quanteon® flow cytometer. EVs stained with CFSE-FITC were gated based on the scatter scale and FITC signal. EV samples stained for CD9 were analyzed then to refine selection of the vesicle population, and finally double stained EVs (for CD9 and CD56) were considered as the NDEVs subpopulation.

2.6.3. Dot Blot

Dot Blot was used to detect the presence of human IgG and ApoB (exclusion markers) in EV fractions after SEC. 25µl of each fraction were blotted onto 0.45µm nitrocellulose membranes and incubated for 15min at RT. Membranes were washed with TBS-Tween 0.1%, and incubated with guanidine chloride 6M for 5min at RT. After 3 more washes with TBS-T 0.5%, the membranes were blocked with TBS-0.5% BSA for 30min and incubated at 4°C overnight with primary antibodies (anti-human IgG-HRP (Duko #P0214) or anti-ApoB (Santa Cruz, # SC-13538)), at a dilution of 1/500 in TBS-BSA 5%. Membranes were washed twice for 15 min with TBS-Tween 0.5% under gentle agitation, incubated with secondary antibody (anti-mouse HRP, dilution 1/10.000 in TBS-BSA 5%) for 1h at RT and washed twice 15min with TBS-Tween 0.5% prior to detection using the Supersignal West Femto 10% – ECL 90% solution. Image acquisition was done with Fusion Solo Western Blot & Chemi Imaging (Vilber®). Dot blot results can be found in supplementary file 3.

2.7. Isolation and content analysis of CD56 positives EVs population

EVs isolated by SEC were concentrated by ultrafiltration (Pierce Protein Concentrators PES 10K, 2-6ml, (ThermoFisher scientific, #88527) at 4000g for 15min at 4°C. Concentrated EVs were resuspended in DPBS to reach a final volume of 500µl. The isolation of an EV subpopulation was carried out on 100µl of concentrated EVs. CD56 (neuronal cell adhesion molecule 1, NCAM1) positive EVs were isolated with the Exo-Flow kit (System Biosciences, #CSFLOWBASICA-1) following the manufacturer's protocol, with biotinylated anti-CD56 antibody (BioLegend, #318319). After elution, EVs were concentrated by centrifugation at 100.000g for 1h30 at 4°C. EV pellets were resuspended in 25µl of RIPA lysis buffer (Triton 0.5%, 25mM Tris pH 7.5, 0.5% NP40), sonicated for 1min on ice, and centrifuged (10.000g, 10 min, 4°C). The supernatant was stored at minus 80°C for further analysis. Concentrations of Aβ42, Aβ40 and total-tau were determined using Simoa (Neurology 3 plex A kit). Lysis buffer compatibility was verified before analysis (Quanterix recommendation for lysis buffer use with Simoa Bead-Based Assays: Tris 25mM pH7-8, Triton – NP-40 ≤ 1%). By using our RIPA buffer, no interference with the quantification of beads-based assays was observed, with no need to adjust calibrators preparation prior to analysis. In order to compare the results, we had to set a protocol indicating that the same quantity of EVs was isolated each time when using the Exo-Flow kit. To that end, we isolated as described above EVs expressing CD56 (NDEVs) by Exo-Flow. We stained EVs with CFSE-FITC (Life technologies ThermoFisher, #C34554A) by incubating

6µl of CFSE-FITC with 500µl of plasma for 1h30 on a rocking wheel. Six different quantities of EVs were used to set the number of EVs giving signal saturation, for which the same and maximal number of EVs is considered to be linked to the beads. Using the concentrated EV fraction (500µl) obtained after ultrafiltration from a control participant, we tested respectively 100µl (± 2.10^5 EVs), 50µl (± 1.10^5 EVs), 10µl (± 2.10^4 EVs), 5µl (± 1.10^4 EVs), 1µl (± 2.10^3 EVs), and a negative control without EVs (only beads and antibody). Nanoparticle tracking analysis (NTA) (ZetaView ®, Particle Metrix) measurement was performed to calculate the EVs number in each condition. 40µl of magnetic beads coupled to biotinylated anti-CD56 antibody were used for every condition. After isolation, bead-EVs complexes were analyzed by FACS (BD FACS Canto II®) to evaluate the FITC signal (associated to EVs signal). Results are presented in supplemental data (see Supplementary Figure 1). Bead saturation occurred at 100µl of EVs. Our measurements indicated that using 100µl of EVs after SEC and concentration to 500µl total volume was a reliable method for obtaining a consistent and maximal number of NDEVs under our experimental conditions.

2.8. Statistical analysis

Statistical analyses were performed using GraphPad Prism 10 software. Parametric tests were performed when data followed a normal distribution. Otherwise, non-parametric tests were performed. When two groups were compared, parametric Student's t-test or non-parametric Mann Whitney test were used, or Welch's t-test when SD

where different between data. For correlations analyses, parametric Pearson's test and non-parametric Spearman's test were used. Simple linear regression was used to illustrate the correlations on the graphs. Significance is indicated as: ns = non-significant, *P < .05, **P < .01, ***P < .001 and ****P < .0001. Analysis of covariance (ANCOVA) was performed to evaluate the effect of age, sex, and APOE status in all the correlation analyses.

3. Results

We first collected plasma samples from 236 CN participants and 55 AD patients and established an accurate and reliable protocol to isolate EVs from those samples; in order to discriminate free-circulating soluble AD biomarkers and those present in blood vesicles originating from the central nervous system. Descriptive parameters of all different groups are listed in Table 1, distinguishing among CN individuals *APOE* e4 carriers (n=68) and *APOE* e4 non-carriers (n=168). The full characterization of EVs isolated from CN is shown in Figure 2.

Table 1. Study's population characteristics. Abbreviations: MMSE = Mini-Mental State Examination. Cognitive assessments were performed within 2 months of the blood draw. APOE e4 carriers (ε4+) and APOE e4 non-carriers (ε4–) indicate individuals carrying at least one e4 allele of the APOE gene (+) or none (–).

Characteristics	Cognitive normal (CN, n = 236)		AD patients (AD, n = 55)	
	***APOE* ε4-** **(n = 168)**	***APOE* ε4+** **(n = 68)**	***APOE* ε4-** **(n = 18)**	***APOE* ε4+** **(n = 37)**
Age at plasma collection (years, mean ± SD)	66.9 ± 7.5	65.3 ± 7.8	68.2 ± 9.5	71.2 ± 8.5
Female (%)	116, (69)	40, (59)	7, (39)	22, (59)
MMSE (out of 30, mean ± SD)	28.7 ± 1	28.6 ± 1	26.3 ± 3.4	23.7 ± 4.1

3.1. AD soluble plasma markers vary according to APOE ε4 genotype or AD status

AD soluble plasma markers were measured across the cohort. Figure 1 shows the quantification of soluble Aβ40, Aβ42 and total-tau in plasma. We observed a significant decrease in soluble plasma Aβ42 and Aβ42/Aβ40 ratio in CN *APOE* ε4 carriers when compared to CN *APOE* ε4 non-carriers (Figure 1.B, P = .019 for Aβ42 and Fig1.D P = .030 for Aβ42/Aβ40). No differences in soluble Aβ40 (Figure 1.A, P = .89) or total-tau (Figure 1.C, P = .83) were observed between CN *APOE* ε4 carriers and non-carriers. In AD patients, we observed significantly lower concentrations of soluble Aβ42 (Figure 1.F; P = .0037), and higher concentrations of total-tau (Figure 1.G, P = .005) than in CN (*APOE* carriers and non-carriers pooled together). The Aβ42/Aβ40 ratio (Figure 1.H) was significantly decreased in AD patients when compared to CN (P < .0001). Of note, the concentration of soluble plasma Aβ40 was also higher in AD patient (Figure 1.E, P = .0027). Values distributions of each biomarker quantified are represented in Figure 1.E' to H'. These two Gaussian distribution models illustrate the fold change in the mean values. The most robust fold change (1.23) appears for the soluble Aβ42/Aβ40 ratio which appears as a prime candidate for clinical diagnostic applications.

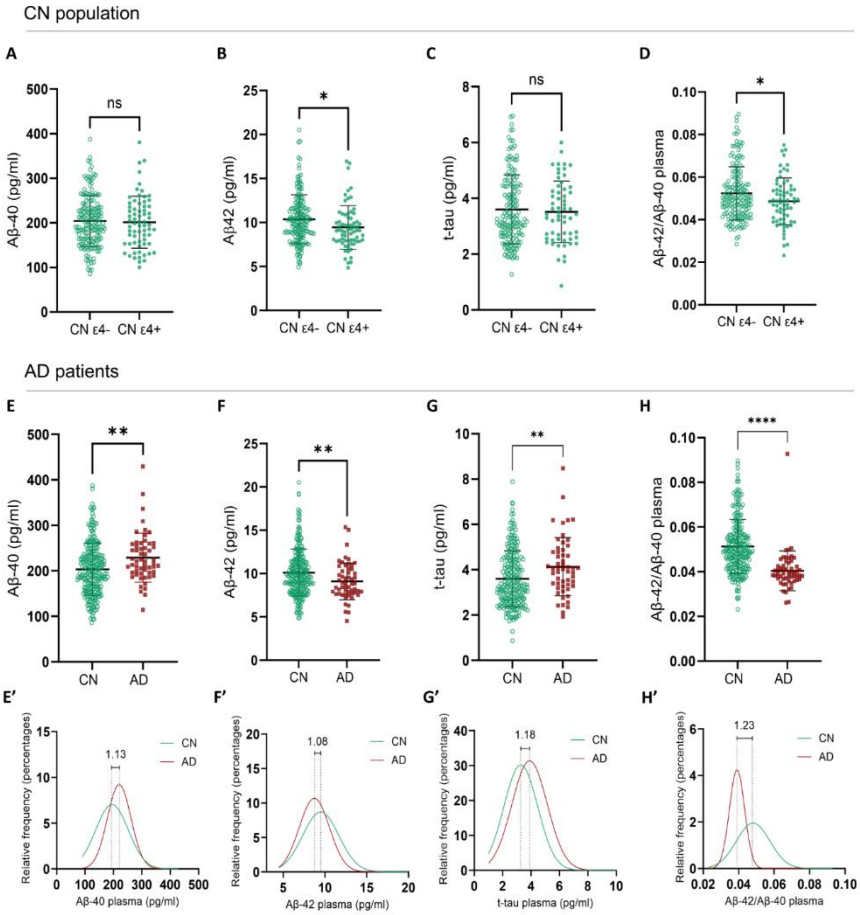

Figure 1. Quantification of soluble amyloid β (Aβ) 42, Aβ40 and total-tau circulating in plasma by Simoa (Neurology 3 plex A, Quanterix).

A to **D:** comparison of soluble plasma AD biomarkers in CN APOE ε4 carriers and ε4 non-carriers. **B.** Plasma soluble Aβ42 is significantly decreased in APOE ε4 carriers (student's t test, P = .0186); **D.** Plasma ratio Aβ42/Aβ40 is also significantly lower in CN APOE ε4 carriers (student's t test, P = .0299), **A** and **C.** there were no significant differences regarding plasma soluble Aβ40 and total-tau. **E** to **H:** comparison of soluble plasma AD biomarkers in AD and CN participants. Gaussian distribution of the values with fold change of the mean value is presented under each graph (**E' to H'**). **E.** Plasma soluble Aβ40 is significantly higher in AD patients (student's t-test, P = .0027), **F.** Aβ42 is lower in AD patients (student's t-test, P = .012), **G.** total-tau is higher in AD patients

(student's t-test, P = .0052); and **H.** plasma ratio Aβ42/β40 is significantly reduced in AD patients when compared to CN participants (student's t-test, P < 0.0001).

3.2. NDEVs represent 3% of the EVs circulating in plasma

To validate our method of EV purification, we first characterized the EVs isolated from the plasma of CN participants. Particle concentration and size distribution was determined in each SEC fraction with Nanoparticle Tracking Analysis (Figure 2.A). Particles were only detected in fractions 7 to 12, with higher concentrations in fractions 8 and 9. The particles detected ranged from 50 nm to 350 nm in size, with most particles measuring 150-200 nm, corresponding to the expected size of EVs. Additional experiments indicated that inclusion markers were strongly enriched in fractions 7 to 12. The expression profiles of these different EV markers were quantified using the ELISA-DELFIA immunoassay (see Methods, Section 2.7), revealing 89% of total CD9 signal, 80% of total CD81 signal, and 73% of total CD63 signal (Figure 2.A'). The exclusion markers were predominantly found in fractions 13 to 24, wherein 89% of Human Serum Albumin, 92% of total IgG, 98% of total protein, and 90% of ApoB were detected. Next, we characterized the subpopulation of brain-derived EVs referred to here as Neurally-derived EVs or NDEVs using flow cytometry. EVs were stained with CFSE-FITC and selected based on the size scatter scale and FITC signal (Figure 2.B). We confirmed that the population selected consisted of EVs by performing double staining with CFSE-FITC and CD9-APC, where 99.36% of the total EV population tested positive. Finally, we added CD56-eFluor450 staining to the CFSE-CD9 condition to quantify the

number of EVs expressing Neuronal Cell Adhesion Molecule 1 (NCAM1 or CD56) and thus derived from the CNS. Only 3% of the CFSE-CD9 positive population tested positive for CD56 (NCAM1), indicating that the NDEVs population represented around 3% (1/30) of the EVs circulating in the bloodstream (Figure 2.B.3). When only stained with CFSE-FITC and CD56-eFluor450 (not CFSE-CD9, data not shown), up to 4% of CFSE-FITC positive events were positive for CD56-eFluor450. This indicates the presence of NDEVs in plasma, representing between 3% and 4% of the total EVs circulating in plasma.

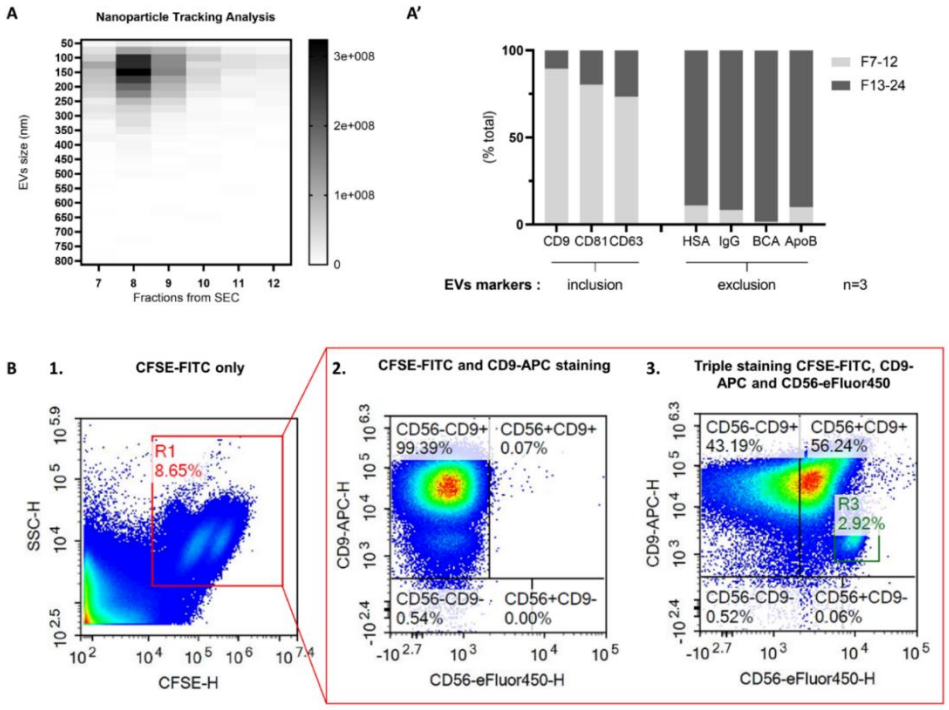

Figure 2. Extracellular vesicles characterization.

A. Nanoparticle tracking analysis (NTA) after size exclusion chromatography of 500µl of plasma. Nanoparticles were only detected in elution fractions 7 to 12 (only these fractions are displayed on the graph here). NTA provided the number and size of particles detected. The mean size of the

particles was 150nm, that corresponds to the expected size of extracellular vesicles (EVs). **A'.** The particles were further characterized by using EVs inclusion markers (CD9, CD81 and CD63) and exclusion markers measured by DELFIA-ELISA (HAS) or human IgG and ApoB measured by dot blot. Protein content was measured by bicinchoninic acid assay (BCA). EVs inclusion markers were highly present in fractions 7 to 12 whereas exclusion markers were almost absent. **B.** Characterization of the neurally-derived EVs (NDEVs) population by flow cytometry (NovoCyte Quanteon). **B.1.** Full EVs population scatter plot using CFSE-FITC staining (x-axis) and side scatter measurement (SSC, y-axis). Gating (R1) was performed to isolate EVs (FITC-positive). **B.2.** Double staining was performed using CFSE-FITC and CD9-APC, as validation step for the EVs population scattering. 99% of the events present in the R1 gate (positive for CFSE-FITC) were positive for CD9-APC, which confirms that the events detected in R1 are EVs. **B.3.** Triple staining for NDEVs population detection was performed using CFSE-FITC, CD9-APC and CD56-eFluor450. The estimated NDEVs population (R3) represent 3% of the total EVs population (R1).

3.3. Relative quantification of NDEVs in plasma

We next investigated whether the number of NDEVs could be used as an AD biomarker in plasma samples. Relative plasma NDEV levels were measured in a subpopulation of CN participants (n = 62, mean age of 64.9 [7.02], mean MMSE of 28.7 [1.15], 32 women [60.4%], *APOE* ε4 carriers/ε4 non-carriers [27/35]) and AD patients (n = 54, mean age of 70.1 [8.82], mean MMSE of 24.2 [4.3], 30 women [54.5]). Results are shown in Figure 3. No significant differences were observed in CN individuals regarding the *APOE* ε4 genotype (Figure 3.A; P = 0.93). Importantly, there was no correlation between age and plasma NDEVs levels in CN *APOE* ε4 carriers or non-carriers (Figure 3.B). Plasma NDEVs levels were not significantly different in AD patients compared to CN individuals (Figure 3.C, P = 0.28). In agreement with this observation, we

did not observe any correlation between NDEVs and MMSE scores in the AD group (Figure 3.D).

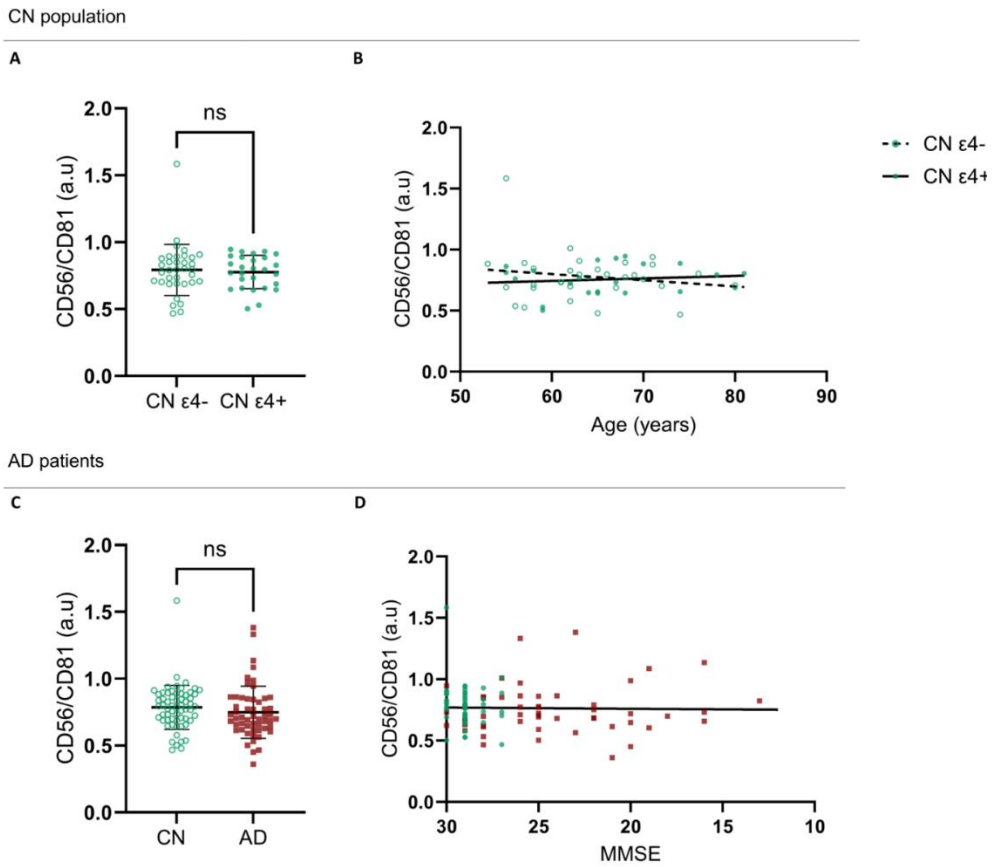

Figure 3. Plasma NDEVs quantifications measured by ELISA-DELFIA immunoassay.

The relative numbers of NDEVs are calculated as the ratio of CD56 signal on CD81 signal. **A.** Measurement of NDEVs in plasma from CN *APOE* ε4 carriers and non-carriers (Mann-Whitney test, $P = 0.93$); **B.** Age-related variation of plasma NDEVs quantity from CN *APOE* ε4 carriers and non-carriers (simple linear regression, Spearman correlation test, $r = -0.006$ and $P = .98$ for ε4 non-carriers; $r = 0.13$ and $P = .55$ for ε4 carriers). **C.** Measurement of NDEVs in plasma from CN participants and AD patients (student's t-test, $P = .28$); **D.** Variation of plasma NDEVs quantity with cognitive loss progression (CN participants are displayed in green, and AD patients in red, Simple linear regression with Spearman correlation test, $r = 0.02$, $P = .84$).

3.4. Inverse correlation between soluble amyloid biomarkers and NDEVs level in CN individuals

Our results indicated that plasma NDEVs numbers do not significantly change (i) with age in CN individuals, (ii) between CN individuals and AD patients, (iii) with decreased MMSE performance. This indicates that the number of plasma NDEVs do not appear as a clinical biomarker to discriminate between CN individuals and AD patients or to monitor cognitive decline [172]. Considering that EVs and in particular exosomes can be produced in multivesicular bodies (MVBs) formed in early endosomes [82] where APP amyloidogenic processing occurs [205] , recent findings showed that Aβ is readily present in extracellular vesicles [206]. We next investigated the correlation between AD soluble plasma biomarkers, NDEVs number and their content in AD biomarkers (i.e. Aβ42, Aβ40 and total tau). Results are summarized in Figure 4 and detailed scatter plots can be found in Supplementary Figure 2. In CN participants (displayed in green on Figure 4), we found a significant negative correlation between the number of plasma NDEVs and the concentration of soluble plasma Aβ42 and Aβ40 (Figure 4, A. and B., Pearson's correlation; for Aβ42: $P < .0001$, $r = –0.51$; for Aβ40: $P = .0003$, $r = –0.45$). For Aβ42, up to 27% of the variation observed among CN participants was explained by the number of NDEVs circulating in the blood (simple linear regression, $R^2 = 0.27$); for Aβ40, it was close to 20% (simple linear regression, $R^2 = 0.20$). In parallel, Aβ content was measured in NDEVs (Figure 4, A'. and B'.). Experimental procedures were set to ensure that equal numbers of EVs were

measured in each condition. High numbers of NDEVs were correlated with high individual content in Aβ42 and Aβ40 (Spearman's correlation, for Aβ42: $P = .015$, $r = 0.47$, for Aβ40: $P = .007$, $r = 0.52$). In AD patients (displayed in red on Figure 4), soluble Aβ42 and Aβ40 concentrations in plasma were not correlated to the quantity of plasma NDEVs (Figure 4, A. and B.) (Pearson correlation, for Aβ42: $P = .22$, $r = –0.17$, for Aβ40: $P = .26$, $r = –0.15$). However, we saw a strong correlation between NDEVs quantity and their content in Aβ in AD patients (Sperman's correlation, for Aβ42: $P = .0065$, $r = 0.69$; and for Aβ40: $P = .0082$, $r = 0.72$).

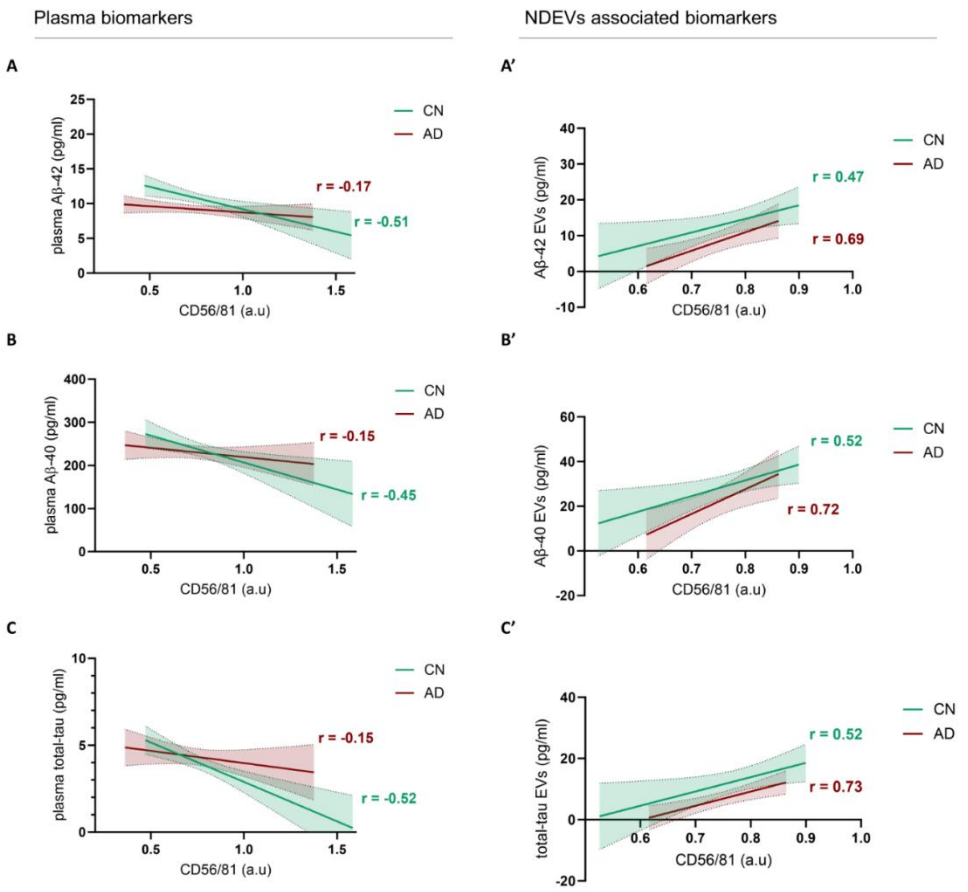

Figure 4. Correlations between plasma biomarkers, plasma NDEVs level and NDEVs associated biomarkers.

Left column (Plasma biomarkers): correlations between plasma soluble AD biomarkers quantity and plasma relative NDEVs quantity (ELISA signal ratio CD56/81) in AD (red) and CN (green) populations. Statistical Analysis: Pearson correlation and simple linear regression were conducted, with 95% confidence intervals displayed for each curve. ANCOVA was performed to assess the confounding effects of age, biological sex, and APOE status. **A.** Strong correlation in CN for soluble Aβ42 and NDEVs quantity in plasma (P = .031, adjusted P = .0049), loss of correlation in AD (P = .22, adjusted P = 0.4123), no differences in slopes (P = .0678), significant difference in intercepts (P = .001); **B.** significant correlation between Aβ40 and NDEVs quantity

in plasma of CN (P = .009, adjusted P = .0313), loss of correlation in AD (P = .26, adjusted P = .5501), no difference in slopes (P = .17), or in intercepts (P = .56); **C.** strong correlation for total-tau and NDEVs in plasma of CN (P = .0002, adjusted P = .0002), and loss of correlation in AD (P = .25, adjusted P = 0.6395), no difference in slopes (P = .064), or in intercepts (P = .2333).

Right column (NDEVs associated biomarkers): correlations between NDEVs content measured by Simoa (N3PA kit) in the same number of EVs (± 2.10^5 EVs, cf. Supplementary File 1 for details), and the relative NDEVs quantity in plasma (ELISA signal ratio CD56/81) in AD and CN populations. Statistical Analysis: Spearman correlation and simple linear regression were conducted, with 95% confidence intervals displayed for each curve. ANCOVA was performed to assess the confounding effects of age, biological sex, and APOE status. **A'.** Strong correlation between Aβ42 carried in NDEVs and NDEVs relative quantity in plasma for both CN (P = .031, adjusted P = .0095) and AD (P = .0048, adjusted P = .0097); **B'.** strong correlation between Aβ40 carried in NDEVs and NDEVs relative quantity in plasma for both CN (P = .014, adjusted P = .0208) and AD (P = .0065, adjusted P = .0119); and **C'.** strong correlation between total-tau carried in NDEVs and NDEVs relative quantity in plasma for both CN (P = .027, adjusted P = .0914) and AD (P = .002, adjusted P = .0082).

3.5. Inverse correlation between soluble total-tau and NDEVs level in CN volunteers

As for Aβ, soluble plasma total-tau in CN individuals negatively correlated with the number of plasma NDEVS (Figure 4.C, Pearson's correlation, $P < .0001$, $r = -0.52$). Measuring EVs content for total-tau, we found a significant correlation between the quantity of total-tau in NDEVs and the number of plasma NDEVs (Figure 4.C', Pearson's correlation, $P < .05$, $r = 0.49$) as observed for Aβ42 and Aβ40. In AD patients, there was no significant correlation between NDEVs levels and soluble plasma total-tau (Figure 4.C), but the content of total-tau in NDEVs strongly correlated with NDEVs quantity (Figure 4.C', Spearman's correlation, $P < .0001$, $r = 0.73$).

3.6. No differences of soluble AD biomarkers quantity linked to NDEVs between AD and CN individuals

We further investigated the potential use of NDEVs-associated amyloid and tau as AD biomarkers. Aβ42, Aβ40 and total-tau quantifications were done on the same number of NDEVs for each participant (see Supplementary Figure 1 for details). For the three biomarkers tested, concentrations were not significantly different in AD compared to CN participants (Figure 5. A, B and D) (Mann Whitney test). Aβ42/Aβ40 ratio was also similar (Figure 5. C) (Mann Whitney test) but we observed a non-significant trend for a decreased Aβ42/40 ratio in the NDEVs of AD patients.

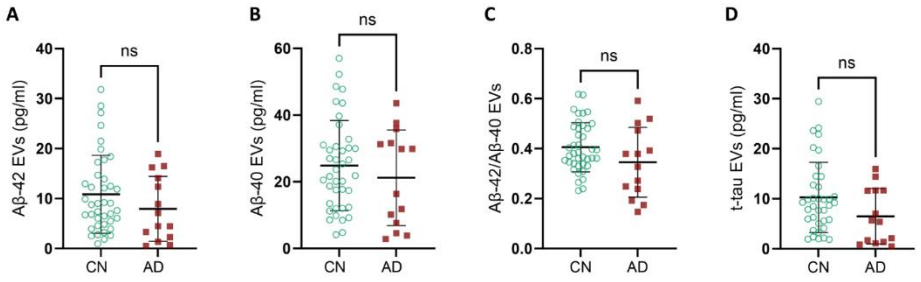

Figure 5. Comparison of the content in AD biomarkers of plasma NDEVs analyzed by Simoa.

For the analysis of NDEVs content, we focused on subgroups distributed across the plasma NDEVs spectrum, ranging from low circulating participants to high circulating participants. In the CN group, n=27, with a mean MMSE of 28.76 [1.27], mean age of 61.78 [14.8], 16 women [59.3%], and mean CD56/81 of 0.768 [0.10]. In the AD group, n=14, with a mean MMSE of 21.9 [5.09], mean age of 66.4 [16.7], 6 women [42.8%], and mean CD56/81 of 0.742 [0.09]. Comparisons were done with Mann Whitney test. **A.** Aβ42 contained in NDEVs do not change in AD ($P = .21$); **B.** Aβ40 either ($P = .46$); **C.** the ratio Aβ42/Aβ40 do not change in AD ($P = .14$); and **D.** total-tau either ($P = 0.06$).

4. Discussion

Blood biomarkers are of growing interest for early detection of AD, monitoring its progression, and measuring the effects of disease-modifying therapies. However, their implementation in clinical practice faces challenges due to low concentrations of AD biomarkers (Aβ, tau) in blood, requiring reliable measurement techniques and standardized sample preparation methods. In our study, we established a standardized protocol to measure free-circulating soluble Aβ42/40/total-tau, NDEVs, and their content in Aβ42/40/tau by Simoa in human plasma samples, with the goal of assessing their potential as AD biomarkers. Our major findings are that (i) Aβ42/40 ratio significantly discriminates between CN individuals and AD patients; (ii) NDEVs are present in the blood (around 3% of total blood EVs), but their number does not change with age or with AD dementia; (iii) in CN individuals, there is an inverse correlation between soluble AD biomarkers and the number of NDEVs. Strikingly, the content of AD biomarkers in NDEVs does not significantly change between CN individuals and AD patients and it does not therefore appear as a diagnostic tool to identify AD patients when quantified by Simoa.

4.1. Plasmatic soluble AD biomarkers

Previous studies have identified significant differences in plasma levels of Aβ40, Aβ42, and total-tau between AD patients and CN individuals[172, 207, 208]. Interestingly, we observed a slight but significant decrease in Aβ42 concentration and Aβ42/40 ratio in CN

APOE ε4 carriers, emphasizing the connection between *APOE* ε4 and amyloid pathology. This suggests plasma Aβ42/40 ratio as a candidate biomarker to detect preclinical stages of at-risk individuals (i.e. *APOE* ε4 carriers) to develop AD. The fold change in the Aβ42/40 ratio between CN and AD patients measured in plasma (1.23) is markedly lower than the one measured in CSF[209]. Amyloid and tau concentrations in plasma are approximately tenfold lower than those in CSF[210, 211]. Conversely, the total protein content in plasma is tenfold higher than in CSF[212], rendering the quantification of plasma biomarkers more exposed to biases likely assay cross reactivities or buffering due to the binding to serum albumin present at high concentration in plasma.

Although we observed a significant increase in soluble total-tau in AD plasma samples, we found it to be a less robust biomarker than Aβ42/40 ratio. These results are consistent with many studies that support that total tau[213-215] is more efficient when used in combination with other biomarkers, such as soluble Aβ42, to identify patients with AD. Though increase in CSF total-tau is used routinely in clinic for AD diagnosis, we are fully aware that phospho-tau measurements (e.g. pTau 181 or pTau 217) are more sensitive to detect AD pathology[213], they were not possible to achieve in the triplex panel available. Further experiments would be useful to complete this biomarkers collection by testing independently pTau biomarkers.

We must assume that only one fraction of Aβ and tau present in the CSF flows to the blood stream, or that peripheral Aβ which has been

shown to regulate Aβ clearance from the CNS might interfere in the measurement. In that respect, isolating NDEVs and measuring NDEVs content is of prime interest, as they might better reflect differences between AD and CN individuals than soluble, free-circulating markers.

4.2. NDEVs as an AD biomarker

The analyze of NDEVS was the second outcome of this study, aiming to evaluate their potential as biomarkers for neurodegenerative conditions and their impact on soluble biomarker measurements, considering their role in amyloid and tau propagation While few studies have explored NDEV quantities as AD biomarkers, Kapogiannis et al.[216] did not observe any differences in NDEVs quantity between AD patients and CN controls using L1CAM as a neuronal marker to identify NDEVs within the total EVs pool. However, the use of L1CAM has become controversial due to its presence in a soluble form in plasma, unrelated to EVs[217]. In our research, we employed a different neuronal marker, NCAM1 (neuronal cell adhesion molecule one, also referred as CD56), expressed by neuronal cells. Despite being expressed by cell types other than neurons and especially NK cells[218], NCAM1 is currently the best available tool to isolate or quantify EVs derived from the CNS in plasma. In the present study, we employed FACS analysis for NDEVs detection as a confirmatory method, as no previous study, thus enabling the validation of NDEVs isolation and the estimation of this EVs subpopulation to comprise 3% of circulating EVs in plasma. In agreement with Kapogiannis' study using L1CAM, we did not find any

significant differences in plasma NDEVs quantity between AD and CN groups in ELISA quantifications. The production of EVs in the brain - at least those than can be monitored in the blood - does not seem to be affected by disease conditions. Consequently, levels of neuronal-derived EVs appears neither as a marker of brain aging nor as an indicator of dementia onset or progression, as no changes were observed in AD patients upon deterioration of the MMSE score. If not the number, the content of NDEVs might then reflect pathological conditions.

4.3. NDEVs content as an AD biomarker

We found that the levels of Aβ42, 40 or total-tau associated to NDEVs were not altered in AD patients when quantified using Simoa. The concept of NDEVs content as an AD biomarker is an emerging field with limited available literature, and there is currently no consensus on the variations observed in AD patients. Other studies using Simoa found similar results regarding Aβ42[216], or total tau[219] carried in NDEVs. Conversely, when quantified by ELISA, significantly elevated Aβ42 levels were reported in plasma NDEVs of AD patients[220-222]. For total-tau quantified by ELISA, similar results as for Aβ42 were reported[221, 222], but other immunoassays gave inconsistent results, with no significant differences of total-tau in NDEVs of AD patients[223]. The inconsistency in results across studies might stem from variations in the techniques used for biomarker quantifications (e.g., Simoa, ELISA kits), NDEVs isolation (e.g., the use of NCAM1 and/or L1CAM as primary target for

NDEV immunoprecipitation), and isolation of extracellular vesicles (EVs) from plasma. Still, our study here supports the hypothesis that neither the number or the content of NDEVs measured in plasma does not discriminate AD patients from CN individuals.

4.4. The relation between plasma NDEVs amount, their content and soluble AD biomarkers could reflect the dynamic of biomarkers production at the neuronal levels that is impaired in AD pathology

Levels of free-circulating Aβ42, Aβ40 and total-tau in plasma inversely correlated with NDEVs quantity in CN individuals, indicating that higher NDEV numbers corresponded to lower soluble amyloid and tau concentrations, including among CN individuals at low-risk (*APOE* ε4 non-carriers). However, the quantity of biomarkers linked to NDEVs was also correlated to NDEVs number (when analyzed on the same amount of NDEVs), with higher numbers of NDEVs circulating associated to higher content in AD biomarkers. Together, these results strongly suggest a link between soluble AD biomarkers and the number of NDEVs, with biomarkers circulating either freely or embedded in EVs, but with a balance between their respective concentrations only in CN individuals (ref fig6). In AD patients, this correlation between soluble AD biomarkers and NDEVs was lost, reflecting potential changes in Aβ production and release during AD pathogenesis. It has been found that Aβ is present in MVBs and can be released into the extracellular space through EVs in neurons. Recent studies have demonstrated the

presence of APP, β- and γ- secretase in exosomes and at the endosomal level[181, 224, 225] providing further evidence of a clear link between amyloid and EVs.

Increased soluble Aβ40 found in the plasma of AD patients may reflect and overall increase in Aβ production in AD condition. Decreased soluble Aβ42 and consequently more pronounced decrease in the Aβ42/40 ratio is likely to reflect Aβ42 aggregation and deposition in AD pathology, leaving less Aβ42 available. Aβ42 aggregates are not detected in the current assays but would be very valuable tool to track AD pathology in blood samples. If plasma Aβ measurement truly reflects Aβ production and release in the brain parenchyma, our result would indicate an equilibrium existing between the release of soluble Aβ and Aβ embedded in vesicles in healthy conditions (CN). This balance seems to be broken in AD conditions, with soluble Aβ42 decrease more likely to be a consequence of amyloid-β deposition the brain than vesicular Aβ (NDEVs) that does not significantly decrease in AD condition. The possible interconnection between these observation and underlying mechanisms is summarized in Figure 6.

4.5. Limitations of this study

In our study, the analysis of NDEVs and the results of the Simoa assay may be constrained by the significant challenge of working with such a small protein fraction. Although the isolation protocol enabled the consistent isolation of NDEVs from each participant, it captured only a small fraction of the total NDEVs pool in plasma, resulting in very low

biomarker quantities for some participants. This limitation could explain the values close to the lowest limit of quantification observed with Simoa when comparing NDEVs content between AD and CN participants (Figure 5). Future studies should focus on improving the isolation protocol to increase the total number of NDEVs, thereby enhancing the concentration of detectable biomarkers. Another limitation was the use of NCAM1, which, although currently the best option, exclusively labeling neurally-derived EVs. Identifying a specific EV marker for neurons could improve the isolation of this particular subpopulation.

5. Conclusions

In conclusion, our study provides valuable insights into the challenges regarding the use of blood biomarkers for AD diagnosis. The intricate relationships observed between NDEVs and soluble AD biomarkers emphasize the need for comprehensive consideration when interpreting biomarker levels in CN participants.

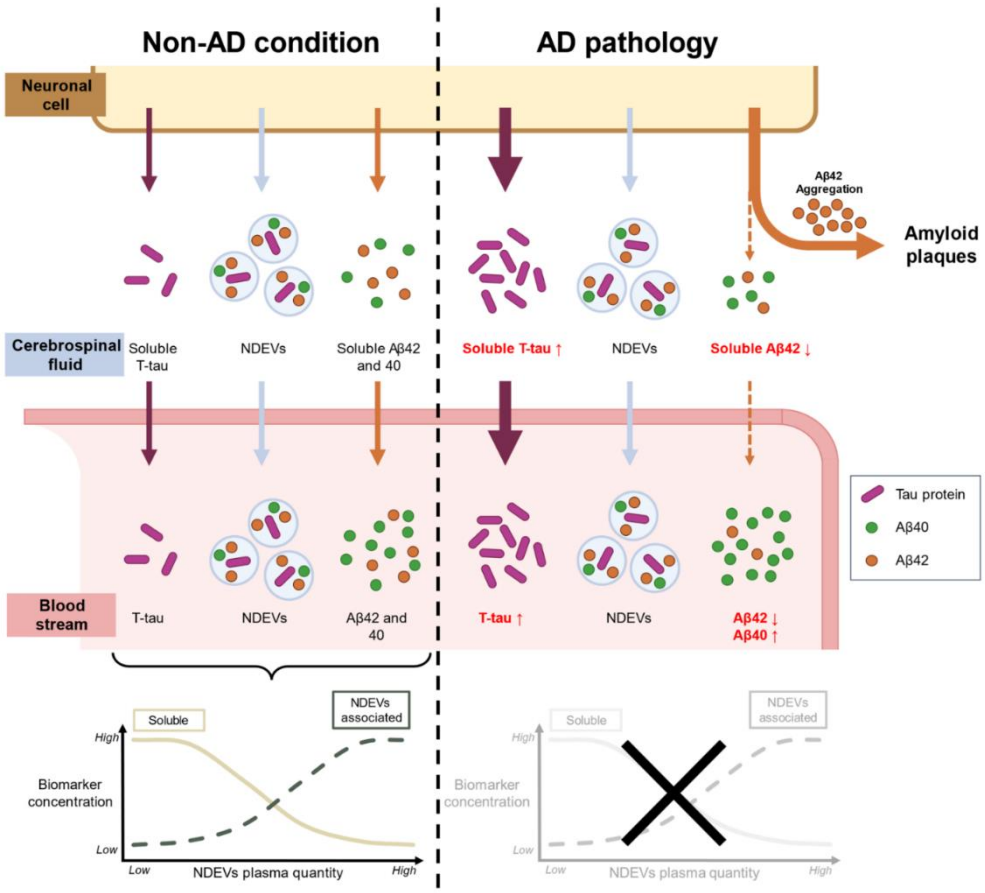

Figure 6. Summary of the main findings.

In the non-AD condition (**left part**), tau protein and amyloid are found either circulating in plasma as soluble (freely circulating) or linked to NDEVs. For total-tau, Aβ42 and Aβ40, the proportion of soluble plasma biomarkers is highly correlated with plasma NDEVs quantity and their content in biomarkers. This distribution between NDEVs and the soluble compartment is balanced in non-AD (as represented in the **bottom-left graph**), reflecting the mechanisms of tau and amyloid production at the neuronal level observed in in vitro models. In AD pathology (**right part**), the release of Aβ and tau is increased, leading to an increased concentration of tau, and a transitional increase of Aβ42-40, in the CSF. This amyloid is more prone to aggregation and will form amyloid plaques, resulting in a decreased quantity in the CSF. The same pattern is observed in the plasma of AD patients, but the dynamics regarding plasma NDEVs are here imbalanced by

the development of AD pathology (as represented in the **bottom-right graph**). The content or number of NDEVs seems not to be good AD biomarkers, whereas variations in plasma soluble biomarkers are more accurate for AD diagnosis.

Declarations

Ethics approval and consent to participate: Participants provided informed consent and demonstrated comprehension of the study's objectives and procedures. All experimental protocols adhered to the ethical standards set forth in the Declaration of Helsinki and underwent approval by local Institutional Review Boards (Institutional Ethics Committee of Clinics Saint-Luc University Hospital, 1200 Brussels, Belgium, Ethical protocols UCL-2022-473; UCL-2016-121 and UCL-2018-119).

Consent for publication: not applicable.

Availability of data and materials: All data collected in the context of this study will be made available in an anonymized form upon the publication of the article.

Competing interests: K.S is a member of the Alzheimer's Research & Therapy editorial board. She was not involved in the assessment or decision-making process for this manuscript.

Funding: This work was supported by the Belgian Fund for Scientific Research (grant numbers ASP40001844, CCL40010417, FNRS J.0106.22); the Fonds de la Recherche Fondamentale Stratégique - Walloon Excellence in Life Sciences and Biotechnology (grant number 40010035); the SAO-FRA Alzheimer's Research Foundation (grant number SAO-FRA 2018/0025, and SAO-FRA 2020/0028); the UCLouvain Action de Recherche Concertée (grant number ARC21/26-114); the Fondation Louvain; the Fondation St Luc, the Fonds européen de développement regional and the Queen Elisabeth Medical Foundation.

Authors contribution: Conceptualization, E.B.; methodology, E.B. and L.D; software, E.B.; formal analysis, E.B., L.D., M.D. and K.S.; investigation, E.B., L.C and B.H.; resources, B.H., P.K.C.; writing—original draft preparation, E.B.; writing—review and editing, E.B.,L.D., L.C., M.D, N.S., B.H and P.K.C.; visualization and figures conception, E.B and L.D; supervision, B.H., P.K.C.; funding acquisition, B.H. and P.K.C. All authors have read and agreed to the published version of the manuscript.

Acknowledgments: We thank all participants and the Stichting Alzheimer's Onderzoek for their help in our study. We thank Daniela Savina, Yasmine Salman, Lisa Quenon and Lara Huyghe for their technical supports.

PART III

GENERAL DISCUSSION

Considerations for the use of plasmatic biomarkers in the AD field

The development of tools to detect and quantify plasma biomarkers has become a key focus in the Alzheimer's disease field and more generally in dementia research over recent years. While several plasma biomarkers have been identified, they were initially restricted to the research domain and have yet to be fully validated to be integrated into clinical practice. The current and emerging plasma biomarker assays in the AD field offer promising diagnostic potential and could serve as valuable preliminary screening tools to assist in diagnosing symptomatic and preclinical asymptomatic individuals. With their ongoing standardization and refinement, they hold the potential to be employed across various stages of AD diagnosis and throughout the continuum of patient care.

Currently available immunoassays

Numerous companies have developed plasma tests targeting specific biomarkers within the AD spectrum, including amyloid-beta forms 42 and 40, as well as tau proteins phosphorylated at different residues. For instance, several immunoassay kits for amyloid detection are available from manufacturers such as Roche Diagnostics, Euroimmun, Fujirebio, and Quanterix. These kits allow the quantification of Aβ42 and Aβ40 in plasma; however, they are currently dedicated to research use only [145, 226]. In our research, we employed the Simoa

technology from Quanterix®, specifically using the Neurology 3-plex A kit to quantify Aβ42 and Aβ40 and the pTau181 V2.1 kit to quantify pTau181. The choice of Simoa was possible due to the recent acquisition of the SR-X™ Biomarker Detection System by the host laboratory. Comparative studies, such as the one conducted in 2023 [145], have demonstrated that the performance of the Simoa assay is comparable to other immunoassays, for example those from Euroimmun and Roche Diagnostics, in measuring the Aβ42/40 ratio in plasma. This study revealed that while these assays could predict amyloid PET positivity with an accuracy represented by an area under the curve (AUC) of 0.7, higher accuracy (AUC of 0.86) was achieved when plasma amyloid was quantified using immunoprecipitation-coupled to mass spectrometry. Despite appearing as a gold standard for biomarker quantification, mass spectrometry remains very hard to implement in clinical use for routine analysis due to its high cost and low throughput compared to immunoassays.

To our knowledge, as of 2022, only one immunoassay for measuring plasma Aβ42/40 has received approval for clinical use, specifically in Japan [227]. In contrast, the research landscape for tau protein biomarkers is more advanced. There are over ten immunoassay kits available for detecting various forms of phosphorylated tau (pTau) in plasma, including pTau181 and pTau217. Currently, these kits are still restricted to research applications. However, in March 2024, the Simoa pTau181 Advantage V2 Kit—used in our study—received Breakthrough Device designation from the U.S. Food and Drug Administration (FDA).

This designation is granted to products that show potential to provide a more effective diagnosis of life-threatening diseases with an unmet medical need. The FDA's recognition of the Simoa pTau181 kit as a breakthrough device highlights its promise in transforming diagnostic approaches for AD, bringing us closer to the routine clinical use of these advanced diagnostic tools. Still, these rapid advances in new diagnostic techniques based on high-sensitivity multiplex plasma assays must be accompanied by rigorous interpretation of the results obtained.

In our study, we established specific plasma thresholds for the Aβ42/40 ratio and phosphorylated tau181 levels to predict amyloid and tau deposition in the brain, as determined by PET imaging (with [^{11}C]-PIB and [^{18}F]-flutemetamol radiotracers for amyloid, and [^{18}F]-MK-6240 for tau). With this information we can predict the A+T+ status of the patients (indicative of AD pathology). This is also a new move in the field, since the A/T/N classification is a biologically-based staging of the disease that categorizes the individuals depending on the presence or not of biomarkers (+/-), with amyloid (A) and tau (T) being taken as references. This leads to the definition of AD individuals as A+T+, of whom some are asymptomatic (preclinical) in the early stages. A major challenge is thus to identify these individuals across the population for early and effective care.

The application of these plasma biomarkers has the potential to be transformative across various clinical and research settings. The

subsequent sections explore potential uses of these plasma thresholds and discuss their place alongside PET-scanner exams.

Plasma biomarkers as a sorting tool

The integration of such plasma biomarker tools into clinical practice could significantly enhance clinical decision-making. They would facilitate more accurate decisions on whether to refer an individual for confirmatory PET/CSF biomarker analysis, investigate alternative causes of symptoms, or develop an appropriate treatment and support plan. This approach could streamline referrals, reduce the number of unnecessary procedures, and ultimately decrease patient waiting times and alleviate the burden on specialist physicians. This is a particular asset in regions where long waiting periods are a critical issue [228].

Plasma biomarkers to enrich AD clinical trials

The use of plasma biomarkers could also enrich clinical trial population by screening out individuals who, for example, lack Aβ pathology. Several clinical trials are currently using plasma biomarker tests to enrich study populations by identifying symptomatic individuals with a high probability of Aβ pathology. This approach minimizes the need for unnecessary PET and/or CSF biomarker analyses that are commonly conducted during pre-trial screening. For instance, the use of plasma pTau181 and Aβ42/Aβ40 measurements to select suitable trial participants has been shown to enhance the efficiency of trial screening

processes, thereby reducing both the burden on participants and the timelines for recruitment [229].

Could plasma biomarkers replace PET and/or CSF biomarker analysis?

Given their less invasive nature and greater accessibility, plasma biomarkers hold the potential to eventually replace PET and/or CSF biomarker analysis in the future [230], and could reduce healthcare disparities by improving access, lowering costs, and addressing concerns associated with the invasiveness of lumbar punctures. Consequently, the use of plasma biomarkers could facilitate earlier diagnosis of AD in the general population. However, for plasma biomarkers to replace PET and/or CSF biomarkers, they must demonstrate high diagnostic performance comparable to current standards. Our research has shown that plasma pTau181 is less effective than CSF pTau181 in predicting tau burden, and the Aβ42/40 ratio does not adequately predict amyloid status, performing even less effectively than pTau181. Due to their peripheral localization, brain-derived plasma biomarkers are much less abundant than those in the CSF, where there is continuous exchange with the brain, especially due to low amount of CSF protein leaking to plasma through the BBB. Moreover, plasma biomarkers exist within a complex protein environment, and their levels could be affected by the expression of peripheral tissues (e.g. Aβ, [231]). Studies has shown that Aβ42 levels are positively correlated fat mass, and a series of observations implicate circulating Aβ in the systemic responses to nutrient excess and suggest

that Aβ is required for the development of insulin resistance in tissues such as the liver and skeletal muscle. These findings indicate the possibility of peripheral amyloid production. Altogether, this makes the establishment of plasma thresholds very challenging. There is a need for standardization of biomarker quantification and plasma preparation to facilitate their clinical implementation, as well as the need to combine different biomarkers to increase accuracy, given that biomarker concentrations in plasma are not as consistent across the AD population as those in CSF [232], especially due to presence of comorbidities such as chronic kidney failure, cancer and chronic inflammatory illness, which may impact plasma protein concentration and thus plasma AD biomarkers. Nevertheless, as technology advances and assays become more sensitive and validated across diverse populations, there is hope that plasma biomarkers may eventually be integrated into routine clinical practice, offering a less invasive and more accessible option for AD diagnosis.

Others potential AD biomarkers

Apart from soluble amyloid peptides and tau proteins, other potential plasma biomarkers are being studied. General biomarkers of neurodegeneration, such as neurofilament light chain proteins (NfL), which are released by degenerating neurons into the CSF and blood, show potential as plasma AD biomarkers. NfL concentrations in blood are correlated with those measured in CSF [233], suggesting their potential application in monitoring neurodegenerative diseases,

including AD. Other biomarkers linked to neuroinflammation, a key component of AD pathology, are also present in blood and could be used as biomarkers. GFAP (glial fibrillary acidic protein), an astrocyte activation marker linked to neuroinflammation, has shown a strong association with amyloid deposits in the brain [234]. However, even though these biomarkers explore other aspects of the disease, their standalone use is outperformed by specific AD biomarkers like amyloid and tau to identify AD pathology alongside other dementias, mainly because they are not specific to AD but are common to all neuroinflammatory and neurodegenerative conditions [235]. Still, we can imagine adding such measurements to those made in our work, which may increase the accuracy of tests, but also cost, when combined with the plasma Aβ42/40 ratio and pTau181.

Is Plasma pTau217 a Superior Biomarker for Alzheimer's Disease Compared to pTau181?

The present work made in this thesis conclude that Aβ42/40 in plasma is outperformed by pTau181. But additionnal measurment were done on our cohort of preclinical AD patients with the measurement of pTau217. Those measurements were possible du to a recent collaboration with the Cliniques Saint Pierre at Ottignies Belgium. Measurement of pTau217 was done by Lumipulse with the kit Lumipulse® G pTau217 (Fujirebio). We decided to analyse blood samples from n=103 participants of our cohort. 80 participants were non-demented, with 41 A-T-, 29 A+T+ 2 A-T+ and 8 A+T-, and 23 demented participants, with 21 A+T+ and 2 A-T-. The A+T+ status was as before determined by tau PET and amyloid PET.

pTau217 is better than pTau181 to predict amyloid and tau deposition evaluated by PET-CT

In the non-demented population and in all the participants, we could find a significant increase of plasma pTau217 in the A+ participants (Figure 1. A and B; Student's T Test, $p < 0.0001$). When compared to measures of plasma pTau181 in this same population, we found that pTau217 predicted with high accuracy amyloid status, with an AUC = 0.91 in all the participants, and in ND participants an AUC of 0.89 (Figure 1. C); which are sensitively way better than performances of pTau181 (with respectively AUC = 0.76 in all the participants and AUC = 0.77 in ND

population). We then performed the same statistics for the prediction of T+ status predetermined by tau PET. Plasma pTau217 was also significantly elevated in T+ participants in both populations (Figure 1. D and E, student's t test, $p < 0.0001$). Compared to pTau181, plasma pTau217 also predicted better T+ status, with AUC=0.92 in all the participants and AUC=0.90 in the ND subgroup, while pTau181 was less strong with only AUC=0.77 in all and 0.75 in the ND group (Figure 1. F).

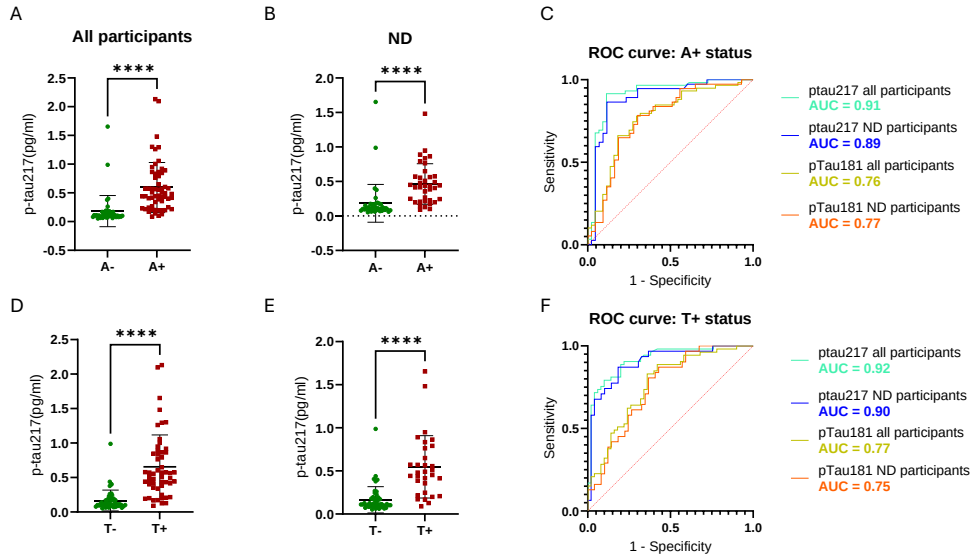

Figure 1. Plasma pTau217 compared to A+ and T+ status. **A**. Plasma pTau217 is significantly increased in A+ participants, **B**. and increased in non-demented participants. **C**. Plasma pTau217 predict better A+ status in both groups (AUC=0.91 and 0.89 when only the ND group is studied) compared to plasma pTau181. **D**. In all participants, pTau217 is increased in T+ participants; **E**. and increased in T+ ND participants. **F**. Compared to pTau181, pTau217 predict much better T+ status in both groups (AUC=0.92 in all the participants, and 0.90 in ND participants).

pTau217 predict better A+T+ status than pTau181

Finally, we examined the prediction of the A+T+ status (or AD status) among both groups with plasma pTau217 and compared it to pTau181. In both groups the quantity of plasmatic pTau217 was significantly increased in A+T+ participants compared to A-T- (Student's t test, *p<0.0001)*. The prediction of A+T+ status was also better with plasma pTau217 in both groups with highly sensitive and specific AUC (in all participants AUC=0.95, and in the ND group AUC=0.93), compared to plasma pTau181 (in all the participants AUC=0.80, and in the ND group AUC=0.79), making plasma pTau217 the best choice for accurate A+T+ diagnosis.

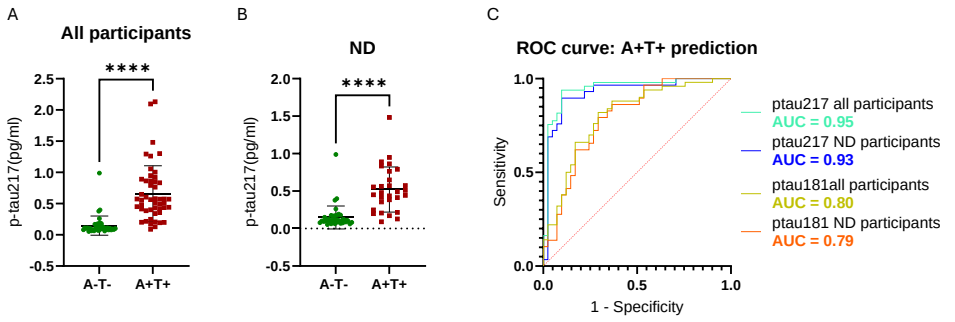

Figure 2. Plasma pTau217 compared to A+T+ status. **A**. In all the participants, pTau217 is significantly increase in A+T+ participants compared to A-T-; **B**. and increase in A+T+ ND participants. **C**. In both groups, plasma pTau217 predicted better A+T+ status (AUC=0.95 in all the participants and 0.93 in the ND group.

Plasma pTau217: to a clinical application?

These preliminary results on plasma pTau217 in a sample of our cohort show promising potential. With an AUC of 0.93 for predicting A+T+ status in a non-demented population, plasma pTau217 is approaching clinically acceptable thresholds for risk assessment. In

contrast, current results for plasma pTau181 and Aβ42/40 are insufficient for definitive AD diagnosis, serving instead to stratify individuals by risk and guide neurologists in deciding whether to pursue further assessments, such as CSF analysis or amyloid and tau PET-CT imaging.

Notably, plasma pTau217 demonstrates performance nearing that of CSF pTau181, which has already been incorporated into clinical practice. For CSF pTau181, the AUC for distinguishing AD patients from controls is 0.98 (CI [0.969-1.000])[236], while plasma pTau217 in our preliminary results achieves an AUC of 0.95 (CI [0.894-0.997]). Importantly, blood sampling is substantially more accessible and less invasive than CSF collection, making venipuncture a preferable, less painful, and less stressful procedure for patients. Our statistical analysis indicates that plasma pTau217 closely approximates the diagnostic accuracy of CSF pTau181.

Other studies have reached the same conclusion: pTau217 is a reliable biomarker for predicting both A+ and T+ status and assessing MCI patients. Most studies indicate that plasma pTau217 outperforms pTau181 and the Aβ42/40 ratio in predicting both amyloid PET and tau PET positivity [237, 238]. Comparisons to CSF pTau217 have shown that plasma pTau217 achieves similar accuracy in identifying brain amyloid deposition [239], however, in cases of low brain amyloid, combining plasma pTau217 with Aβ42/40 can further improve diagnostic accuracy [237]. It has also been observed that plasma pTau217 immunoassays

(Simoa, Lumipulse, MSD) perform as well as the gold standard—pTau217 measurement by mass spectrometry—in identifying amyloid PET-positive individuals in MCI populations [240]. Overall, studies on pTau217 consistently suggest that plasma pTau217 could be transformative for AD diagnosis, particularly in MCI populations, with performance comparable to CSF analysis, making it likely for clinical application in the coming years.

In our view, biomarkers such as plasma pTau217 hold significant promise for AD diagnosis and monitoring, potentially offering convenient access to reliable indicators of amyloid and tau pathology in the brain.

Considerations for the study of extracellular vesicles in biofluids

From the study of blood biomarkers, a new area of interest has emerged: extracellular vesicles (EVs). The scientific community now acknowledges their presence in the blood. Several studies, particularly in cancer research, have shown that the content of these vesicles can indicate their cellular origin and potentially be used as biomarkers for monitoring disease progression or for diagnosis. Additionally, research teams in pharmacology are exploring the use of EVs produced in vitro for targeted drug delivery, aiming to increase the efficiency of future treatments. While research dedicated to EVs is rapidly evolving, it faces significant challenges, particularly due to the small size of these vesicles, which hampers their use as biomarkers or in therapeutic applications. These EVs hold promise for Alzheimer's research, where they could be investigated as potential biomarkers for early diagnosis or as vectors for delivering therapeutic agents, opening new avenues for understanding and treating neurodegenerative diseases.

EVs in blood: the challenge of EVs purification

Due to their size, EVs isolation protocols need to be standardized to ensure good purity from common contaminants found in blood and maintain reproducibility between experiments. The major confounders in EVs isolation and detection are lipoproteins and plasma proteins, both abundant in blood. The lipoproteins are included in the family of

particles described as “non-vesicular extracellular particles” (NVEPs) [241], including high-density, low-density, intermediate-density and very low-density lipoproteins (HDL, LDL, IDL, VLDL). Those different structures overlap in size, density and molecular composition with EVs present in blood, requiring an extremely standardized protocol for isolation and characterization of EVs from blood. Depending on the technique used for EVs isolation, some contamination with lipoprotein structures can occur. The other main confounders are the circulating soluble proteins found in blood. These proteins are of major concern when researchers study the content of blood EVs, as soluble protein contamination in EV fractions could compromise the accuracy of the results. The main soluble proteins circulating in the blood are serum albumin, immunoglobulins and fibrinogen which are ten times concentrated than AD plasma biomarkers, tau and pTau proteins and amyloid β peptides isoforms [242, 243].

Since 2014 and the first publication of guidelines for EVs isolation, two major updates have been published (one in 2018 and one in 2024) trying to improve EVs isolation protocols to resolve the impact of confounders (described above). First, the conditions of venipuncture and blood processing need to be consistent across the entire cohort of participants. In our research, we ensured consistency by using a 21g needle and processing the plasma within 2 hours. Those two points are crucial since using a small needle activates the platelets and promotes hemolysis, two main events leading to contamination of EVs preparation. The MISEV 2024 guidelines [241] recommend using either

plasma or serum samples, but advise against using hemolysate samples. While routine hemolysis analysis are not commonly performed in most non-clinical laboratories, the guidelines suggest at least a visual inspection for hemolysis, which we also conducted in our research.

Methods for EVs isolation are crucial for downstream analytical assays from blood plasma or serum. These methods rely on four primary principles: size, density, charge, and molecular composition. Common techniques include ultracentrifugation, density gradient centrifugation, size-exclusion chromatography, and emerging affinity-based chromatography. However, no single method can exclusively isolate all EVs, as they often overlap in size and density with platelets and lipoproteins. The combination of several methods is preferable if the EVs preparation needs to be pure, although it comes at the cost of reducing the total number of EVs collected. In our isolation of EVs from plasma, size-exclusion chromatography efficiently separates EVs from soluble proteins, but some NVEPs may still contaminate the EV pool. Adding a filtration step with specific pore sizes increased EV purity and concentrated the total EV pool. Alternatively, a density gradient centrifugation step could have been used to separate NVEPs, though this might compromise protocol consistency and results in poor EV recovery.

Ideally, the isolation protocol should be tailored to the specific goals of the experiment, balancing the need for high EV yield with the desire for high purity and reproducibility.

EVs as biomarkers of Alzheimer's disease

EVs have the potential to enhance the accuracy of diagnosing and monitoring neurodegenerative diseases in several ways. One significant aspect is that some EVs found in the blood are directly derived from brain cells. The main challenge is to identify specific markers on the surface of EVs originating from the brain, which would enable more precise studies of this specific subpopulation of EVs. Currently, the two main neuronal EV markers used are LCAM1 and NCAM, which are expressed by both neurons and glial cells, but are not entirely specific to these cell types. In our study we decided to use NCAM considering recent controversy suggesting that LCAM1 may be present in plasma as soluble clusters rather than within EVs. Nevertheless, NCAM is also expressed by NK (natural killer) cells, which are produced in the bone marrow and secondary lymphoid tissues (distributed throughout the body), and make up about 10% of circulating lymphocytes. NK cells play a role in early cytotoxic responses against viruses, parasites and microbial pathogens, and in tumor immunosurveillance. Their activation leads to the secretion of various cytokines and chemokines that recruit other immune effector cells to the target site. These different components are believed to be secreted in EVs, meaning that EVs derived from NK cells are present in the blood as well [244]. To isolate brain-derived EVs, a specific NK cell marker not expressed by neurons, such as CD16 (also known as Fc gamma receptor IIIa), could be used to deplete the pool of CD56-positive EVs [245]. However, adding a second immunoprecipitation step to the isolation process in our study could

have reduced the quantity and integrity of the NDEVs. Another approach is to search for other specific neuronal membrane markers that might be present in EVs derived from neurons. Still, there is no evidence that NK derived EVs could contain amyloid peptides or tau proteins. Currently, there is no consensus on the preferred use of NCAM or LCAM1.

Despite the challenges in isolating NDEVs, this specific type of EV has the potential to carry pathological markers of neurodegenerative diseases. In our study, we measured amyloid-beta (Aβ42 and Aβ40) levels in NDEVs. Given that the cohort in our study is larger than the population used for NDEVs measurement, future research could extend the measurement of amyloid biomarkers to include the entire cohort and incorporate additional markers such as pTau181. Additionally, there is a need for comprehensive work to identify novel biomarkers beyond amyloid and tau. Recent studies have identified the N-methyl-D-aspartate receptor 2A (NMDA2A) as an AD biomarker present in NDEVs in blood [242]. This protein is a receptor for the neurotransmitter glutamate and plays a key role in strengthening synaptic interactions, which are important for learning and memory. Changes in NMDA receptors are reported to occur early in AD pathology. A significant decrease in NMDAR2A levels has been found in EVs of AD patients, compared to CN controls and patients with dementia due to Parkinson's disease, which may reflect neuronal synaptic loss more directly than the measurement of CD56 positive EVs amount as conducted in our study. Another study measured TDP-43 and full-length tau proteins in plasma EVs using dedicated immunoassays [246], allowing for the specific

measurement of tau 3R-repeat and 4R-repeat isoforms. They found that TDP-43 levels in EVs were high in patients with amyotrophic lateral sclerosis, and the EV tau ratio 3R/4R was low in patients with supranuclear palsy and high in patients with frontotemporal dementia.

Another approach involves the measurement of EV miRNAs (microRNAs). These small non-coding RNAs, which modulate RNA expression, have been found to reflect several pathogenic processes. Their dysregulation has been associated with the pathological status of AD [247]. Although these miRNAs can circulate freely in blood plasma or CSF, they are more stable when contained within small EVs, such as exosomes. Studies of exosomal miRNAs in the context of AD have identified specific miRNAs that are either up-regulated or down-regulated in AD patients, distinguishing them from CN healthy participants and those with other neurodegenerative diseases [248, 249].

These results are encouraging regarding the potential of measuring other biomarkers in AD, especially tau protein isoforms, which are known to help in the differential diagnosis of neurodegenerative diseases.

Potential use of EVs as therapeutic agents

One potential use of EVs could be as carriers for delivering new drugs to the brain. A significant limitation in treating AD is the need for drugs to cross the BBB to effectively reach brain lesions. Apart from

drugs injected directly into the spinal cord, most immunotherapies have limited ability to cross the BBB. It has been confirmed that EVs can cross the BBB, and EVs from various sources can enter the CNS [250]. The use of EVs for drug delivery could facilitate the BBB crossing and increase the specific targeting of cells. The pioneering work in this field was published over a decade ago. Researchers incorporated short interfering RNAs (siRNAs) against BACE1 into EVs derived from murine dendritic cells, which were engineered to express Lamp2b (an exosomal membrane protein) fused with the neuron-specific RVG peptide. When injected intravenously, the RVG-targeted EVs demonstrated specific delivery of the siRNA to the CNS and resulted in a knockdown of *BACE1*, a protease involved in amyloid-beta production, in wild-type mice [251]. More recent studies have reviewed the current progress on stem cell-derived EVs. The advantage of using stem cells lies in their ability to differentiate into any cell type, allowing for the production of EVs derived from various cell types. Stem cell-derived EVs have been reported to reduce the age-related senescence and tissue dysfunction in mice [252]. This effect could be mainly due to the role EVs play in maintaining cellular homeostasis by removing excess, unwanted, or damaged biomolecules.

However, this beneficial effect could be counterbalanced by the potential role of NDEVs in spreading tau and amyloid, which could make these EVs both protective and disease-promoting in certain contexts. Stem cell-derived EVs could also be used as cargo for drug delivery, allowing easy BBB crossing. In an era of emerging new treatments for AD,

with the recent FDA approvals of Aducanumab and Lecanemab in the U.S, it is conceivable that such anti-amyloid and future anti-tau drugs could be delivered directly to the brain parenchyma by EVs, specifically targeting neurons and AD-related lesions.

PART IV

GENERAL CONCLUSION

PART IV. GENERAL CONCLUSION

This work was the first to establish an extensive plasma biobank at UCLouvain within the context of AD research. We have now collected more than 500 plasma samples from 400 individuals, ranging from cognitively normal persons to preclinical AD patients and those with AD dementia. We have evaluated the amyloid and tau status of over 200 participants using a dedicated PET scanner, and since the end of 2023, we have collected follow-up data spanning 1 to 2 years from our patients. This biobank has the potential to be shared with other universities for the development of new immunoassay kits or the study of novel plasma biomarkers. We are currently expanding our plasma sample collection to include other clinical centers in Wallonia (Charleroi and Ottignies) by the second semester of 2024, which will further enrich our cohort with additional AD patient samples.

Our research has enabled us to establish various thresholds for predicting AD status based on plasma ratios of Aβ42/40 and pTau181. The innovative aspect of our approach lies in the use of tau and amyloid PET to enrich our cohort with preclinical AD patients. This has allowed us to calculate pathological thresholds within a cognitively normal population, whereas most studies typically use only cognitively impaired AD patients and cognitively normal participants.

Moreover, our work on NDEVs has highlighted the significant challenges associated with their isolation and the standardization of content measurements. Despite these challenges, we have demonstrated that the quantity of NDEVs circulating in the blood can

interfere with the quantification of soluble biomarkers in cognitively normal participants, as a portion of these biomarkers are directly linked to circulating NDEVs.

In conclusion, we do believe that this thesis represents a significant advancement in AD research through the establishment of a comprehensive plasma biobank and the development of novel biomarkers for early detection and diagnosis. Our findings provide valuable insights into the pathophysiology of AD and open up new avenues for collaborative research and clinical applications.

List of abbreviations

A+	Amyloid pathology presence
AD	Alzheimer's Disease
ADAD	Autosomal dominant AD
AICD	Amyloid intracellular domain
APOE	Apolipoprotein E gene
apoE	Apolipoprotein
APOER	Apolipoprotein receptor
APP	Amyloid precursor protein
AUC	Area under the curve
Aβ	Amyloid beta
CBD	Corticobasal dementia
CI	Confidence interval
CN	Cognitively normal
CNS	Central nervous system
CSF	Cerebrospinal fluid
CTF α and β	C-terminal fragment α and β
ECLIA	Electrochemiluminescence immunoassay
ELISA	Enzyme-Linked Immunosorbent Assay
EOAD	Early onset AD
ESCRT	Endosomal sorting complex required for transport
EVs	Extracellular vesicles
FAD	Familial AD
FAT	Fast axonal transport
FcRn	Neonatal Fc receptor
FDA	Food and Drug
FTLD	Fronto-temporal dementia
GMM	Gaussian mixture model
IgG	Immunoglobulin G
LAMP1-2	Lysosome-associated membrane protein 1 and 2
LDL	Low-density lipoproteins
LH	Likelihood ratio
LMPs	Lysosomal membrane proteins
LOAD	Late onset AD
LRP	Lipoprotein receptor-related protein

LRP1	Lipoprotein receptor-related protein 1
MA	Maladie d'Alzheimer
MCI	Mild cognitive impairment
MMSE	Mini Mental State Evaluation
MoCA	Montréal Cognitive Assessment
MRI	Magnetic resonance imaging
MSD	Meso Scale Discovery
MTBR	Microtubule-binding repeat
MVE	Multivesicular endosome
N+	Presence of neurodegeneration
NCAM	Neuronal cell adhesion molecule
NCT	Nicastrin
NDEVs	Neurally derived EVs
NFTs	Neurofibrillary tangles
NMDAR	N-methyl-D-aspartic acid receptor
p75NRT	p75 neurotrophin receptor
PET	Positron emission tomography
PSP	Progressive supranuclear palsy
pTau	Phosphorylated tau
SEC	Size exclusion chromatography
Simoa	Single molecule array
T+	Tau pathology presence
TEMs	Tetraspanin-enriched microdomains

Bibliography

1. Lane, C.A.-O., J. Hardy, and J.M. Schott, *Alzheimer's disease*. (1468-1331 (Electronic)).
2. *Alzheimer's Disease International. World Alzheimer Report 2019*. . 2019.
3. Alzheimer A Fau - Stelzmann, R.A., et al., *An English translation of Alzheimer's 1907 paper, "Uber eine eigenartige Erkankung der Hirnrinde"*. (0897-3806 (Print)).
4. Brion, J.-P.P., H.; Nunez, J.; Flament-Durand, J. r., *Mise en évidence immunologique de la protéine tau au niveau deslésions de dégénérescence neurofibrillaire de la maladie d'Alzheime*. Arch. Biol., 1985. **95**: p. 229–235.
5. Glenner, G.G. and C.W. Wong, *Alzheimer's disease and Down's syndrome: Sharing of a unique cerebrovascular amyloid fibril protein*. Biochemical and Biophysical Research Communications, 1984. **122**(3): p. 1131-1135.
6. Khachaturian, Z.S., *Diagnosis of Alzheimer's disease*. (0003-9942 (Print)).
7. Mirra, S.S., et al., *The Consortium to Establish a Registry for Alzheimer's Disease (CERAD). Part II. Standardization of the neuropathologic assessment of Alzheimer's disease*. (0028-3878 (Print)).
8. Newell, K.L., et al., *Application of the National Institute on Aging (NIA)-Reagan Institute criteria for the neuropathological diagnosis of Alzheimer disease*. (0022-3069 (Print)).
9. Ferri, C.P., et al., *Global prevalence of dementia: a Delphi consensus study*. (1474-547X (Electronic)).
10. *Dementia*. 15 March 2023, World Health Organisation.
11. Blennow, K., H. de Leon Mj Fau - Zetterberg, and H. Zetterberg, *Alzheimer's disease*. (1474-547X (Electronic)).
12. van der Flier, W.M., et al., *Early-onset versus late-onset Alzheimer's disease: the case of the missing APOE ε4 allele*. (1474-4465 (Electronic)).
13. Mecocci, P., et al., *Brain Aging and Late-Onset Alzheimer's Disease: A Matter of Increased Amyloid or Reduced Energy?* Journal of Alzheimer's Disease, 2018. **64**: p. S397-S404.
14. Jacobs, D., et al., *Age at onset of Alzheimer's disease: relation to pattern of cognitive dysfunction and rate of decline*. (0028-3878 (Print)).
15. Panegyres, P.K. and H.Y. Chen, *Differences between early and late onset Alzheimer's disease*. (2165-591X (Print)).
16. Jefferies, K. and N. Agrawal, *Early-onset dementia*. Advances in Psychiatric Treatment, 2009. **15**(5): p. 380-388.
17. Baillon, S., et al., *Prevalence and Severity of Neuropsychiatric Symptoms in Early- Versus Late-Onset Alzheimer's Disease*. American Journal of Alzheimer's Disease & Other Dementias®, 2019. **34**(7-8): p. 433-438.
18. *From the Centers for Disease Control and Prevention. Public*

health and aging: trends in aging--United States and worldwide. (0098-7484 (Print)).

19. Qiu, C., E. Kivipelto M Fau - von Strauss, and E. von Strauss, *Epidemiology of Alzheimer's disease: occurrence, determinants, and strategies toward intervention*. (1294-8322 (Print)).
20. Robinson, M., B.Y. Lee, and F.T. Hane, *Recent Progress in Alzheimer's Disease Research, Part 2: Genetics and Epidemiology*. Journal of Alzheimer's Disease, 2017. **57**(2): p. 317-330.
21. Yamazaki, Y., et al., *Apolipoprotein E and Alzheimer disease: pathobiology and targeting strategies*. Nature Reviews Neurology, 2019. **15**(9): p. 501-518.
22. Singh, P.P., M. Singh, and S.S. Mastana, *APOE distribution in world populations with new data from India and the UK*. Annals of Human Biology, 2006. **33**(3): p. 279-308.
23. Engelborghs, S., et al., *Prospective Belgian study of neurodegenerative and vascular dementia: APOE genotype effects*. (0022-3050 (Print)).
24. Serrano-Pozo, A., S. Das, and B.T. Hyman, *APOE and Alzheimer's disease: advances in genetics, pathophysiology, and therapeutic approaches*. The Lancet Neurology, 2021. **20**(1): p. 68-80.
25. Zhao, N., et al., *Alzheimer's risk factors age, APOE genotype, and sex drive distinct molecular pathways*. Neuron, 2020. **106**(5): p. 727-742. e6.
26. Tanzi, R.E., *The genetics of Alzheimer disease. LID - 10.1101/cshperspect.a006296 [doi] LID - a006296*. (2157-1422 (Electronic)).
27. Maloney, J.A., et al., *Molecular mechanisms of Alzheimer disease protection by the A673T allele of amyloid precursor protein*. (1083-351X (Electronic)).
28. Zheng, H. and E.H. Koo, *Biology and pathophysiology of the amyloid precursor protein*. (1750-1326 (Electronic)).
29. Müller, U.C., T. Deller, and M. Korte, *Not just amyloid: physiological functions of the amyloid precursor protein family*. (1471-0048 (Electronic)).
30. Goate, A., et al., *Segregation of a missense mutation in the amyloid precursor protein gene with familial Alzheimer's disease*. (0028-0836 (Print)).
31. Jacobsen, K.T. and K. Iverfeldt, *Amyloid precursor protein and its homologues: a family of proteolysis-dependent receptors*. Cellular and Molecular Life Sciences, 2009. **66**(14): p. 2299-2318.
32. Zhang, Y.-W., et al., *APP processing in Alzheimer's disease*. Molecular Brain, 2011. **4**(1): p. 3.
33. Kuhn, P.H., et al., *ADAM10 is the physiologically relevant, constitutive alpha-secretase of the amyloid precursor protein in primary neurons*. (1460-2075 (Electronic)).
34. Yu, G., et al., *Nicastrin modulates presenilin-mediated notch/glp-1 signal transduction and betaAPP processing*. (0028-0836 (Print)).
35. Takasugi, N., et al., *The role of presenilin cofactors in the γ-secretase complex*. Nature, 2003. **422**(6930): p. 438-441.
36. Kuhn, A.J. and J. Raskatov, *Is the p3 Peptide (Aβ17-40, Aβ17-42) Relevant to the Pathology of Alzheimer's Disease?1*. (1875-8908 (Electronic)).
37. Kuhn, A.J., et al., *Alzheimer's Disease "Non-amyloidogenic" p3*

Peptide Revisited: A Case for Amyloid-α. (1948-7193 (Electronic)).
38. Tomita, T., *Molecular mechanism of intramembrane proteolysis by γ-secretase*. (1756-2651 (Electronic)).
39. Chen, G.-f., et al., *Amyloid beta: structure, biology and structure-based therapeutic development*. Acta Pharmacologica Sinica, 2017. **38**(9): p. 1205-1235.
40. De Felice, F.G., et al., *Abeta oligomers induce neuronal oxidative stress through an N-methyl-D-aspartate receptor-dependent mechanism that is blocked by the Alzheimer drug memantine*. (0021-9258 (Print)).
41. Rönicke, R., et al., *Early neuronal dysfunction by amyloid β oligomers depends on activation of NR2B-containing NMDA receptors*. Neurobiology of aging, 2011. **32**(12): p. 2219-2228.
42. Wang, H.-Y., et al., *α7 nicotinic acetylcholine receptors mediate β-amyloid peptide-induced tau protein phosphorylation*. Journal of Biological Chemistry, 2003. **278**(34): p. 31547-31553.
43. Hashimoto, Y., et al., *Molecular characterization of neurohybrid cell death induced by Alzheimer's amyloid-β peptides via p75NTR/PLAIDD*. Journal of neurochemistry, 2004. **90**(3): p. 549-558.
44. Fernandez-Vizarra, P., et al., *Immunoglobulin G Fc receptor deficiency prevents Alzheimer-like pathology and cognitive impairment in mice*. Brain, 2012. **135**(9): p. 2826-2837.
45. Roychaudhuri, R., et al., *Amyloid beta-protein assembly and Alzheimer disease*. (0021-9258 (Print)).
46. Shi, J., et al., *Mutation screening and association study of the neprilysin gene in sporadic Alzheimer's disease in Chinese persons*. The Journals of Gerontology Series A: Biological Sciences and Medical Sciences, 2005. **60**(3): p. 301-306.
47. Deane, R., et al., *RAGE mediates amyloid-β peptide transport across the blood-brain barrier and accumulation in brain*. Nature medicine, 2003. **9**(7): p. 907-913.
48. Shibata, M., et al., *Clearance of Alzheimer's amyloid-β 1-40 peptide from brain by LDL receptor–related protein-1 at the blood-brain barrier*. The Journal of clinical investigation, 2000. **106**(12): p. 1489-1499.
49. Cockerill, I., et al., *Blood-Brain Barrier Integrity and Clearance of Amyloid-β from the BBB*. (0065-2598 (Print)).
50. Ramanathan, A., et al., *Impaired vascular-mediated clearance of brain amyloid beta in Alzheimer's disease: the role, regulation and restoration of LRP1*. Frontiers in aging neuroscience, 2015. **7**: p. 136.
51. Deane, R., et al., *IgG-assisted age-dependent clearance of Alzheimer's amyloid β peptide by the blood–brain barrier neonatal Fc receptor*. Journal of Neuroscience, 2005. **25**(50): p. 11495-11503.
52. Sardar Sinha, M., et al., *Alzheimer's disease pathology propagation by exosomes containing toxic amyloid-beta oligomers*. (1432-0533 (Electronic)).
53. Gallardo, G. and D.M. Holtzman, *Amyloid-β and Tau at the Crossroads of Alzheimer's Disease*. (0065-2598 (Print)).
54. Guo, T., W. Noble, and D.P. Hanger, *Roles of tau protein in health and disease*. (1432-0533 (Electronic)).
55. Jeganathan, S., et al., *Global hairpin folding of tau in solution*.

Biochemistry, 2006. **45**(7): p. 2283-2293.
56. He, H.J., et al., *The proline-rich domain of tau plays a role in interactions with actin*. BMC cell biology, 2009. **10**: p. 1-12.
57. Morris, M., et al., *Tau post-translational modifications in wild-type and human amyloid precursor protein transgenic mice*. Nature neuroscience, 2015. **18**(8): p. 1183-1189.
58. Li, L., et al., *Tau Ubiquitination in Alzheimer's Disease*. (1664-2295 (Print)).
59. Ittner, L.M., et al., *Dendritic function of tau mediates amyloid-β toxicity in Alzheimer's disease mouse models*. Cell, 2010. **142**(3): p. 387-397.
60. Janelidze, S., et al., *Plasma P-tau181 in Alzheimer's disease: relationship to other biomarkers, differential diagnosis, neuropathology and longitudinal progression to Alzheimer's dementia*. Nature medicine, 2020. **26**(3): p. 379-386.
61. Barthélemy, N.R., et al., *Cerebrospinal fluid phospho-tau T217 outperforms T181 as a biomarker for the differential diagnosis of Alzheimer's disease and PET amyloid-positive patient identification*. Alzheimer's research & therapy, 2020. **12**: p. 1-11.
62. Cohen, T.J., et al., *Intrinsic tau acetylation is coupled to auto-proteolytic tau fragmentation*. PloS one, 2016. **11**(7): p. e0158470.
63. Min, S.-W., et al., *Critical role of acetylation in tau-mediated neurodegeneration and cognitive deficits*. Nature medicine, 2015. **21**(10): p. 1154-1162.
64. Cohen, T.J., et al., *The acetylation of tau inhibits its function and promotes pathological tau aggregation*. Nature communications, 2011. **2**(1): p. 252.
65. Swatek, K.N. and D. Komander, *Ubiquitin modifications*. Cell research, 2016. **26**(4): p. 399-422.
66. Grumati, P. and I. Dikic, *Ubiquitin signaling and autophagy*. Journal of Biological Chemistry, 2018. **293**(15): p. 5404-5413.
67. Kim, J.H., et al., *CHIP-mediated hyperubiquitylation of tau promotes its self-assembly into the insoluble tau filaments*. Chemical Science, 2021. **12**(15): p. 5599-5610.
68. Dickey, C.A., et al., *Deletion of the ubiquitin ligase CHIP leads to the accumulation, but not the aggregation, of both endogenous phospho-and caspase-3-cleaved tau species*. Journal of Neuroscience, 2006. **26**(26): p. 6985-6996.
69. Ghag, G., et al., *Soluble tau aggregates, not large fibrils, are the toxic species that display seeding and cross-seeding behavior*. Protein Science, 2018. **27**(11): p. 1901-1909.
70. Chen, Q., et al., *Tau protein is involved in morphological plasticity in hippocampal neurons in response to BDNF*. (1872-9754 (Electronic)).
71. DeKosky, S.T. and S.W. Scheff, *Synapse loss in frontal cortex biopsies in Alzheimer's disease: correlation with cognitive severity*. (0364-5134 (Print)).
72. Hanger, D.P., D. Goniotaki, and W. Noble, *Synaptic Localisation of Tau*. (0065-2598 (Print)).
73. Colin, M., et al., *From the prion-like propagation hypothesis to therapeutic strategies of anti-tau immunotherapy*. Acta Neuropathologica, 2020. **139**(1): p. 3-25.
74. Banks, W.A., *From blood-brain barrier to blood-brain interface:*

new opportunities for CNS drug delivery. (1474-1784 (Electronic)).
75. Erickson, M.A. and W.A. Banks, *Blood-brain barrier dysfunction as a cause and consequence of Alzheimer's disease*. (1559-7016 (Electronic)).
76. Combs, B., et al., *Tau and Axonal Transport Misregulation in Tauopathies*. (0065-2598 (Print)).
77. Morfini, G., et al., *Conventional kinesin: Biochemical heterogeneity and functional implications in health and disease*. (1873-2747 (Electronic)).
78. van Niel, G., G. D'Angelo, and G. Raposo, *Shedding light on the cell biology of extracellular vesicles*. Nature Reviews Molecular Cell Biology, 2018. **19**(4): p. 213-228.
79. Raposo, G. and W. Stoorvogel, *Extracellular vesicles: exosomes, microvesicles, and friends*. (1540-8140 (Electronic)).
80. Hurley, J.H., *ESCRT complexes and the biogenesis of multivesicular bodies*. (0955-0674 (Print)).
81. Saftig, P. and J. Klumperman, *Lysosome biogenesis and lysosomal membrane proteins: trafficking meets function*. Nature Reviews Molecular Cell Biology, 2009. **10**(9): p. 623-635.
82. Piper, R.C. and D.J. Katzmann, *Biogenesis and function of multivesicular bodies*. (1081-0706 (Print)).
83. Takahashi, R.H., et al., *Intraneuronal Alzheimer abeta42 accumulates in multivesicular bodies and is associated with synaptic pathology*. (0002-9440 (Print)).
84. Xiao, T., et al., *The role of exosomes in the pathogenesis of Alzheimer' disease*. (2047-9158 (Print)).
85. Falker, C., et al., *Exosomal cellular prion protein drives fibrillization of amyloid beta and counteracts amyloid beta-mediated neurotoxicity*. (1471-4159 (Electronic)).
86. Wakabayashi, T., et al., *Analysis of the γ-secretase interactome and validation of its association with tetraspanin-enriched microdomains*. Nature Cell Biology, 2009. **11**(11): p. 1340-1346.
87. Seipold, L. and P. Saftig, *The Emerging Role of Tetraspanins in the Proteolytic Processing of the Amyloid Precursor Protein*. Frontiers in Molecular Neuroscience, 2016. **9**.
88. Braak, H., et al., *Staging of Alzheimer disease-associated neurofibrillary pathology using paraffin sections and immunocytochemistry*. (0001-6322 (Print)).
89. Ruan, Z., *Extracellular vesicles drive tau spreading in Alzheimer's disease*. Neural Regeneration Research, 2022. **17**(2).
90. Wang, Y., et al., *The release and trans-synaptic transmission of Tau via exosomes*. Molecular Neurodegeneration, 2017. **12**(1): p. 5.
91. Chen, C.C., et al., *Elucidation of Exosome Migration across the Blood-Brain Barrier Model In Vitro*. (1865-5025 (Print)).
92. Morad, G., et al., *Tumor-Derived Extracellular Vesicles Breach the Intact Blood-Brain Barrier via Transcytosis*. (1936-086X (Electronic)).
93. Bateman Randall, J., et al., *Clinical and Biomarker Changes in Dominantly Inherited Alzheimer's Disease*. New England Journal of Medicine. **367**(9): p. 795-804.
94. Leuzy, A., et al., *In vivo Detection of Alzheimer's Disease*. (1551-4056 (Electronic)).

95. Jack Jr, C.R., et al., *Revised criteria for diagnosis and staging of Alzheimer's disease: Alzheimer's Association Workgroup*. Alzheimer's & Dementia, 2024. **n/a**(n/a).
96. Bayart, J.-L., et al., *Analytical and clinical performances of the automated Lumipulse cerebrospinal fluid Aβ42 and T-Tau assays for Alzheimer's disease diagnosis*. Journal of Neurology, 2019. **266**(9): p. 2304-2311.
97. Janelidze, S., et al., *CSF Aβ42/Aβ40 and Aβ42/Aβ38 ratios: better diagnostic markers of Alzheimer disease*. Annals of Clinical and Translational Neurology, 2016. **3**(3): p. 154-165.
98. Thal, D.R., et al., *Phases of A beta-deposition in the human brain and its relevance for the development of AD*. (0028-3878 (Print)).
99. Klunk, W.E., et al., *Imaging brain amyloid in Alzheimer's disease with Pittsburgh Compound-B*. Annals of Neurology, 2004. **55**(3): p. 306-319.
100. Morbelli, S. and M. Bauckneht, *Amyloid PET Imaging: Standardization and Integration with Other Alzheimer's Disease Biomarkers*. (1940-6029 (Electronic)).
101. Pemberton, H.A.-O., et al., *Quantification of amyloid PET for future clinical use: a state-of-the-art review*. (1619-7089 (Electronic)).
102. Villain, N., et al., *Regional dynamics of amyloid-β deposition in healthy elderly, mild cognitive impairment and Alzheimer's disease: a voxelwise PiB–PET longitudinal study*. Brain, 2012. **135**(7): p. 2126-2139.
103. Hanseeuw, B.A.-O., et al., *Defining a Centiloid scale threshold predicting long-term progression to dementia in patients attending the memory clinic: an [(18)F] flutemetamol amyloid PET study*. (1619-7089 (Electronic)).
104. Johnson, K.A., et al., *Appropriate use criteria for amyloid PET: a report of the Amyloid Imaging Task Force, the Society of Nuclear Medicine and Molecular Imaging, and the Alzheimer's Association*. (1535-5667 (Electronic)).
105. Shoghi-Jadid, K., et al., *Localization of Neurofibrillary Tangles and Beta-Amyloid Plaques in the Brains of Living Patients With Alzheimer Disease*. The American Journal of Geriatric Psychiatry, 2002. **10**(1): p. 24-35.
106. Mathis, C.A., et al., *Small-molecule PET Tracers for Imaging Proteinopathies*. Seminars in Nuclear Medicine, 2017. **47**(5): p. 553-575.
107. Villemagne, V.L., et al., *In vivo evaluation of a novel tau imaging tracer for Alzheimer's disease*. European Journal of Nuclear Medicine and Molecular Imaging, 2014. **41**(5): p. 816-826.
108. Pascoal, T.A., et al., *Longitudinal 18F-MK-6240 tau tangles accumulation follows Braak stages*. (1460-2156 (Electronic)).
109. Sperling, R.A., et al., *Toward defining the preclinical stages of Alzheimer's disease: recommendations from the National Institute on Aging-Alzheimer's Association workgroups on diagnostic guidelines for Alzheimer's disease*. (1552-5279 (Electronic)).
110. Albert, M.S., et al., *The diagnosis of mild cognitive impairment due to Alzheimer's disease: recommendations from the National Institute on Aging-Alzheimer's Association workgroups on diagnostic guidelines for Alzheimer's disease*. (1552-5279 (Electronic)).

111. Folstein, M.F., S.E. Folstein, and P.R. McHugh, *"Mini-mental state"*. Journal of Psychiatric Research, 1975. **12**(3): p. 189-198.
112. *Quantrix.com*. [cited 2018.
113. Lewczuk, P., et al., *Cerebrospinal Fluid Aβ42/40 Corresponds Better than Aβ42 to Amyloid PET in Alzheimer's Disease*. (1875-8908 (Electronic)).
114. Ashton, N.A.-O., et al., *Plasma p-tau231: a new biomarker for incipient Alzheimer's disease pathology*. (1432-0533 (Electronic)).
115. Moscoso, A., et al., *Time course of phosphorylated-tau181 in blood across the Alzheimer's disease spectrum*. (1460-2156 (Electronic)).
116. Hebert, L.E., et al., *Alzheimer disease in the United States (2010-2050) estimated using the 2010 census*. Neurology, 2013. **80**(19): p. 1778-1783.
117. Hardy, J.A. and G.A. Higgins, *Alzheimer's Disease: The Amyloid Cascade Hypothesis*. Science, 1992. **256**(5054): p. 184-185.
118. Vadukul, D.M., et al., *An evaluation of the self-assembly enhancing properties of cell-derived hexameric amyloid-β*. Scientific Reports, 2021. **11**(1): p. 11570.
119. Vrancx, C., et al., *Mechanism of Cellular Formation and In Vivo Seeding Effects of Hexameric β-Amyloid Assemblies*. Molecular Neurobiology, 2021. **58**(12): p. 6647-6669.
120. Mawuenyega, K.G., et al., *Decreased Clearance of CNS β-Amyloid in Alzheimer's Disease*. Science, 2010. **330**(6012): p. 1774-1774.
121. Andreasen, N., et al., *Cerebrospinal Fluid ^{2}-Amyloid(1-42) in Alzheimer Disease: Differences Between Early- and Late-Onset Alzheimer Disease and Stability During the Course of Disease*. ARCH NEUROL, 1999. **56**.
122. Wiltfang, J., et al., *Amyloid β peptide ratio 42/40 but not Aβ42 correlates with phospho-Tau in patients with low- and high-CSF Aβ40 load*. Journal of Neurochemistry, 2007. **101**(4): p. 1053-1059.
123. Hanseeuw, B.J., et al., *Association of Amyloid and Tau With Cognition in Preclinical Alzheimer Disease: A Longitudinal Study*. JAMA Neurology, 2019. **76**(8): p. 915.
124. Jack, C.R., et al., *NIA-AA Research Framework: Toward a biological definition of Alzheimer's disease*. Alzheimer's & Dementia, 2018. **14**(4): p. 535-562.
125. Donohue, M.C., et al., *Association Between Elevated Brain Amyloid and Subsequent Cognitive Decline Among Cognitively Normal Persons*. JAMA, 2017. **317**(22): p. 2305.
126. Park, S.A., et al., *Promising Blood Biomarkers for Clinical Use in Alzheimer's Disease: A Focused Update*. Journal of Clinical Neurology, 2022. **18**(4): p. 401.
127. Bateman, R.J., et al., *Human amyloid-β synthesis and clearance rates as measured in cerebrospinal fluid in vivo*. Nature Medicine, 2006. **12**(7): p. 856-861.
128. Rissin, D.M., et al., *Single-molecule enzyme-linked immunosorbent assay detects serum proteins at subfemtomolar concentrations*. Nature Biotechnology, 2010. **28**(6): p. 595-599.
129. Verberk, I.M.W., et al., *Plasma Amyloid as Prescreener for the Earliest A lzheimer Pathological Changes*. Annals of Neurology, 2018. **84**(5): p. 648-658.
130. Cheng, L., et al., *Plasma Aβ as a biomarker for predicting Aβ-PET*

status in Alzheimer's disease : a systematic review with meta-analysis. Journal of Neurology, Neurosurgery & Psychiatry, 2022. **93**(5): p. 513-520.

131. Janelidze, S., et al., *Plasma β-amyloid in Alzheimer's disease and vascular disease*. Scientific Reports, 2016. **6**(1): p. 26801.
132. Nakamura, A., et al., *High performance plasma amyloid-β biomarkers for Alzheimer's disease*. Nature, 2018. **554**(7691): p. 249-254.
133. Ovod, V., et al., *Amyloid β concentrations and stable isotope labeling kinetics of human plasma specific to central nervous system amyloidosis*. Alzheimer's & Dementia, 2017. **13**(8): p. 841-849.
134. Schindler, S.E., et al., *High-precision plasma β-amyloid 42/40 predicts current and future brain amyloidosis*. Neurology, 2019. **93**(17): p. e1647-e1659.
135. Giudici, K.V., et al., *Assessment of Plasma Amyloid-β 42/40 and Cognitive Decline Among Community-Dwelling Older Adults*. JAMA Network Open, 2020. **3**(12): p. e2028634.
136. Verberk, I.M.W., et al., *Plasma amyloid is associated with the rate of cognitive decline in cognitively normal elderly: the SCIENCe project*. Neurobiology of Aging, 2020. **89**: p. 99-107.
137. Sims, J.R., et al., *Donanemab in Early Symptomatic Alzheimer Disease: The TRAILBLAZER-ALZ 2 Randomized Clinical Trial*. JAMA, 2023. **330**(6): p. 512.
138. Van Dyck, C.H., et al., *Lecanemab in Early Alzheimer's Disease*. New England Journal of Medicine, 2023. **388**(1): p. 9-21.
139. Corder, E.H., et al., *Gene Dose of Apolipoprotein E Type 4 Allele and the Risk of Alzheimer's Disease in Late Onset Families*. Science, 1993. **261**(5123): p. 921-923.
140. Farrer, L.A., *Effects of Age, Sex, and Ethnicity on the Association Between Apolipoprotein E Genotype and Alzheimer Disease: A Meta-analysis*. JAMA, 1997. **278**(16): p. 1349.
141. Roses, M.D.A.D., *APOLIPOPROTEIN E ALLELES AS RISK FACTORS IN ALZHEIMER'S DISEASE*. Annual Review of Medicine, 1996. **47**(1): p. 387-400.
142. Jansen, W.J., et al., *Prevalence of Cerebral Amyloid Pathology in Persons Without Dementia: A Meta-analysis*. JAMA, 2015. **313**(19): p. 1924.
143. Brand, A.L., et al., *The performance of plasma amyloid beta measurements in identifying amyloid plaques in Alzheimer's disease: a literature review*. Alzheimer's Research & Therapy, 2022. **14**(1): p. 195.
144. Palmqvist, S., et al., *Performance of Fully Automated Plasma Assays as Screening Tests for Alzheimer Disease–Related β-Amyloid Status*. JAMA Neurology, 2019. **76**(9): p. 1060.
145. Janelidze, S., et al., *Head-to-Head Comparison of 8 Plasma Amyloid-β 42/40 Assays in Alzheimer Disease*. JAMA Neurology, 2021. **78**(11): p. 1375.
146. Chang, L., et al., *Single molecule enzyme-linked immunosorbent assays: Theoretical considerations*. Journal of Immunological Methods, 2012. **378**(1-2): p. 102-115.
147. Hirtz, C., et al., *Comparison of ultrasensitive and mass spectrometry quantification of blood-based amyloid biomarkers for Alzheimer's disease diagnosis in a memory clinic cohort*. Alzheimer's Research & Therapy, 2023. **15**(1): p. 34.

148. Udeh-Momoh, C., et al., *Blood Derived Amyloid Biomarkers for Alzheimer's Disease Prevention*. The Journal Of Prevention of Alzheimer's Disease, 2021: p. 1-10.
149. Vergallo, A., et al., *Plasma amyloid β 40/42 ratio predicts cerebral amyloidosis in cognitively normal individuals at risk for Alzheimer's disease*. Alzheimer's & Dementia, 2019. **15**(6): p. 764-775.
150. Smirnov, D.S., et al., *Plasma biomarkers for Alzheimer's Disease in relation to neuropathology and cognitive change*. Acta Neuropathologica, 2022. **143**(4): p. 487-503.
151. Janelidze, S., et al., *Detecting amyloid positivity in early Alzheimer's disease using combinations of plasma Aβ42/Aβ40 and p-tau*. Alzheimer's & Dementia, 2022. **18**(2): p. 283-293.
152. Keshavan, A., et al., *Population-based blood screening for preclinical Alzheimer's disease in a British birth cohort at age 70*. Brain, 2021. **144**(2): p. 434-449.
153. Li, Y., et al., *Validation of Plasma Amyloid-β 42/40 for Detecting Alzheimer Disease Amyloid Plaques*. Neurology, 2022. **98**(7): p. e688-e699.
154. Zicha, S., et al., *Comparative analytical performance of multiple plasma Aβ42 and Aβ40 assays and their ability to predict positron emission tomography amyloid positivity*. Alzheimer's & Dementia, 2023. **19**(3): p. 956-966.
155. De Meyer, S., et al., *Comparison of ELISA- and SIMOA-based quantification of plasma Aβ ratios for early detection of cerebral amyloidosis*. Alzheimer's Research & Therapy, 2020. **12**(1): p. 162.
156. Milà-Alomà, M., et al., *Plasma p-tau231 and p-tau217 as state markers of amyloid-β pathology in preclinical Alzheimer's disease*. Nature Medicine, 2022.
157. Karikari, T.K., et al., *Blood phosphorylated tau 181 as a biomarker for Alzheimer's disease: a diagnostic performance and prediction modelling study using data from four prospective cohorts*. The Lancet Neurology, 2020. **19**(5): p. 422-433.
158. Mielke, M.M., et al., *Comparison of Plasma Phosphorylated Tau Species With Amyloid and Tau Positron Emission Tomography, Neurodegeneration, Vascular Pathology, and Cognitive Outcomes*. JAMA Neurology, 2021. **78**(9): p. 1108.
159. Kent, S.A., T.L. Spires-Jones, and C.S. Durrant, *The physiological roles of tau and Aβ: implications for Alzheimer's disease pathology and therapeutics*. Acta Neuropathologica, 2020. **140**(4): p. 417-447.
160. Kuo, Y.-M., et al., *Elevated Aβ42 in Skeletal Muscle of Alzheimer Disease Patients Suggests Peripheral Alterations of AβPP Metabolism*. The American Journal of Pathology, 2000. **156**(3): p. 797-805.
161. Kuo, Y.-M., et al., *Amyloid-β Peptides Interact with Plasma Proteins and Erythrocytes: Implications for Their Quantitation in Plasma*. Biochemical and Biophysical Research Communications, 2000. **268**(3): p. 750-756.
162. Lopez, O.L., et al., *Plasma amyloid levels and the risk of AD in normal subjects in the Cardiovascular Health Study*. Neurology, 2008. **70**(19): p. 1664-1671.
163. Braak, H. and E. Braak, *Frequency of Stages of Alzheimer-Related Lesions in Different Age*

Categories. Neurobiology of Aging, 1997. **18**(4): p. 351-357.
164. Roy, M., et al., *Age-associated evolution of plasmatic amyloid in mouse lemur primates: relationship with intracellular amyloid deposition*. Neurobiology of Aging, 2015. **36**(1): p. 149-156.
165. Villemagne, V.L., et al., *Amyloid β deposition, neurodegeneration, and cognitive decline in sporadic Alzheimer's disease: a prospective cohort study*. The Lancet Neurology, 2013. **12**(4): p. 357-367.
166. Hanseeuw, B.J., et al., *Defining a Centiloid scale threshold predicting long-term progression to dementia in patients attending the memory clinic: an [18F] flutemetamol amyloid PET study*. European Journal of Nuclear Medicine and Molecular Imaging, 2021. **48**(1): p. 302-310.
167. Fraley, C., et al., *Gaussian Mixture Modelling for Model-Based Clustering, Classification, and Density Estimation*. 2022.
168. Scheltens, P., et al., *Alzheimer's disease*. (1474-547X (Electronic)).
169. Minter, M.R., J.M. Taylor, and P.A.-O. Crack, *The contribution of neuroinflammation to amyloid toxicity in Alzheimer's disease*. (1471-4159 (Electronic)).
170. Chen, Y. and Y. Yu, *Tau and neuroinflammation in Alzheimer's disease: interplay mechanisms and clinical translation*. (1742-2094 (Electronic)).
171. Cacace, R., K. Sleegers, and C. Van Broeckhoven, *Molecular genetics of early-onset Alzheimer's disease revisited*. (1552-5279 (Electronic)).
172. Colmant, L.A.-O., et al., *Definition of a Threshold for the Plasma Aβ42/Aβ40 Ratio Measured by Single-Molecule Array to Predict the Amyloid Status of Individuals without Dementia*. *LID - 10.3390/ijms25021173 [doi] LID - 1173*. (1422-0067 (Electronic)).
173. Mendes, A.A.-O., et al., *Head-to-head study of diagnostic accuracy of plasma and cerebrospinal fluid p-tau217 versus p-tau181 and p-tau231 in a memory clinic cohort*. (1432-1459 (Electronic)).
174. Kwon, H.S., et al., *Predicting amyloid PET positivity using plasma p-tau181 and other blood-based biomarkers*. (2352-8729 (Print)).
175. Thijssen, E.H., et al., *Diagnostic value of plasma phosphorylated tau181 in Alzheimer's disease and frontotemporal lobar degeneration*. (1546-170X (Electronic)).
176. Winston, C.N., et al., *Evaluation of Blood-Based Plasma Biomarkers as Potential Markers of Amyloid Burden in Preclinical Alzheimer's Disease*. (1875-8908 (Electronic)).
177. Tissot, C., et al., *Comparing tau status determined via plasma pTau181, pTau231 and [(18)F]MK6240 tau-PET*. (2352-3964 (Electronic)).
178. Zhang, X.X., et al., *The Epidemiology of Alzheimer's Disease Modifiable Risk Factors and Prevention*. (2426-0266 (Electronic)).
179. Barthélemy, N.R., et al., *Highly accurate blood test for Alzheimer's disease is similar or superior to clinical cerebrospinal fluid tests*. (1546-170X (Electronic)).
180. Therriault, J., et al., *Association of Phosphorylated Tau Biomarkers With Amyloid Positron Emission Tomography vs Tau Positron Emission Tomography*. (2168-6157 (Electronic)).
181. Coleman, B.M. and A.F. Hill, *Extracellular vesicles--Their role in the packaging and spread of misfolded proteins associated with*

neurodegenerative diseases. (1096-3634 (Electronic)).
182. Congdon, E.E., et al., *Tau-targeting therapies for Alzheimer disease: current status and future directions*. (1759-4766 (Electronic)).
183. Sevigny, J., et al., *The antibody aducanumab reduces Aβ plaques in Alzheimer's disease*. (1476-4687 (Electronic)).
184. van Dyck, C.H., et al., *Lecanemab in Early Alzheimer's Disease*. (1533-4406 (Electronic)).
185. Mintun, M.A., et al., *Donanemab in Early Alzheimer's Disease*. (1533-4406 (Electronic)).
186. Prince, M.e.a., *The Global Impact of Dementia: An Analysis of Prevalence, Incidence, Cost and Trends*. . Alzheimer's Disease International, 2015. **World Alzheimer Report 2015**.
187. Jie, C., et al., *Tauvid™: The First FDA-Approved PET Tracer for Imaging Tau Pathology in Alzheimer's Disease*. Pharmaceuticals, 2021. **14**(2): p. 110.
188. Hansson, O., *Biomarkers for neurodegenerative diseases*. Nature Medicine, 2021. **27**(6): p. 954-963.
189. Sevigny, J., et al., *The antibody aducanumab reduces Aβ plaques in Alzheimer's disease*. Nature, 2016. **537**(7618): p. 50-56.
190. Swanson, C.J., et al., *A randomized, double-blind, phase 2b proof-of-concept clinical trial in early Alzheimer's disease with lecanemab, an anti-Aβ protofibril antibody*. Alzheimer's Research & Therapy, 2021. **13**(1).
191. Andreasson, U., K. Blennow, and H. Zetterberg, *Update on ultrasensitive technologies to facilitate research on blood biomarkers for central nervous system disorders*. Alzheimer's & Dementia: Diagnosis, Assessment & Disease Monitoring, 2016. **3**(1): p. 98-102.
192. Schindler, S.E., et al., *High-precision plasma β-amyloid 42/40 predicts current and future brain amyloidosis*. 2019(1526-632X (Electronic)).
193. Mayeux, R., et al., *Plasma A[beta]40 and A[beta]42 and Alzheimer's disease: relation to age, mortality, and risk*. 2003(1526-632X (Electronic)).
194. Doecke, J.D., et al., *Total Aβ₄₂/Aβ₄₀ ratio in plasma predicts amyloid-PET status, independent of clinical AD diagnosis*. Neurology, 2020. **94**(15): p. e1580-e1591.
195. Pichet Binette, A., et al., *Confounding factors of Alzheimer's disease plasma biomarkers and their impact on clinical performance*. Alzheimer's & Dementia, 2022.
196. Ruan, Z., et al., *Alzheimer's disease brain-derived extracellular vesicles spread tau pathology in interneurons*. (1460-2156 (Electronic)).
197. Gomes, P., et al., *Extracellular vesicles and Alzheimer's disease in the novel era of Precision Medicine: implications for disease progression, diagnosis and treatment*. Exp Neurol, 2022. **358**: p. 114183.
198. Asai, H., et al., *Depletion of microglia and inhibition of exosome synthesis halt tau propagation*. Nature Neuroscience, 2015. **18**(11): p. 1584-1593.
199. Beretta, C., et al., *Extracellular vesicles from amyloid-β exposed cell cultures induce severe dysfunction in cortical neurons*. Scientific Reports, 2020. **10**(1).

200. Yuyama, K. and Y. Igarashi, *Exosomes as Carriers of Alzheimer's Amyloid-ss*. Front Neurosci, 2017. **11**: p. 229.
201. Malm, T., S. Loppi, and K.M. Kanninen, *Exosomes in Alzheimer's disease*. Neurochemistry International, 2016. **97**: p. 193-199.
202. Norman, M.A.-O., et al., *L1CAM is not associated with extracellular vesicles in human cerebrospinal fluid or plasma*. (1548-7105 (Electronic)).
203. Böing, A.N., et al., *Single-step isolation of extracellular vesicles by size-exclusion chromatography. LID - 10.3402/jev.v3.23430 [doi]*. (2001-3078 (Print)).
204. Théry, C., et al., *Minimal information for studies of extracellular vesicles 2018 (MISEV2018): a position statement of the International Society for Extracellular Vesicles and update of the MISEV2014 guidelines*. Journal of Extracellular Vesicles, 2018. **7**(1): p. 1535750.
205. Choy, R.W., R. Cheng Z Fau - Schekman, and R. Schekman, *Amyloid precursor protein (APP) traffics from the cell surface via endosomes for amyloid β (Aβ) production in the trans-Golgi network*. (1091-6490 (Electronic)).
206. Imanbekova, M., et al., *Identification of amyloid beta in small extracellular vesicles via Raman spectroscopy*. (2516-0230 (Electronic)).
207. Simrén, J., et al., *The diagnostic and prognostic capabilities of plasma biomarkers in Alzheimer's disease*. Alzheimer's & Dementia, 2021. **17**(7): p. 1145-1156.
208. Vergallo, A., et al., *Plasma amyloid β 40/42 ratio predicts cerebral amyloidosis in cognitively normal individuals at risk for Alzheimer's disease*. Alzheimer's & Dementia, 2019. **15**(6): p. 764-775.
209. Wojdała, A.L., et al., *CSF and plasma Aβ42/40 across Alzheimer's disease continuum: comparison of two ultrasensitive Simoa® assays targeting distinct amyloid regions*. 2024. **62**(2): p. 332-340.
210. Feinkohl, I., et al., *Plasma Amyloid Concentration in Alzheimer's Disease: Performance of a High-Throughput Amyloid Assay in Distinguishing Alzheimer's Disease Cases from Controls*. (1875-8908 (Electronic)).
211. Marques, M.A., et al., *Peripheral amyloid-beta levels regulate amyloid-beta clearance from the central nervous system*. (1387-2877 (Print)).
212. Song, F., et al., *Meta-analysis of plasma amyloid-β levels in Alzheimer's disease*. (1875-8908 (Electronic)).
213. Brickman, A.M., et al., *Plasma p-tau181, p-tau217, and other blood-based Alzheimer's disease biomarkers in a multi-ethnic, community study*. Alzheimer's & Dementia, 2021. **17**(8): p. 1353-1364.
214. Irwin, D.J., et al., *CSF tau and β-amyloid predict cerebral synucleinopathy in autopsied Lewy body disorders*. (1526-632X (Electronic)).
215. Riemenschneider, M., et al., *Tau and Abeta42 protein in CSF of patients with frontotemporal degeneration*. (0028-3878 (Print)).
216. Kapogiannis, D., et al., *Association of Extracellular Vesicle Biomarkers With Alzheimer Disease in the Baltimore Longitudinal Study of Aging*. JAMA Neurology, 2019. **76**(11): p. 1340.
217. Norman, M., et al., *L1CAM is not associated with extracellular*

vesicles in human cerebrospinal fluid or plasma. Nature Methods, 2021. **18**(6): p. 631-634.

218. Poznanski, S.M. and A.A. Ashkar, *Shining light on the significance of NK cell CD56 brightness*. Cellular & Molecular Immunology, 2018. **15**(12): p. 1071-1073.
219. Shi, M., et al., *CNS tau efflux via exosomes is likely increased in Parkinson's disease but not in Alzheimer's disease*. (1552-5279 (Electronic)).
220. Winston Cn Fau - Goetzl, E.J., et al., *Growth Hormone-Releasing Hormone Modulation of Neuronal Exosome Biomarkers in Mild Cognitive Impairment*. (1875-8908 (Electronic)).
221. Jia, L., et al., *Concordance between the assessment of Aβ42, T-tau, and P-T181-tau in peripheral blood neuronal-derived exosomes and cerebrospinal fluid*. Alzheimer's & Dementia, 2019. **15**(8): p. 1071-1080.
222. Fiandaca, M.S., et al., *Identification of preclinical Alzheimer's disease by a profile of pathogenic proteins in neurally derived blood exosomes: A case-control study*. (1552-5279 (Electronic)).
223. Guix, F.X., et al., *Detection of Aggregation-Competent Tau in Neuron-Derived Extracellular Vesicles*. *LID - 10.3390/ijms19030663 [doi] LID - 663*. (1422-0067 (Electronic)).
224. Rajendran, L., et al., *Alzheimer's disease beta-amyloid peptides are released in association with exosomes*. (0027-8424 (Print)).
225. Sharples, R.A., et al., *Inhibition of gamma-secretase causes increased secretion of amyloid precursor protein C-terminal fragments in association with exosomes*. (1530-6860 (Electronic)).
226. Figdore, D.J., et al., *Performance of the Lumipulse plasma Aβ42/40 and pTau181 immunoassays in the detection of amyloid pathology*. (2352-8729 (Print)).
227. *Sysmex Files for Manufacturing and Marketing Approval*

for an Assay Kit that Assists in Identification of Amyloid Beta (Aβ)

Accumulation in the Brain, in *Sysmex Corporation*. 2022, Sysmex Corporation.
228. Mattke, S., et al., *Blood-based biomarkers for Alzheimer's pathology and the diagnostic process for a disease-modifying treatment: Projecting the impact on the cost and wait times*. Alzheimer's & Dementia: Diagnosis, Assessment & Disease Monitoring, 2020. **12**(1).
229. Rissman, R.A.-O., et al., *Plasma Aβ42/Aβ40 and phospho-tau217 concentration ratios increase the accuracy of amyloid PET classification in preclinical Alzheimer's disease*. (1552-5279 (Electronic)).
230. Bittner, T., *What Are the Remaining Challenges before Blood-Based Biomarkers for Alzheimer's Disease Can Be Used in Clinical Practice?* The Journal of Prevention of Alzheimer's Disease, 2022. **9**(4): p. 567-568.
231. Czeczor, J.K. and S.L. McGee, *Emerging roles for the amyloid precursor protein and derived peptides in the regulation of cellular and systemic metabolism*. Journal of Neuroendocrinology, 2017. **29**(5).
232. Palmqvist, S., et al., *Performance of Fully Automated Plasma Assays as Screening Tests for Alzheimer Disease-Related β-Amyloid Status*. (2168-6157 (Electronic)).

233. Jeppsson, A., et al., *Plasma and cerebrospinal fluid concentrations of neurofilament light protein correlate in patients with idiopathic normal pressure hydrocephalus*. Fluids and Barriers of the CNS, 2023. **20**(1): p. 54.
234. Shir, D., et al., *Association of plasma glial fibrillary acidic protein (GFAP) with neuroimaging of Alzheimer's disease and vascular pathology*. (2352-8729 (Print)).
235. Chatterjee, P., et al., *Plasma glial fibrillary acidic protein is elevated in cognitively normal older adults at risk of Alzheimer's disease*. Translational Psychiatry, 2021. **11**(1): p. 27.
236. Leitão, M.J., et al., *Clinical validation of the Lumipulse G cerebrospinal fluid assays for routine diagnosis of Alzheimer's disease*. Alzheimer's Research & Therapy, 2019. **11**(1): p. 91.
237. Devanarayan, V.A.-O., et al., *Plasma pTau217 predicts continuous brain amyloid levels in preclinical and early Alzheimer's disease*. (1552-5279 (Electronic)).
238. Lehmann, S.A.-O.X., et al., *Clinical value of plasma ALZpath pTau217 immunoassay for assessing mild cognitive impairment*. (1468-330X (Electronic)).
239. Ashton, N.J., et al., *Diagnostic Accuracy of a Plasma Phosphorylated Tau 217 Immunoassay for Alzheimer Disease Pathology*. (2168-6157 (Electronic)).
240. Janelidze, S.A.-O., et al., *Head-to-head comparison of 10 plasma phospho-tau assays in prodromal Alzheimer's disease*. (1460-2156 (Electronic)).
241. Welsh, J.A.-O., et al., *Minimal information for studies of extracellular vesicles (MISEV2023): From basic to advanced approaches*. (2001-3078 (Electronic)).
242. Tian, C., et al., *Blood extracellular vesicles carrying synaptic function- and brain-related proteins as potential biomarkers for Alzheimer's disease*. Alzheimer's & Dementia, 2023. **19**(3): p. 909-923.
243. Lucien, F., et al., *MIBlood-EV: Minimal information to enhance the quality and reproducibility of blood extracellular vesicle research*. Journal of Extracellular Vesicles, 2023. **12**(12): p. 12385.
244. Chan, A.A.-O.X., et al., *Natural Killer Cell-Derived Extracellular Vesicles as a Promising Immunotherapeutic Strategy for Cancer: A Systematic Review. LID - 10.3390/ijms24044026 [doi] LID - 4026*. (1422-0067 (Electronic)).
245. Hofmann, L., et al., *The Potential of CD16 on Plasma-Derived Exosomes as a Liquid Biomarker in Head and Neck Cancer. LID - 10.3390/ijms21113739 [doi] LID - 3739*. (1422-0067 (Electronic)).
246. Chatterjee, M., et al., *Plasma extracellular vesicle tau and TDP-43 as diagnostic biomarkers in FTD and ALS*. Nature Medicine, 2024. **30**(6): p. 1771-1783.
247. Olsson, B., et al., *CSF and blood biomarkers for the diagnosis of Alzheimer's disease: a systematic review and meta-analysis*. The Lancet Neurology, 2016. **15**(7): p. 673-684.
248. Gámez-Valero, A., et al., *Exploratory study on microRNA profiles from plasma-derived extracellular vesicles in Alzheimer's disease and dementia with Lewy bodies*. Translational Neurodegeneration, 2019. **8**(1): p. 31.
249. Nie, C., et al., *Differential Expression of Plasma Exo-miRNA in Neurodegenerative Diseases by*

Next-Generation Sequencing. Frontiers in Neuroscience, 2020. **14**.

250. Shi, M., et al., *New windows into the brain: Central nervous system-derived extracellular vesicles in blood*. (1873-5118 (Electronic)).

251. Alvarez-Erviti, L., et al., *Delivery of siRNA to the mouse brain by systemic injection of targeted exosomes*. Nature Biotechnology, 2011. **29**(4): p. 341-345.

252. Rather, H.A., et al., *Therapeutic efficacy and promise of stem cell-derived extracellular vesicles in Alzheimer's disease and other aging-related disorders*. Ageing Research Reviews, 2023. **92**: p. 102088.

Supplementary materials of PART II.

"Comparison of plasma soluble and extracellular vesicles-associated biomarkers in Alzheimer's Disease patients and cognitively normal individuals"

Supplementary file 1: Validation protocol for NDEVs isolation using Exoflow technique.

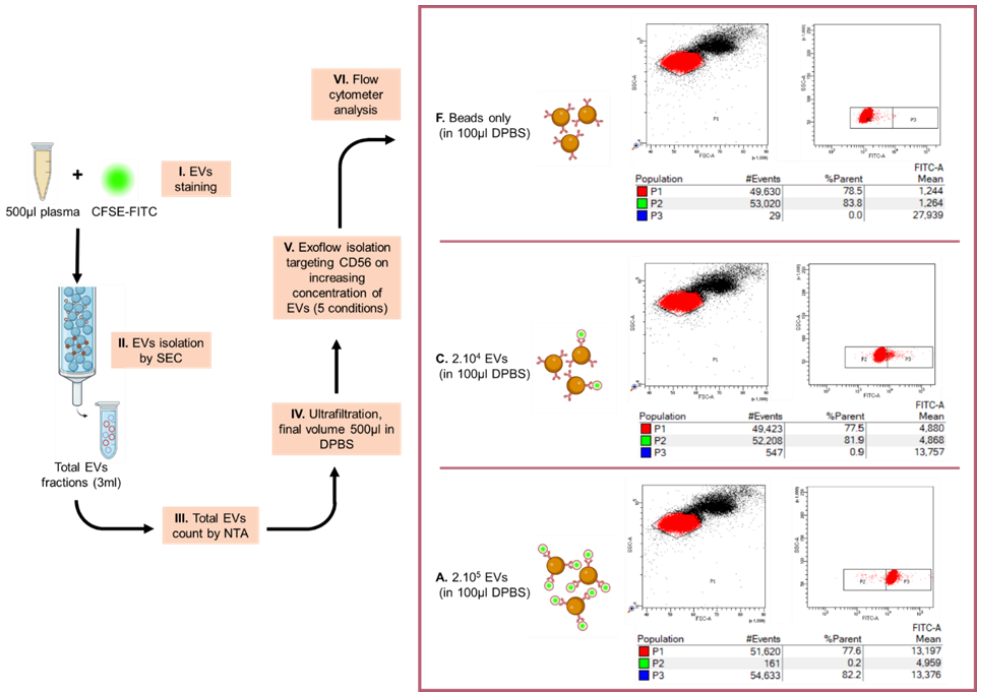

I. Plasma sample was incubated with 6µl of CFSE-FITC at RT for 2h. **II.** EVs were isolated by size exclusion chromatography, by collecting EVS fractions (F7 to 12 = 3ml total volume). **III.** Number of EVs were count by NTA to determine EVs quantity to use in Exolfow protocol. **IV.** 3ml of eluted EVs were concentrated by ultrafiltration (10kDa filter, 4°C, 45min at 4000g), final volume was 500µl. **V.** Exoflow with anti-CD56 antibody was

performed in 5 different conditions : **A.** 100µl of concentrated EVs (+/– 2.105 EVs), B.50µl (+/–1.105 EVs), **C.**10µl (+/–2.104 EVs), D.5µl (+/–1.104 EVs), E.1µl (+/– 2.103 EVs) and **F.** magnetic beads without EVs. We used the same amount of beads solution (40µl) and antibody (10µl, dilution 1/5). Exoflow isolation was performed following manufacturer protocol (System Biosciences, #CSFLOWBASICA-1). **VI.** Post isolation beads were analyzed by flow cytometry for FITC signal. Beads population was selected based on size scatter and forward scatter (population P1), and with negative FITC signal (population P2). Positive population (P3) was considered positive above log104 of FITC signal. Saturation point was reach with condition A. 2.105 EVs.

Supplementary file 2: Detailed scatter plots of the correlation between plasma soluble biomarkers quantity, plasma NDEVs quantity and their content in AD biomarkers.

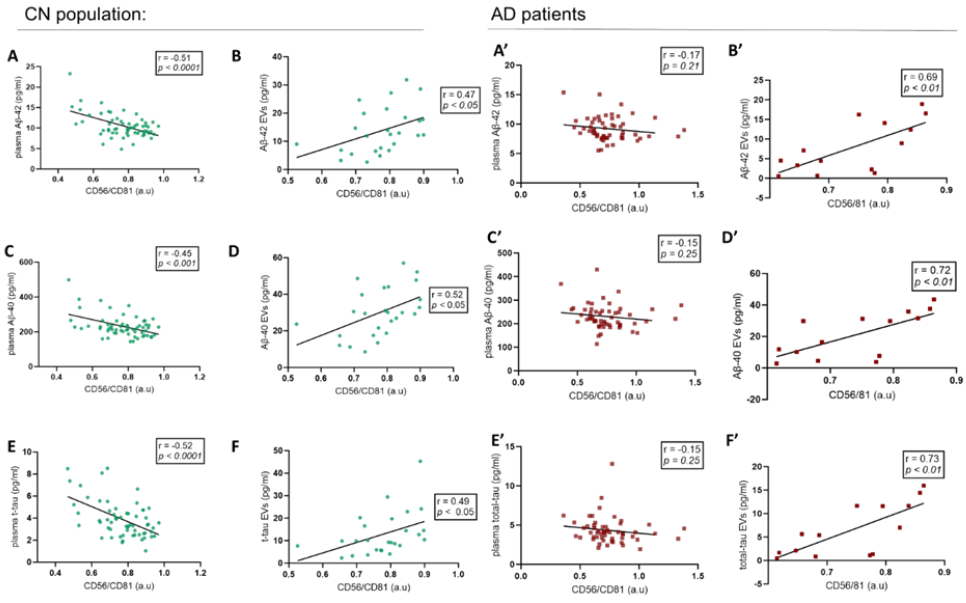

Population details for figures A, A', C, C', E and E' can be found on paragraph 3.2. For the analysis of NDEVs content, we focused on subgroups distributed across the plasma NDEVs spectrum, ranging from low circulating participants to high circulating participants. In the CN group, n=27, with a mean MMSE [SD] of 28.76 [1.27], mean age [SD] of 61.78 [14.8], 16 women [59.3%], and mean CD56/81 of 0.768 [0.10]. In the AD group, n=14, with a mean MMSE [SD] of 21.9 [5.09], mean age [SD] of 66.4 [16.7], 6 women [42.8%], and mean CD56/81 of 0.742 [0.09].

Supplementary file 3: Dot blot results for EVs characterization

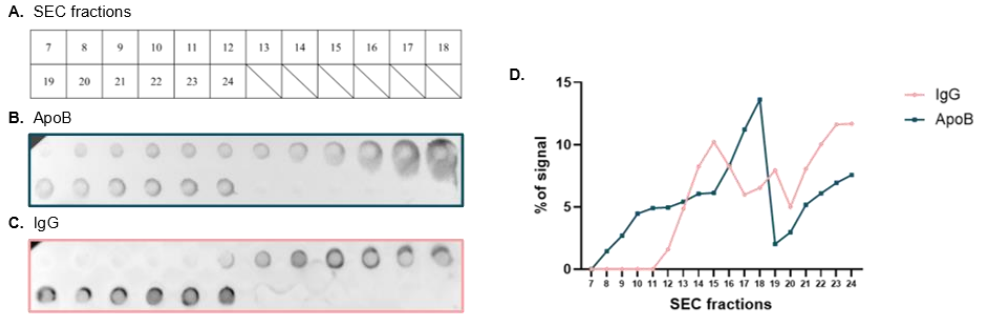

Exclusion markers tested are apolipoprotein B (ApoB) and human IgG.A. Schematic display of the dot blots showing the localization of the fractions spotted on the membrane (fractions 7 to 24). Fractions before 7 were not analyzed due to the absence of particles detected by NTA in fractions 1 to 6. Putative EV particles were present in fractions 7 to 12. B. Raw dot blot results for ApoB detection (protocol detail in section 2.6.3). C. Raw dot blot result for IgG detection. D. Quantification of the signal in dot blots for ApoB and IgG. IgG is detected mostly after fraction 12 (98.41% of the signal), while the ApoB signal is detected in fractions 7 to 12 (18.46% of the signal), with the signal peaking in fractions 13 to 24 (81.54% of the signal).